Fakultät für Medizin
Institut für Pharmakologie und Toxikologie

Phosphorylation of the β_1-adrenoceptor

Laura Emily Hinz

Vollständiger Abdruck der von der Fakultät für Medizin der Technischen Universität München zur Erlangung des akademischen Grades eines

Doctor of Philosophy (Ph.D.)

genehmigten Dissertation.

Vorsitzender: Univ-Prof. Dr. Arthur Konnerth

Betreuer: Univ-Prof. Dr. Dr. Stefan Engelhardt

Prüfer der Dissertation:
1. Univ-Prof. Dr. Bernhard Küster
2. Assoc. Prof. Rory Koenen, Ph.D.

Die Dissertation wurde am 14.03.2017 bei der Technischen Universität München eingereicht und durch die Fakultät für Medizin am 12.06.2017 angenommen.

Abstract

β-adrenoceptors belong to the family of G protein-coupled receptors (GPCRs), the largest group of membrane proteins in mammals. Phosphorylation of GPCRs is an essential regulatory mechanism. It leads to β-arrestin binding, which controls key processes such as desensitization and internalization.

Even though the human β_1-adrenoceptor (ADRB1) is of tremendous importance in a number of diseases, its phosphorylation remains poorly understood. To address this question, we overexpressed the ADRB1 in human embryonic kidney cells and purified the receptor via crosslink immunoprecipitation. The purified β_1-adrenoceptor was then used to perform qualitative and quantitative mass spectrometry. We were able to elucidate the phosphorylation pattern of the human β_1-adrenoceptor *in vitro* and identified six previously unknown phosphorylation sites in the third intracellular loop and the receptor's C-terminus.

Labeling HEK293 cells with stable heavy isotopes (SILAC) led to the discovery of a stimulation-dependent regulation of four of these phosphorylation sites (Ser260, Ser274, Ser312 and Ser412). Furthermore, mutagenesis studies in stably transfected HEK293 cells revealed the impact of phosphorylation for arrestin binding and internalization of the receptor. Fluorescence resonance energy transfer experiments with β_1-adrenoceptor variants carrying point mutations of putative phosphorylation sites identified two C-terminal phosphosites as the receptor's arrestin recognition site. This highly conserved site Ser461/462 not only determined arrestin recruitment to the β_1-adrenoceptor, but was also crucial for receptor internalization.

As arrestin recruitment leads to an alternative G protein-independent signal transduction in many GPCRs, among them the β_2-adrenoceptor, we investigated whether ADRB1 phosphorylation is linked to MAPK1/3 activation. However, in this regard the ADRB1 and the ADRB2 seem to differ, as we did not observe phosphorylation-dependent MAP kinase activation after ADRB1 stimulation.

Our approach led to the successful identification of six novel and two previously known phosphorylation sites in the ADRB1 and to the discovery of the β_1-adrenoceptor's arrestin recognition site.

Contents

1 Introduction

1.1 The sympathetic nervous system

The sympathetic nervous system is part of the autonomous nervous system, which controls the body's unconscious actions like heartbeat, breathing and blood pressure. This helps the human body react to stressful situations. When the sympathetic nervous system is activated, the adrenal glands excrete the catecholamines epinephrine and norepinephrine (Figure 1.1). Additionally norepinephrine is released from sympathetic nerve endings. Epinephrine and norepinephrine then activate α- and β-adrenoceptors.

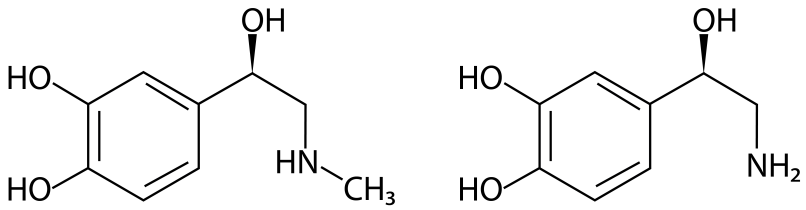

Figure 1.1: **Epinephrine and norepinephrine.**
The catecholamines epinephrine (**left hand side**) and norepinephrine (**right hand side**) are the endogenous ligands for the adrenoceptors.

Depending on the organ this leads to different responses. In the heart, catecholamine-induced activation of the β_1-adrenoceptor (ADRB1) leads to positive chronotropy (increase in heart rate), dromotropy (increase in atrioventricular conduction), inotropy (increase in heart contractility) and bathmotropy (decrease in excitation threshold). In the intestines, adrenoceptor activation causes vasoconstriction, which reduces blood flow to intestinal organs so more blood can be supplied to vital organs, such as the brain or the heart. All of these mechanisms lead to an adaptation to stress stimuli.

The counterpart of the sympathetic nervous system is the parasympathetic nervous system, which stimulates tasks like digestion and controls homeostasis containment.

This thesis deals with one of the β-adrenoceptors, the β_1-adrenoceptor, which is the central receptor for sympathetic signal transduction in the heart. The ADRB1 belongs to the family of G protein-coupled receptors (GPCRs).

1.2 G protein-coupled receptors

G protein-coupled receptors form the largest group of mammalian surface receptors. They account for one third to one half of all known drug targets (Pierce et al., 2002; Overington et al., 2006; Salon et al., 2011).

GPCRs transduce extracellular signals into the cell via guanine nucleotide-binding proteins or G proteins (Pierce et al., 2002). All G proteins are GTPases, which means that they have the ability to hydrolyze guanosine triphosphate (GTP) into guanosine diphosphate (GDP). Through this mechanism, G proteins act as molecular switches. They are active, when bound to GTP and inactive, when bound to GDP. Guanine nucleotide exchange factors facilitate the switch from GDP to GTP. After this exchange the G protein is put in an active state (Figure 1.2).

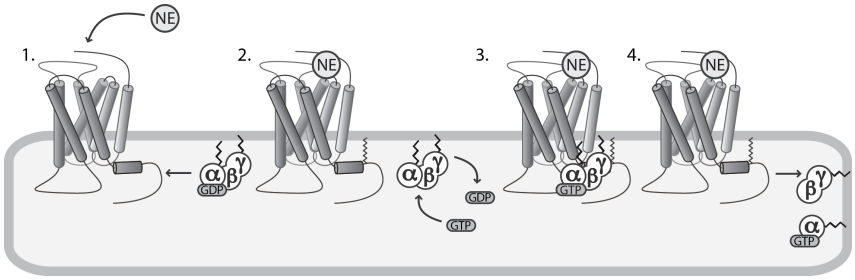

Figure 1.2: **The cycle of GPCR activation and G protein dissociation.**
G proteins are inactive when bound to GDP and active when bound to GTP. Once a G protein dissociates, it starts signaling. (**1**) After ligand activation of the GPCR, the receptor attracts a heterotrimeric G protein. (**2**) The inactive G protein binds to the receptor and the affinity for GDP is lowered, while at the same time the affinity for GTP increases. (**3**) The active G protein is bound to the GPCR. (**4**) Upon a conformational change of the GPCR the heterotrimeric G protein dissociates in the α- (G_α) and βγ-subunits ($G_{\beta\gamma}$). G_α moves away from $G_{\beta\gamma}$ via lateral diffusion and initiates downstream signal transduction (e.g. activation of adenylyl cyclase). $G_{\beta\gamma}$ forms a stable complex and remains anchored to the membrane via G_γ.
GDP = guanosine diphosphate, GTP = guanosine triphosphate, NE = norepinephrine.

There are two different classes of G proteins: First small monomeric G proteins, like Ras, which is involved in the MAP kinase pathway and second larger

heterotrimeric G proteins, which consist of three subunits, the G_α-, G_β- and G_γ-subunit (Zhang et al., 2015). The guanine nucleotide binding pocket is located in the G_α-subunit. G proteins that interact with GPCRs typically are heterotrimeric G proteins. They functionally couple GPCRs to other signaling molecules like enzymes or ion channels (Rockman et al., 2002).

GPCRs share a highly conserved structure of seven transmembrane-spanning domains (Figure 1.3), which is why they are also called seven-transmembrane receptors or heptahelical receptors (Pierce et al., 2002). These transmembrane domains consist of hydrophobic α-helices, which are connected through three intracellular (ICL-1 – ICL-3) and three extracellular (ECL-1 – ECL-3) loops (Figure 1.4). Using the similarities of the transmembrane domains, GPCRs have been grouped into five different classes (A-E) (Attwood and Findlay, 1994), which are not all found in humans. Fredriksson et al., 2003 classified the human GPCRs further and divided them into five different families: The rhodopsin family, the secretin family, the glutamate family, the adhesion family and the frizzled/tas2 receptor family. Their genome analysis shows more than 800 GPCRs, with over 50 % being olfactory receptors. The International Union of Basic and Clinical Pharmacology (IUPHAR) currently uses parts of both classification systems: They divide the GPCRs into Class A (rhodopsin family), Class B (secretin family), Class C (glutamate family), adhesion family and frizzled family (Alexander et al., 2013). The β-adrenoceptors belong to the rhodopsin family, which forms the largest family of GPCRs (Deupi and Kobilka, 2007). Class A receptors from the rhodopsin family can be further grouped in 19 subgroups (A1-A19) (Joost and Methner, 2002).

While the transmembrane-spanning domains are highly conserved, both the extracellular N-terminus (amino-terminus) and the intracellular C-terminus (carboxy-terminus) show great variations. This becomes clear, when looking closely at the β_1-adrenoceptor and the β_2-adrenoceptor, which are very similar receptors, but only share 54 % sequence homology (Frielle et al., 1987).

Even though G protein-coupled receptors are similar in overall structure and mechanistic function, they have a wide variety of binding partners. Their ligands range from small subatomic particles like photons, which activate rhodopsin, to ions and small molecules (Deupi and Kobilka, 2007). The natural ligands for the β_1-adrenoceptor are the catecholamines epinephrine and norepinephrine (Figure 1.1).

The interaction between GPCRs and G proteins and other interacting proteins is mainly facilitated by the third intracellular loop and the C-terminus while ligand binding takes place in the N-terminus and the transmembrane-spanning domains (Lefkowitz, 2007).

Many rhodopsin-like receptors, such as the β_1-adrenoceptor contain a cysteine-rich region intracellularly, at which the receptors are palmitoylated (Figure 1.3 [purple]).

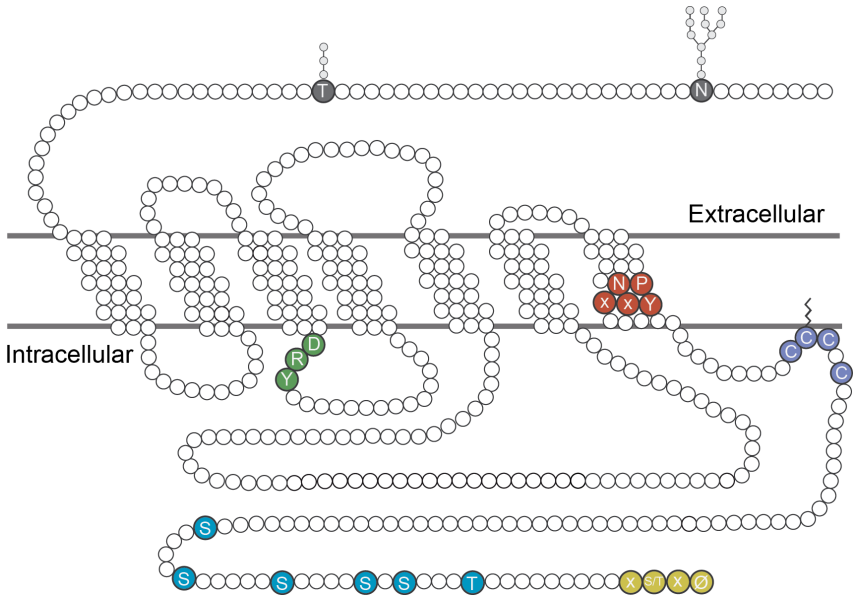

Figure 1.3: **Conserved motifs in G protein-coupled receptors.**
G protein-coupled receptors consist out of seven conserved transmembrane domains, an extracellular N-terminus and an intracellular C-terminus. Depicted in grey are sites for N- and O-glycosylation, respectively. Furthermore the DRY motif (green) is highly conserved in many GPCRs, as is the NPxxY motif (red), which is linked to receptor activation. Marked in purple is a cysteine-rich region, in which a lipid anchor is inserted into the membrane. This leads to the formation of helix 8. Many putative phosphorylation sites (blue) are located at the C-terminus. So is the PDZ type I domain (yellow), which is found at the C-terminal end of many G protein-coupled receptors. N = asparagine, T = threonine, D = aspartate, R = arginine, Y = tyrosine, P = proline, x = any amino acid (except for proline), C = cysteine, S = serine, S/T = serine or threonine, Ø = bulky hydrophobic amino acid (phenylalanine, isoleucine, leucine, methionine, valine, tryptophan).

This fatty acid integrates into the membrane and leads to the formation of an additional small intracellular loop following transmembrane domain seven, termed helix 8 (Palczewski et al., 2000; Kirchberg et al., 2011). As seen in figure 1.4, the helices are arranged in a counter-clockwise manner with helix 8 being orthogonal to the other transmembrane domains.

Apart from the general composition of seven transmembrane-spanning domains, GPCRs also share conserved structures within these domains. Many G protein-coupled receptors share a three-amino acid motif at the end of helix 3, the DRY motif (Figure 1.3 [green]), that consists of aspartate (D), arginine (R) and tyrosine (Y) residues. The significance of the DRY motif is not yet fully understood, an activation site (Warne et al., 2008) or an arrestin binding motif (Marion et al., 2006) is proposed. Another conserved sequence is the NPxxY motif (Figure 1.3 [red]) at the end of transmembrane domain 6, consisting out of asparagine (N), proline (P), two other amino acids and tyrosine (Y). This sequence, which is present in many GPCRs, is linked to receptor activation (Barak et al., 1995; Fritze et al., 2003). Apart from activation-related motifs, many GPCRs contain a protein-protein interaction domain at the far distal C-terminus, the PDZ (post synaptic density protein 95, Drosophila disc large tumor suppressor and zonula occludens-1 protein) type I domain (Figure 1.3 [yellow], Chapter 1.4.2). This domain can be involved in downstream signal transduction and internalization of the GPCR (Cao et al., 1999).

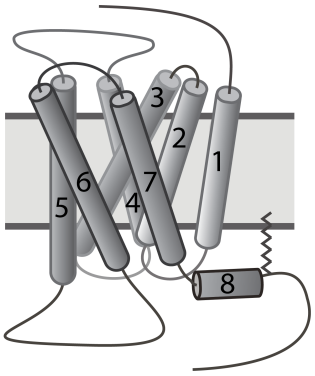

Figure 1.4: **Schematic illustration of domain juxtaposition in class A GPCRs.**
Class A GPCR structure containing the extracellular N-terminus, the intracellular C-terminus, the seven transmembrane domains and intra- and extracellular loops. 1-7 = transmembrane domain 1 to 7. 8 = helix 8, which forms after fatty acid addition in a cysteine-rich region of the intracellular C-terminus.

The GPCR classification was originally performed on gene level, because the exact protein structure was only known for very few GPCRs. This is due to their usually very low expression rates, their often very long and unstructured C- and N-termini and solubility problems, which are typical for membrane proteins.

Therefore the, by now numerous, available crystal structures usually contain several thermostabilizing mutations as well as truncations of the C- and N-terminus, respectively. Regarding crystallography of β-adrenoceptors, recent years have

brought great advances. The structure of the turkey ADRB1 was solved both in the inactive (Warne et al., 2008) as well as in the active state, when bound to antagonists and agonists (Warne et al., 2011; Warne et al., 2012) as well as in an agonist-free state (Huang et al., 2013) . The β_2-adrenoceptor (ADRB2) structure is even solved for the human receptor, also in its inactive (Rasmussen et al., 2007) and active (Rasmussen et al., 2011b) state as well as when bound to G_s (Rasmussen et al., 2011a).

1.2.1 G protein-coupled receptor signal transduction

G protein-coupled receptors receive signals from the extracellular space and transmit them into the cytosol via G proteins. Currently two models for G protein/GPCR interaction are being discussed. The *precoupling model* (Neubig et al., 1988; Nobles et al., 2005) assumes that the G protein in its inactive state is already bound to the GPCR and upon GPCR activation becomes activated itself. The *collision coupling model* (Tolkovsky and Levitzki, 1978) states that once the receptor is activated, it attracts an inactive G protein, which then becomes activated. There is evidence for both of these models and it is possible that different modes of binding occur in different GPCRs.

How a GPCR transduces incoming signals depends on its associated G protein. There are more than 20 different G proteins known so far, which can be grouped into five main families: G_s, G_i/G_o, G_q, $G_{12/13}$ and G_v (Oka et al., 2009). In humans however, the G_v family seems to be absent. Stimulatory G_s proteins signal via an activation of the membrane-bound adenylyl cyclase (Figure 1.5). This enzyme produces the second messenger cyclic adenosine monophosphate (cAMP) out of adenosine triphosphate (ATP), which then activates protein kinase A (PKA). One GPCR can activate multiple G proteins and one G_α-subunit can activate multiple adenylyl cyclase enzymes, thus leading to an amplification of the signal (Lambert, 2008).

When the G protein-coupled receptor changes its conformation, it induces the dissociation of the heterotrimeric G protein into the different subunits. The G_α-subunit moves via lateral diffusion away from the $\beta\gamma$-subunits, which then form a stable complex, the $G_{\beta\gamma}$-complex (Gilman, 1987; Pierce et al., 2002; Preininger and Hamm, 2004). The $G_{\beta\gamma}$-complex stays anchored to the membrane via a lipid anchor on the G_γ-subunit (Figure 1.2). The $G_{\beta\gamma}$-complex has many different signaling functions, one of which is to inhibit the G_α-subunit (Clapham and Neer, 1997). Signaling stops when the intrinsic GTPase activity of the G_α-subunit hydrolyzes GTP into GDP. How long a G protein stays active mainly depends on the activity of

the intrinsic GTPase. This activity increases when G_α is bound to either its target protein or a *regulator of G protein signaling* (RGS) (Gerber et al., 2016).

Inhibitory G_i proteins cause either an inhibition of the adenylyl cyclase or an activation of phosphodiesterases (PDE) or both. PDEs stop cAMP signaling through the degradation of cAMP to adenosine 5'-monophosphate (Strada et al., 1974). G_i proteins and PDE can hence both be seen as antagonistic to G_s proteins, since they both lead to a decrease in cAMP levels. $G_{q/11}$ and $G_{12/13}$ proteins activate phospholipase C and the Rho family of GTPases, respectively (Birnbaumer, 2007). In mammals signaling via those two G proteins often leads to smooth muscle contractions (Wynne et al., 2009).

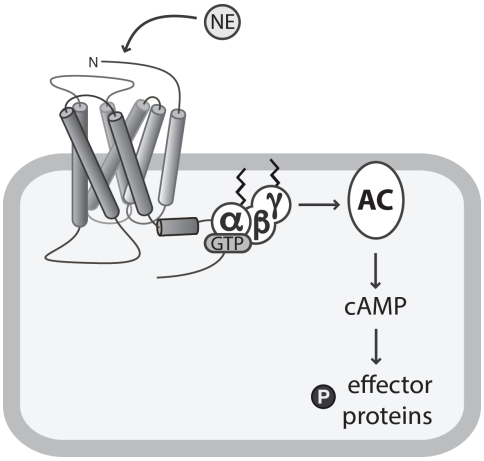

Figure 1.5: **Schematic overview of signal transduction via stimulatory G proteins using the example of the β_1-adrenoceptor.**
The β_1-adrenoceptor is usually coupled to a stimulatory G protein. Upon catecholamine binding the ADRB1 changes its conformation which leads to the dissociation of the trimeric G protein. The G_α-subunit activates the membrane-anchored adenylyl cyclase. This enzyme produces cAMP out of ATP. cAMP activates PKA. Through phosphorylation of different downstream effector proteins in the heart e.g. the voltage dependent calcium channel, PKA activation results in an increase in inotropy.
Abbreviations: AC = adenylyl cyclase, ATP = adenosine triphosphate, cAMP = cyclic adenosine monophosphate, NE = norepinephrine, PKA = protein kinase A.

Activation of G protein-coupled receptors does not only lead to G protein-mediated canonical signal transduction, but can also result in G protein-independent signaling via the binding of arrestin proteins (Chapter 1.4).

1.2.2 Adrenoceptors

The adrenoceptors all belong to the rhodopsin group of G protein-coupled receptors, i.e. are all class A GPCRs. There a nine different adrenoceptor subtypes. Six α-adrenoceptors and three β-adrenoceptors. The α-adrenoceptors are grouped into α_{1A}, α_{1B}, α_{1C} and α_{2A}, α_{2B}, α_{2C}. The β-adrenoceptors comprise the β_1-adrenoceptor, β_2-adrenoceptor and the β_3-adrenoceptor (Strosberg, 1993).

These receptors elicit different responses to the same stimulus (epinephrine and norepinephrine), depending on the type of G protein they couple to (Chapter 1.2.1). In mammals the α_{1A}-adrenoceptor, for example, is predominantly coupled to G proteins from the G_q/G_{11} family and receptor stimulation leads to smooth muscle contraction. On the other hand the β_2-adrenoceptor is physiologically G_s-coupled and thus stimulation of this receptor leads to smooth muscle relaxation. Therefore the distribution of the different adrenoceptors in the effector tissues is the key to understanding the role of the adrenoceptors and not the agonists themselves, since they are the same for all adrenoceptors.

Receptor	**Predominant cell type**	**Agonist affinity**	**Mechanism**
α_1	smooth muscle cells	NE > epinephrine	$G_q \rightarrow Ca^{2+}\uparrow$
α_2	smooth muscle cells platelets	epinephrine > NE	$G_i \rightarrow$ cAMP $\downarrow$
β_1	cardiac myocytes	epinephrine = NE	$G_s \rightarrow$ cAMP $\uparrow$
β_2	smooth muscle cells	epinephrine > NE	$G_s \rightarrow$ cAMP $\uparrow$ $G_i \rightarrow$ cAMP $\downarrow$
β_3	adipocytes	NE > epinephrine	$G_s \rightarrow$ cAMP $\uparrow$

NE = norepinephrine

Physiologically and pathophysiologically very important are the β-adrenoceptors. As mediators of cellular responses after activation of the sympathetic nervous system, they represent the target of widely used therapeutic agents (Insel et al., 2007; Lymperopoulos et al., 2013; Ahles and Engelhardt, 2014). The by far best studied β-adrenoceptor is the β_2-adrenoceptor, which has served as a prototype receptor for a plethora of GPCR studies (Lefkowitz and Shenoy, 2005).

1.2.3 Physiology of the β_1-adrenoceptor

The β_1-adrenoceptor is predominantly located in the heart and sympathetic nervous system, but can also be found in other tissues such as lung, blood and placenta (human protein atlas: Uhlén et al., 2015). As a class A GPCR, the ADRB1 is generally coupled to a stimulatory G_s protein. This means it signals via the cAMP-dependent PKA pathway (Figure 1.5). Activation of protein kinase A leads to phosphorylation of a variety of effector proteins, for example the voltage dependent calcium channel (Zhao et al., 1994; Catterall, 2000), the ryanodine receptor (Marx et al., 2000) and phospholamban (Simmerman and Jones, 1998). In the heart, where this GPCR is predominantly located, this results in an increase in heart frequency and myocardial contractility (Lohse et al., 2003). This is a physiological response to a stress stimulus.

1.2.4 Polymorphisms of the β_1-adrenoceptor

The gene sequence of the human ADRB1 shows a high degree of variability. This variability results in many synonymous and nonsynonymous polymorphisms (Ahles et al., 2015). Especially nonsynonymous polymorphisms, which lead to an exchange of one amino acid for another in the protein are of high interest. The two most frequent ones are the N-terminal p.Ser49Gly (Maqbool et al., 1999; Börjesson et al., 2000) and p.Arg389Gly (Tesson et al., 1999; Mason et al., 1999) in the proximal C-terminus. This terminology means that in the ADRB1 protein (p) at the given amino acid position, here 49 and 389, respectively, the amino acid that is mentioned first can be substituted for the second one. Looking at the first example, this means that in some cases the serine residue is replaced by glycine.

The p.Arg389Gly polymorphism is located at the receptor‘s putative G protein binding site, which hints at a potential functional importance of this single nucleotide polymorphism (SNP). In the Caucasian and Asian population the allele frequency is 74 % for the arginine allele and 26 % for the glycine allele (Mason et al., 1999). In the African American population however the allele frequency of the arginine allele is considerably lower at 58 % (Ahles and Engelhardt, 2014). Several clinical trials have found the Arg389 variant of the ADRB1 to exhibit a weak, but significant correlation with hypertension (Gjesing et al., 2007; Tikhonoff et al., 2008; Johnson et al., 2011). Many clinical trials have either found or not found polymorphism specific differences in susceptibility to different cardiovascular diseases, especially heart failure. However, due to profound differences of this polymorphism in patients from different ethnic backgrounds, it remains unclear whether one variant of the polymorphism actually constitutes an advantage over the other regarding

cardiac health (Ahles and Engelhardt, 2014). What is known so far is that healthy individuals carrying the Arg389 variant show a stronger response to β-agonists and -antagonists (Sofowora et al., 2003; Bruck et al., 2005).

1.3 Phosphorylation of proteins

Phosphorylation is the most common post-translational protein modification in signal transduction (Manning et al., 2002). In eukaryotes three amino acids can be phosphorylated: serine, threonine and tyrosine (Figure 1.6). The ratio of phosphorylated amino acids in a vertebrate cell is 1800:200:1 for pSer:pThr:pTyr (Mann et al., 2002). Tyrosine residues are predominantly phosphorylated in low abundant proteins and this phosphorylations tends to be less stable than serine and threonine phosphorylation (Olsen et al., 2006).

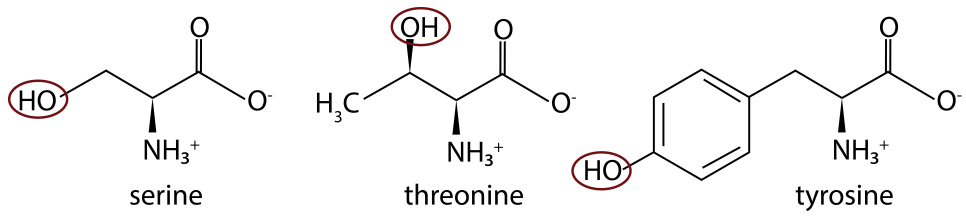

Figure 1.6: **Serine, threonine and tyrosine are commonly phosphorylated in proteins.** These three amino acids all carry a hydroxy group (red circles), which can interact with inorganic phosphate to form a phosphomonoester bond.

Adding or removing a phosphate group often leads to activation of the modified protein. In signal transduction phosphorylation can act as a *molecular switch* and this can hence be seen as *phosphoregulation*. An example for this is the MAP kinase pathway, a network of three classes of kinases which activate each other through phosphorylation (Pearson et al., 2001). However phosphorylation is not just a motif in signal transduction. It is also involved in protein degradation, gene expression and apoptosis (Manning et al., 2002). It is thought that up to 30 % of all proteins are phosphorylated at one or more sites (Ubersax and Ferrell, 2007).

1.3.1 Kinases and phosphatases

Kinases and phosphatases are enzymes which phosphorylate and dephosphorylate proteins. They are highly abundant proteins, which make up about two percent

of the human genome, accounting for about 500 kinases and 100 phosphatases (Venter et al., 2001). Kinases catalyze the formation of a phosphomonoester bond between an inorganic phosphate group and a hydroxy group of the target protein (Figure 1.6 and 1.7). The energy for this reaction comes from the ubiquitous energy carrier adenosine triphosphate, which is transformed into the less energy-rich adenosine diphosphate (ADP).

Eukaryotic kinases can be divided by their specificity into serine/threonine-specific and tyrosine-specific kinases (Hanks and Hunter, 1995). Some kinases are also bispecific, which means they are able to phosphorylate serine and threonine residues as well as tyrosines. Which serine, threonine and tyrosine residues are phosphorylated depends largely on their position within the protein and the amino acids surrounding them. Contrary to what their class name suggests, serine/threonine-specific kinases do not have the same affinity towards phosphorylating serine and threonine residues, respectively. Most serine/threonine-specific kinases preferentially phosphorylate serine residues (Ubersax and Ferrell, 2007).

Some kinases have specific consensus sequences, for example protein kinase A has the following consensus sequence: Arg-Arg-X-Ser/Thr-Φ, with Φ being a small hydrophobic amino acid (Ubersax and Ferrell, 2007) and X being any amino acid except for proline. Incorporation of proline into a protein disrupts the secondary structure of that protein, which destroys the PKA consensus site (Morgan and Rubenstein, 2013).

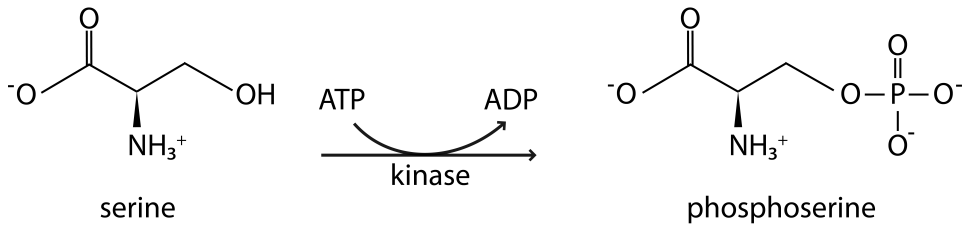

Figure 1.7: **Serine phosphorylation reaction.**
Serine is phosphorylated by a serine/threonine-specific kinase. This kinase catalyzes the formation of a phosphomonoester bond between the hydroxy group of the serine residue and orthophosphate, which is derived from the conversion of ATP to ADP.

Phosphatases are the physiological antagonists of kinases. They remove phosphorylations from proteins through hydrolytic cleavage of the phosphomonoester bond. They do not reverse the kinase reaction i.e. they cannot reconstitute ATP out of ADP. Rather the action of phospatases leads to the release of inorganic phosphate. Analogous to kinases, phosphatases can be grouped into serine/threonine-

specific phosphatases, tyrosine-specific phosphatases and bispecific phosphatases. In contrast to serine/threonine-specific kinases, serine/threonine-specific phosphatases preferentially interact with threonine residues (Ubersax and Ferrell, 2007). Some phosphatases also recognize a consensus sequence (Shi, 2009).

G protein-coupled receptor kinases

G protein-coupled receptor kinases (GRKs) play a central role for GPCR phosphorylation. They belong to the family of serine/threonine-specific kinases and are expressed in seven different isoforms. GRK1 (Benovic et al., 1986; Palczewski et al., 1988) and GRK7 are only expressed in the retina and are involved in phototransduction (Weiss et al., 2001). GRK4 is predominantly expressed in lung, brain and both male and female reproductive organs (human protein atlas: Uhlén et al., 2015). GRK2, 3, 5 and GRK6 are widely expressed and can phosphorylate a plethora of different G protein-coupled receptors. However, in the heart, where the ADRB1 is predominantly found, only three GRK isoforms are expressed (GRK 2, 3 and 5) (Belmonte and Blaxall, 2011). GRK 2 and 3 are located in the cytosol. Once the β-adrenoceptor is activated, GRKs interact with $G_{\beta\gamma}$ and subsequently translocate to the cell membrane (Pitcher et al., 1992). GRK5 is constitutively expressed at the cell membrane and interacts with the membrane via electrostatic interactions of its basic carboxy terminus with the membrane phospholipids (Premont et al., 1994; Kunapuli et al., 1994).

G protein-coupled receptor kinases phosphorylate serine and threonine residues in the third intracellular loop and in in the C-terminus of GPCRs (Reiter and Lefkowitz, 2006). In contrast to protein kinase A there is no well defined consensus sequence for GRKs (Olivares-Reyes et al., 2001; Kim et al., 2005). This makes a bioinformatical prediction of putative GRK phosphorylation sites difficult. In the β_2-adrenoceptor GRK phosphorylation sites are located in the receptor's C-terminus (Drake et al., 2006; Nobles et al., 2011).

1.3.2 Phosphorylation of G protein-coupled receptors

After activation, a GPCR undergoes a conformational change, where the transmembrane domains are shifted relative to each other. This makes the receptor more accessible to different kinases (Palczewski et al., 1991), most often GRKs, protein kinase A and protein kinase C (PKC).

Phosphorylation of G protein-coupled receptors by GRKs only occurs after agonist activation (Benovic et al., 1986). There are two main reasons for this: First

the aforementioned better accessibility after the ligand-induced conformational change which transforms the GPCR into a good substrate for the kinases, and second the activation of GRKs by activated G protein-coupled receptors (Palczewski et al., 1991). When the GPCR is activated, the trimeric G protein dissociates and while the α-subunit diffuses away, the βγ-subunit stays in place, anchored to the membrane. This βγ-subunit can then act as an anchor for several GRKs to bind to, which increases GPCR phosphorylation (Pitcher et al., 1992).

This phosphorylation facilitates interactions with other proteins, for example with the two non-visual arrestins β-arrestin1 and 2 (Gurevich and Gurevich, 2004; Tilley et al., 2009; Shukla et al., 2014). β-arrestin binding can lead to desensitization, internalization (Chapter 1.4.2) and activation of non-canonical signaling pathways (Chapter 1.4.2).

Phosphorylation of the human β_1-adrenoceptor and the β_2-adrenoceptor

So far the phosphorylation pattern of the β_1-adrenoceptor remains largely elusive (Cotecchia et al., 2012). Until now three phosphosites in the human β_1-adrenoceptor are known: Serine 312 is phosphorylated by protein kinase A (Gardner et al., 2004) and serine 412 is phosphorylated by protein kinase B (Gavi et al., 2007). Serine 475 is shown to be phosphorylated as part of the PDZ type I domain (Chapter 1.4.2, Nooh et al., 2014), however the responsible kinase is not known yet. Apart from these sites, no other phosphorylation sites have been identified.

This picture looks very different for the closely related β_2-adrenoceptor. For this receptor the phosphosites have been very well described (Nobles et al., 2011). Apart from PKA and different GRKs the serine/threonine kinases ATM (ataxia teleangiectasia mutated) and ATR (ataxia telangiectasia and rad3-related protein) are involved in receptor phosphorylation. A similar putative ATM/ATR site can also be found on the β_1-adrenoceptor for the serine residue at position 168 in the second intracellular loop. Figure 1.8 depicts the known PKA phosphorylation site and possible other phosphosites in the intracellular loops and on the carboxy terminus.

Unfortunately it is not possible to infer the exact phosphorylation sites of the β_1-adrenoceptor from the already known phosphosites of the β_2-adrenoceptor for two reasons. First the amino acid sequence in the transmembrane domains is fairly conserved between the ADRB1 and the ADRB2. However, when it comes to the intracellular loops and the C-terminus, where phosphorylation takes place, sequence conservation is very poor. The second reason is the lack of consensus sequences for G protein-coupled receptor kinases.

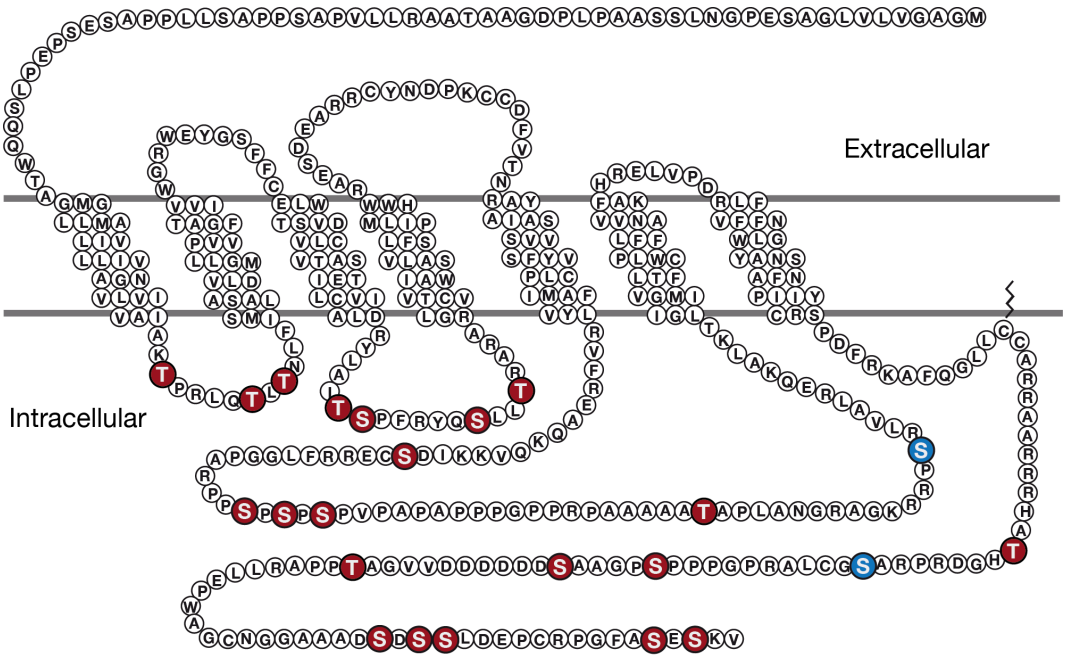

Figure 1.8: **Potential intracellular phosphorylation sites of the β_1-adrenoceptor.** Red: putative phosphorylation sites for G protein-coupled receptor kinases; Blue: Ser312 is a known protein kinase A phosphorylation site and Ser412 is known to be phosphorylated by protein kinase B.

1.4 Phosphorylation-dependent signaling: Recruitment of arrestins

Protein phosphorylation on intracellular serine and threonine residues is described as a prerequisite for arrestin binding (Vishnivetskiy et al., 2007).

Mammals express four different arrestin proteins: Two visual arrestins (arrestin-1 and -4) and two non-visual arrestins (arrestin-2 and -3, also termed β-arrestin1 and β-arrestin2) (Gurevich and Gurevich, 2004). While the visual arrestins are only found in the retina, the non-visual arrestins are found in many different tissues (human protein atlas: Uhlén et al., 2015).

The first function that was discovered for arrestin proteins was the ability to terminate GPCR signaling (Chapter 1.4.2), hence the name arrestin (Premont and Gainetdinov, 2007). Apart from sterically hindering G protein binding, arrestin recruitment also leads to internalization through the clathrin-mediated endocytosis

pathway. Furthermore arrestins can act as scaffolds for proteins of several different signal transduction cascades to bind to (Miller and Lefkowitz, 2001; McDonald, 2000).

1.4.1 Arrestin binding and activation

In order for arrestins to bind to GPCRs generally two prerequisites have to be met: 1) agonist-induced activation of the GPCR and 2) phosphorylation of the GPCR by GRKs (Lohse and Hoffmann, 2014). Arrestin proteins contain two specialized regions to sense whether these prerequisites are met. They have a phosphorylation sensor in the polar core of the protein and an activation sensor, which to date has not been fully understood.

Even though these two requirements apply to all GPCRs, there seems to be no conserved arrestin binding motif that is the the same for all G protein-coupled receptors. While the phosphorylation sites responsible for arrestin binding are most often located in ICL-3 or the receptor's C-terminus, for some receptors they can also be found in ICL-1 (follitropin receptor, Nakamura et al., 1998), or ICL-2 (μ-opioid receptor, Celver et al., 2001). Not only is there no conservation as to the location of the required phosphosites, but there is also no consistency among the different GPCRs regarding the number of phosphorylation sites needed for arrestin binding. For the P2Y1 receptor two phophosites facilitate arrestin binding (Reiner et al., 2009; Qi et al., 2011). While a cluster of four phosphorylation sites in the proximal C-terminus of the β_2-adrenoceptor is sufficient to induce arrestin binding (Krasel et al., 2008), an engineered hyperphosphorylation of this receptor leads to an even stronger recruitment of arrestin proteins (Zindel et al., 2015). These differences clearly show that there must be an individual arrestin binding motif for each GPCR separately.

Arrestin binding to a GPCR uncouples the receptor from its respective G protein, which leads to GPCR desensitization (Chapter 1.4.2). It furthermore results in the stabilization of the GPCR in a state of high agonist affinity (De Lean et al., 1980; Lohse et al., 1984) and it also induces a conformational change within the arrestin protein itself. This conformational change is believed to be the basis of the arrestin's ability to impact GPCR downstream signal transduction (Chapter 1.4.2).

β-arrestin-dependent G protein-coupled receptor classification

While it is generally thought that all GPCRs can bind β-arrestins, there seems to be a great deal of variability concerning the individual β-arrestin binding sites, which

have to be analyzed for each GPCR independently (Chapter 1.4.1). However, there are two distinct patterns of arrestin binding, that many GPCRs exhibit. According to Oakley et al., 2000, GPCRs can be categorized with regard to their interactions with arrestins as Class A and B receptors. This classification is not to be confused with the general GPCR classification of classes A-E (Chapter 1.2). In this definition class A receptors, for example the β_2-adrenoceptor bind β-arrestin2 with higher affinity than β-arrestin1 and do not interact with visual arrestins. Their interaction with β-arrestin2 is transient and they undergo a rapid recycling back to the membrane.

In contrast to that class B receptors like the angiotensin II type 1A receptor show a similar affinity for both β-arrestin1 and 2 and also bind to visual arrestins. Their binding is stronger, which causes them to internalize together with the bound arrestin and therefore they are only slowly recycled back to the membrane (Oakley et al., 2000). So far it is not definitely known whether the β_1-adrenoceptor belongs to the class A or class B receptors. However, there is recent evidence that the binding of β-arrestin1 and β-arrestin2 to the β_1-adrenoceptor depends on which variant of the p.Arg389Gly polymorphism (Chapter 1.2.4) the ADRB1 carries (Ahles et al., 2015; McCrink et al., 2016).

1.4.2 Functional implications of arrestin recruitment

Arrestin binding to G protein-coupled receptors leads to desensitization (Chapter 1.4.2) of the GPCR, to receptor internalization (Chapter 1.4.2) and to non-canonical signal transduction (Chapter 1.4.2).

Desensitization

Repetitive stimulation of GPCRs leads to a decrease in receptor response. This means that the same amount of catecholamines will result in a lower amount of produced cAMP as compared to a receptor that is stimulated for the first time. This depicts a negative feedback mechanism to protect the cell from overstimulation (Ferguson, 2001). In case of rhodopsin it is also the basis for the adaptation to different levels of light intensity (Arshavsky, 2002; Ridge et al., 2003).

The molecular basis for this desensitization of a GPCR is receptor phosphorylation by GRKs (Bouvier et al., 1988) (Figure 1.9 [2]) and subsequent binding of arrestins (Lohse et al., 1990) (Figure 1.9 [3]). These proteins physically uncouple the receptor from its G protein and cause the cessation of cAMP production. Since this process is strongly agonist-dependent, it is also termed *homologous desensitization* (Lohse et al., 1990) to distinguish it from the agonist-independent

heterologous desensitization, which is found after phosphorylation by kinases other than GRKs such as PKA or PKC. In contrast to homologous desensitization the latter process is more generalized and also switches off unactivated receptors.

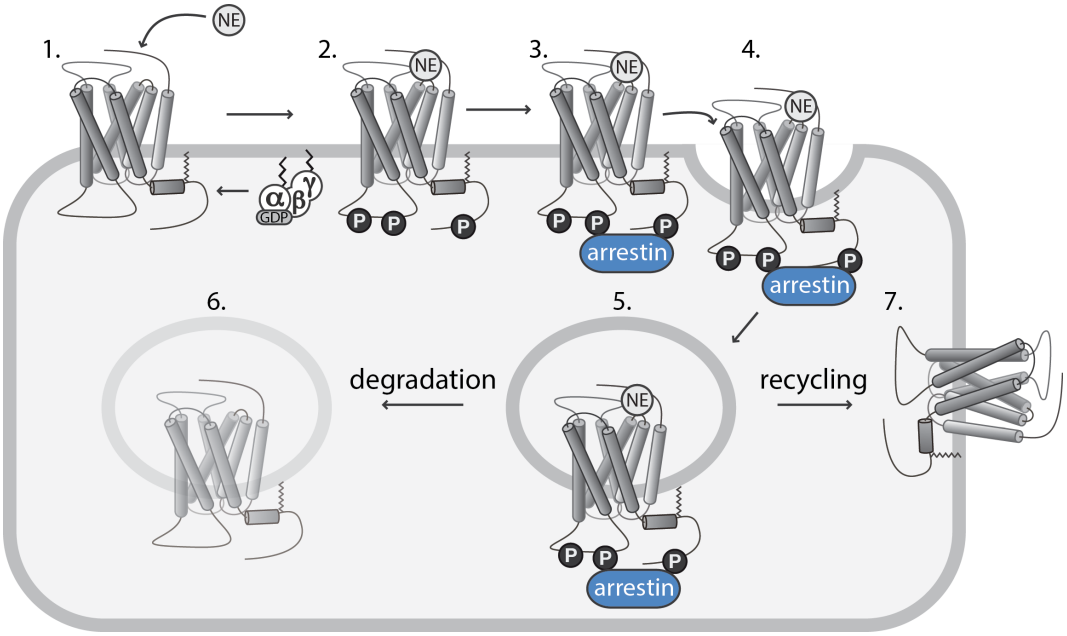

Figure 1.9: **Desensitization and internalization of a G protein-coupled receptor using the example of the β_1-adrenoceptor.**
After activation (**1**) the receptor recruits a trimeric G protein and the canonical signaling starts (Figure 1.10). (**2**) The GPCR is then phosphorylated by different kinases for example G protein-coupled receptor kinases and protein kinase A. (**3**) This leads to the attraction of *docking proteins* such as β-arrestins. Binding of arrestins results in *desensitization* of the receptor which means that the GPCR stops canonical signal transduction. (**4** and **5**) Arrestin recruitment also leads to endocytosis or internalization of the receptor. The receptor is then either degraded (**6**) or recycled (**7**) and brought back to the plasma membrane.

Internalization

The second process responsible for a decrease in cAMP production after repetitive agonist stimulation is internalization. Arrestin recruitment leads to endocytosis of the GPCR via caveolae and clathrin-coated pits (Figure 1.9 [4]). β-arrestins interact directly with clathrin or with the clathrin adapter protein AP2 (Goodman et al., 1996; Goodman et al., 1997; Oakley et al., 1999; Laporte et al., 2002). The receptor can

then be either degraded through the endosome lysosome system (Figure 1.9 [6]) or recycled and brought back to the membrane (Figure 1.9 [7]).

Internalization of the β_1-adrenoceptor however, is still a highly discussed subject. Its internalization has been shown to depend on the different kinases, which phoshorylate the receptor. This phosphorylation then leads to clathrin-mediated endocytosis as described above and to internalization via invaginations of the plasma membrane, called caveolae (Rapacciuolo et al., 2003). Other authors have found the ADRB1 not to internalize at all (Eichel et al., 2016), to exhibit an endophilin-dependent internalization (Boucrot et al., 2015) or to internalize depending on the receptor's PDZ type I domain (Figure 1.3 [red]). This is a protein-protein interaction domain at the far distal C-terminus which impacts internalization for many GPCRs, as shown for the β_2-adrenoceptor (Cao et al., 1999). PDZ is an acronym for post synaptic density protein 95, Drosophila disc large tumor suppressor and zonula occludens-1 protein. These were the first three proteins which were found to contain this conserved domain (Kennedy, 1995). This domain is made up of the following sequence: X-(S/T)-X-Ø, with X at positions -1 and -3 as any amino acid, serine or threonine at position -2 and a bulky hydrophobic amino acid (Ø) at position 0 (Sheng and Sala, 2001).

Many different downstream proteins interact with the PDZ type I domain. For the β_1-adrenoceptor there is evidence, that SAP97 (synapse-associated protein 97) is of great importance for receptor internalization and receptor recycling (Gardner et al., 2007). It was reported by the same group, that phosphorylation of serine 312 by protein kinase A acts in concert with the PDZ type I domain regarding the internalization of the ADRB1 (Gardner et al., 2004).

Signal transduction via arrestins

Other effects of β-arrestin binding include GPCR ubiquitination (Shenoy and Lefkowitz, 2003) and the triggering of an alternative signaling pathway where β-arrestin itself acts as a signal transducer (Luttrell and Gesty-Palmer, 2010).

Apart from canonical signal transduction via G proteins (Chapter 1.2.1) recent data suggests that GPCRs can also signal alternatively via β-arrestins (Figure 1.10; Shenoy et al., 2006; Shukla et al., 2014). The idea is that β-arrestins also undergo a conformational change after binding to GPCRs. This involves the rotation of the two domains relative to each other (Gurevich and Gurevich, 2006), which is thought to uncover binding sites for various other proteins. Thus β-arrestins act as adaptor proteins and can form scaffolds, to which other proteins can bind to (Rockman et al., 2002). So far this signal transduction pathway is not fully understood, but signaling

via MAP kinase 1/3 (MAPK1/3), PKB, c-src (proto-oncogene tyrosine-protein kinse src) and JNK (c-Jun N-terminal kinase) is proposed (Irannejad et al., 2013; Smith and Rajagopal, 2016). One possible pathway leads to an activation of the MAP kinase pathway involving MAPK1/3 through an EGFR (epidermal growth factor receptor) transactivaton (Noma et al., 2007). This process seems to be G protein-independent. However, it is very likely that other ways of activating MAPK1/3 in a G_s protein-independent fashion exist, such as $G_{\beta\gamma}$-dependent MAPK1/3 activation (Hawes et al., 1995).

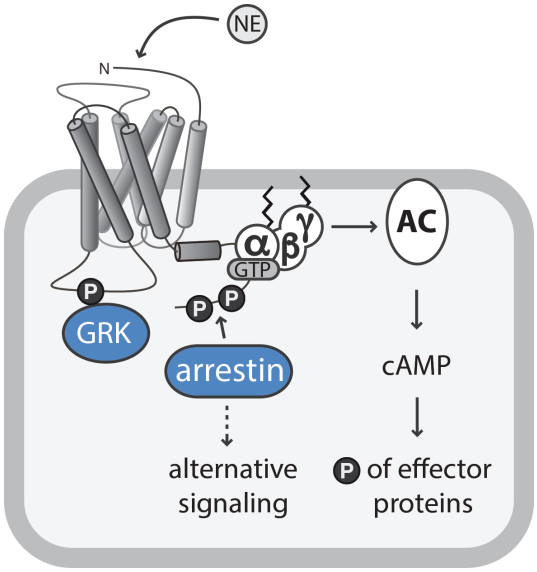

Figure 1.10: **Schematic overview of GPCR signaling**
GPCRc can signal via the non-canonical (**left hand side**) and the canonical (**right hand side**) pathway. cAMP = cyclic adenosine monophosphate, GRK = G protein-coupled receptor kinase, GTP = guanosine triphosphate, NE = norepinephrine, P = inorganic phosphate and phosphorylation, respectively.

This alternative signal transduction is also known as *biased agonism* or *functional selectivity* (Kenakin, 2007). This is the case when an agonist only activates one signaling pathway, either the G protein-coupled pathway or the alternative signaling pathway. If the GPCR couples to more than one G protein e.g. the β_2-adrenoceptor, which is able to couple to G_s and G_i (Daaka et al., 1997), biased agonism can also refer to an agonist, that only activates one of these pathways.

A very well characterized biased agonist is carvedilol (Wisler et al., 2007), which is reported to be an inverse agonist concerning G protein signaling, but a weak

agonist when signaling via β-arrestins. The receptor‘s phosphorylation is a key factor for this alternative signaling (Lefkowitz and Shenoy, 2005; Premont and Gainetdinov, 2007).

1.4.3 Fluorescence resonance energy transfer-based real time measurement of arrestin recruitment

Fluorescence resonance energy transfer (FRET) is a technique to study inter- and intra-molecular interactions. It is based on different variants of the green fluorescent protein (GFP). The basis for this technique are two fluorophores with overlapping excitation and emission spectra, respectively. If the excitation spectrum of the second fluorophore is within the emission spectrum of the first fluorophore and both fluorophores are in close proximity, energy can be transferred from one fluorophore to the other, without losses. This technique can be used to determine whether two molecules are close to each other. This is referred to as *inter*molecular FRET (Figure 1.11 [A]).

Apart from intermolecular FRET, also *intra*molecular FRET can be performed. In this method the two fluorophores are inserted into one protein and the energy transfer occurs upon conformational changes within the protein. This technique can therefore be used to detect GPCR activation. For this, a fluorophore is inserted into the third intracellular loop the the GPCR and the second one is fused to the receptor's C-terminus (Lohse et al., 2008).

Intermolecular FRET can thus be used to study β-arrestin recruitment to GPCRs. Both the β-arrestin and the GPCR are tagged with a variant of GFP (Vilardaga et al., 2003; Krasel et al., 2005; Krasel et al., 2008). A prominent FRET pair is the combination of yellow fluorescent protein (YFP) and cyan fluorescent protein (CFP), or variants of these proteins, such as Cerulean (Cer), a brighter variant of CFP. CFP can be excited at 430 nm and emits light at 480 nm. This is within the excitation spectrum of YFP, which then emits light at 535 nm (Hou et al., 2011). When YFP-tagged arrestin binds to a GPCR that is fused to CFP, light emission at 535 nm (from YFP) increases, while the emission from CFP at 480 nm decreases (Figure 1.11). The FRET ratio is the ratio of YFP emission divided by CFP emission. Here it can be seen as a parameter for arrestin binding. When YFP-tagged arrestin is bound to a G protein-coupled receptor the FRET ratio increases and when it diffuses away the FRET ratio decreases.

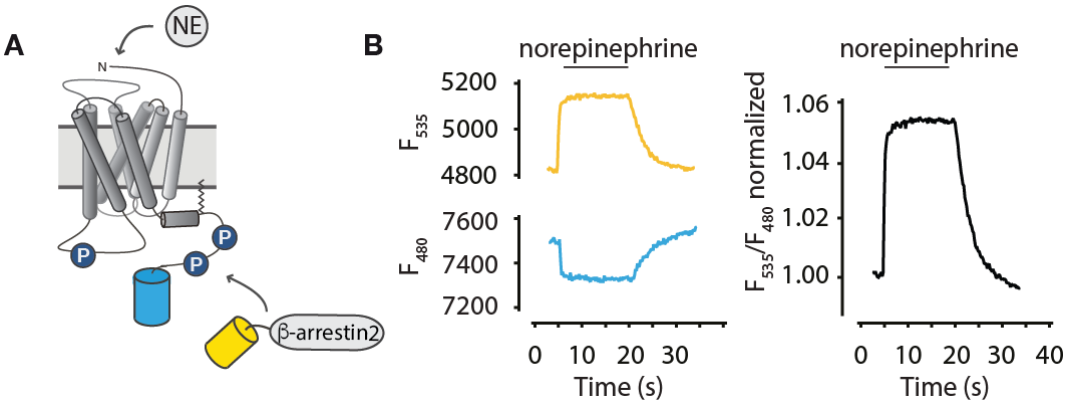

Figure 1.11: **Overview of fluorescence resonance energy transfer experiments.** (**A**) β-arrestin fluorescence resonance energy transfer (FRET) experiments. ADRB1 variants are fused to Cerulean and β-arrestin2 is tagged with a yellow fluorescent protein (YFP). After receptor activation with norepinephrine (NE), the ADRB1 is phosphorylated, which leads to β-arrestin2 binding. (**B**) Representative FRET tracings. After arrestin binding, the two fluorophores are in close proximity, which induces FRET, leading to an increase in emission at 535 nm (yellow tracing), a decrease in emission at 480 nm (blue tracing) and an overall increase in FRET ratio (black tracing). This change in the FRET ratio can be used as a parameter for β-arrestin2 recruitment to the ADRB1.

1.5 Analysis of phosphorylation

There are several ways to detect protein phosphorylation. Among them the most prominent ones are radioactive phosphorylation assays, site-directed mutagenesis, biochemical assays with phosphosite specific antibodies and mass spectrometry. One of the biggest problems, when trying to assess the phosphorylation status of a given protein is that usually only a small part of all proteins that potentially could be phosphorylated is actually phosphorylated (Cantin et al., 2007). Furthermore membrane proteins, like the β_1-adrenoceptor are even in an overexpression system only expressed in very low amounts. This means that a method with a high sensitivity is needed.

1.5.1 Phosphosite deletion and phosphomimicking

To analyze the impact of single phosphorylation sites the serine or threonine residue can be exchanged for either alanine, glutamate or aspartate. The conversion of a

serine/threonine residue to an alanine resembles the unphosphorylated state of this residue (Bemben et al., 2014), since alanine, which has no side chain, cannot be phosphorylated (Figure 1.12). This is termed phosphosite deletion.

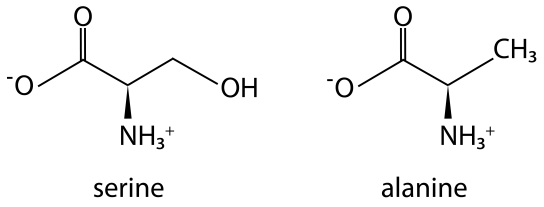

Figure 1.12: **Phosphosite deletion.**
Alanine is substituted to resemble the unphosphorylated state of a serine residue

The opposite of the deletion of a certain phosphosite is phosphomimicking (Blundell et al., 2009). Here, the serine/threonine residue in question is exchanged for either glutamate or aspartate (Figure 1.13). The side chains of these two amino acids very closely resemble the phosphorylated state of the serine/threonine residue. These techniques allow for a thorough investigation of different phosphorylation sites.

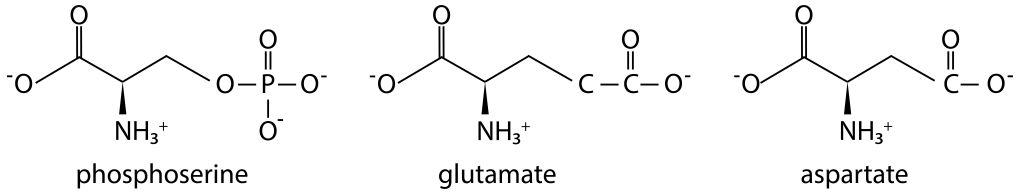

Figure 1.13: **Phosphomimicking.**
Serine is substituted for glutamate or aspartate to resemble the phosphorylated state of the serine residue

1.5.2 Mass spectrometry to assess protein phosphorylation

Mass spectrometry (MS) provides the high sensitivity needed to analyze phosphorylated membrane proteins and it can also be used in a high-throughput format.

There are two different approaches in proteomics: *top down* proteomics, where the protein is analyzed as a whole and *bottom up* proteomics, where proteins are digested into peptides and the identified peptides are allocated to certain proteins. The latter is the more common approach.

A typical workflow of a *bottom up* MS experiment contains four steps. The first step is the digestion of the protein (Chapter 1.5.2), followed by different methods to reduce sample complexity, such as an enrichment of phosphopeptides (Chapter 1.5.2) or other post-translational modifications (PTMs), two dimensional gel electrophoresis or chromatographic techniques such as ion exchange chromatography. The sample preparation should consist of two or more different dimensions, i.e. a combination of at least two of these methods in order to reduce sample complexity and thus to produce high quality MS data. The complexity reduction is a crucial step, because mass spectrometers can usually only detect proteins which differ no more that four orders of magnitude in abundance (Schiess et al., 2009). However, typical samples such as blood can differ up to ten orders of magnitude when it comes to protein abundance. A comparison of a very highly abundant protein such as albumin with low abundant proteins, such as cytokines is therefore very difficult. Or in other words, a highly abundant protein may mask the signal of the protein of interest, if it has a low abundance and no adequate complexity reduction was performed.

Nowadays most mass spectrometers are coupled to a liquid chromatography (LC) machine, which means that it is often enough to only perform one additional purification step, as the LC itself already represents one of the two needed dimensions in sample preparation. The third step then is the mass spectrometry itself and the last step is the analysis of the data.

Protein purification

Integral membrane proteins such as the β_1-adrenoceptor are usually expressed in very low amounts. In order to further analyze a protein, one of the first steps is a purification and concentration of the protein. Since these proteins are a part of the membrane, they first have to be solubilized. Solubilization is the excavation of a membrane protein from the phospholipid bilayer into solution. This means that the phospholipids that used to surround the protein in the membrane have to be replaced by detergents. These detergents bind to the hydrophobic parts of a transmembrane protein and inhibit its aggregation.

Immunoprecipitation (IP) is a simple way to purify proteins. It can either be used alone or as the first step in the purification process. This method uses the specificity of the interaction between an antibody and its antigen to purify the desired protein. Usually the antibody is bound to a substrate, often in form of beads (Kaboord and Perr, 2008). They can be made out of agarose, resin or metal. When the antibody-covered beads are mixed with a cell lysate, the antibodies bind to the antigens

(Figure 1.14). The next step is dependent on the kind of beads that have been used. Metal beads can easily be separated from the cell lysate using a magnet. Agarose or resin beads are usually centrifuged and then found at the bottom of the reaction tube, while the cell lysate remains in the supernatant. By washing the beads several times, the remaining proteins from the cell lysate are eliminated.

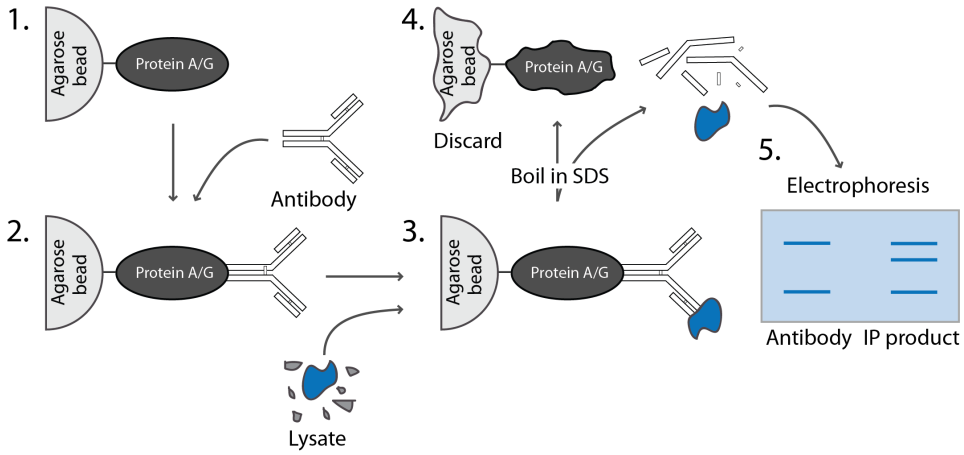

Figure 1.14: **Schematic overview of immunoprecipitation with agarose beads.**
(**1**) Agarose beads are covered with protein A and protein G. (**2**) Antibodies bind through their F_c part to protein A and G, respectively. (**3**) When antibody-covered beads and cell lysate are mixed, the antibodies bind to their antigen. The remainder of the cell lysate is eliminated by multiple washing steps, which include centrifuging of the sample and buffer replacement. (**4**) The antibody-antigen-bead-complex is boiled in a SDS-based buffer. This leads to the dissociation of the antibody from the antigen. As a side effect both the antibody and protein A and protein G denaturate. **(5**) As result of the denaturation of the antibody, an immunoblot shows the desired protein as well as the heavy and the light chain of the antibody.
SDS = sodium dodecyl sulfate

The next step is to sever the bond between the antibody and the antigen. This is often done by adding a strong detergent, such as sodium dodecyl sulfate (SDS) and heating the immunoprecipitation products to a temperature above 90 °C. Another way is to lower the pH to approximately 2, which also weakens the antibody-antigen interaction. The immunoprecipitation products can then be visualized using gel electrophoresis and Coomassie Brilliant Blue staining or western blot.

A problem with the traditional immunoprecipitation method is that the antibody is always part of the IP product. This can perturb further analyses, for example if the desired protein runs at the same height on an SDS gel as the heavy or the light chain of an antibody. In this case detection with Coomassie Brilliant Blue or by western blot is very difficult. One way to eliminate the antibody from the IP product is to covalently bind the antibody to the substrate material. There are two ways to do this. First the antibody can bind to the beads via protein A and protein G, respectively, as in the traditional IP method. Then a crosslinker can be used to covalently crosslink the antibody to the beads. The second alternative is to bind the antibody directly and covalently to the beads without using protein A or protein G (Kaboord and Perr, 2008).

Figure 1.15 depicts the traditional and the crosslinked IP method. In both methods the bond between the antigen and the antibody has to be disturbed in such a way that the antibody itself is not denatured. This means that using SDS and heat does not work for this approach. A common way to elute the antigen from the antibody covered beads is by using a low pH.

Digestion of the protein

In *top down* proteomics, a protein needs to be digested by proteases before it can be analyzed via mass spectrometry. For this the protein needs to be in a denatured state, so that the protease has access to all parts of the protein. When a protein is still folded a protease might only be able to cleave the outer parts of this protein, leaving the inner core intact. Therefore proteins are denatured before digestion.

A common denaturating agent is urea. However urea cannot reduce covalent disulfide bonds, which occur in many proteins between two cysteine residues stabilizing the protein fold or linking different protein domains together. For this dithiothreitol (DTT) is used. After reduction of the disulfide bonds with DTT, the cysteines are exposed and could potentially again form new disulfide bonds. In order to prevent this, free cysteines are alkylated with 2-iodoacetamide (IAA). After alkylation, no new disulfide bonds can form. However, this represents a modification of cysteine residues which must be taken into consideration in the analysis later on, because this alkylation changes the mass of all peptides which contain a cysteine residue.

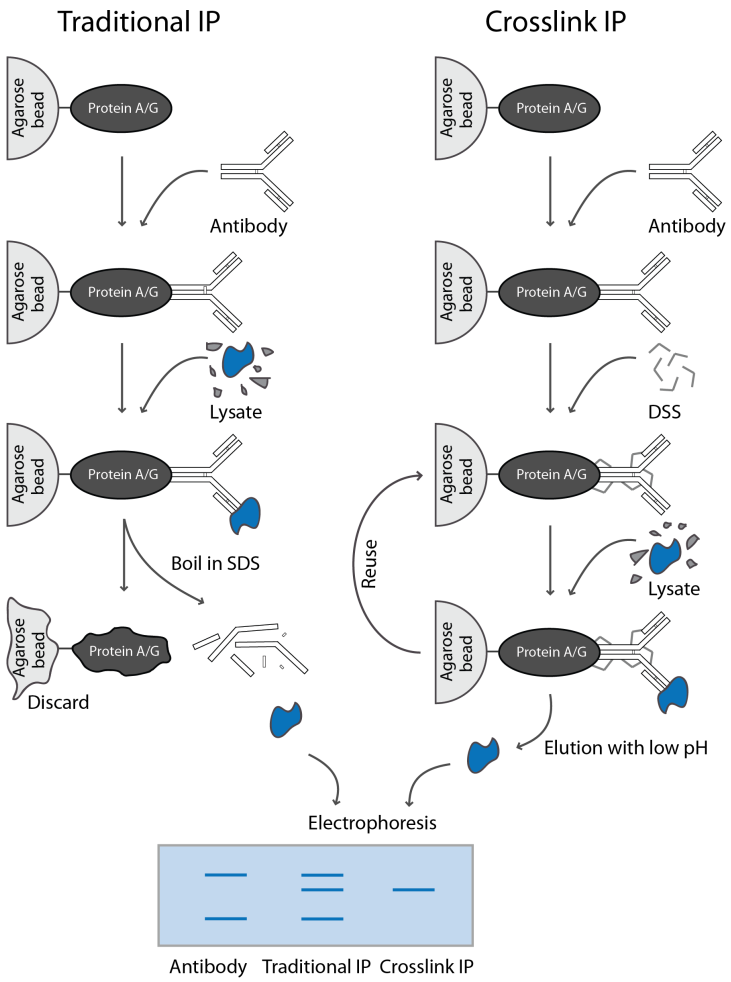

Figure 1.15: **Traditional and crosslink immunoprecipication.**
Comparison of the traditional immunoprecipitation (**left hand side**) and the crosslink immunoprecipitation (**right hand side**). Through covalent linking of the antibody to Protein A/G with the crosslinker disuccinimidyl suberate (DSS) the antibody does not co-elute together with the desired antigen. Figure adapted from Pierce company website.

There are several proteases that can be used for protein digestion. The most common protease used in proteomics is trypsin (Hustoft et al., 2010). It hydrolyzes the peptide bond on the carboxy terminal side of lysine and arginine residues, except if a proline residue is directly located after the lysine or arginine residue. This has the advantage, that every peptide contains a basic amino acid residue at its C-terminus. At pH < 3 these residues are positively charged. This means that each tryptic peptide will have at least two positive charges. One on the N-terminal side and the other on the C-terminal side at either lysine or arginine. This double charge is especially important for MS/MS measurements (Chapter 1.5.2), because it means that all fragment ions are still positively charged and can therefore be measured.

Apart from trypsin, other proteases can also be used, for example chymotrypsin, V8 protease, papain, LysC and GluC. For this work the proteases trypsin, LysC and chymotrypsin were used.

Phosphopeptide enrichment

Usually only a small portion of the proteins in a cell is phosphorylated. The phosphorylated species is in an equilibrium with its unphosphorylated counterpart, with the majority of the proteins being unphosphorylated (Steen et al., 2006). This can be enhanced by agonist stimulation. In case of the β_1-adrenoceptor stimulation with epinephrine or norepinephrine leads to an increase in phosphorylation of the β_1-adrenoceptor. However, even after β-adrenergic stimulation the rate of phosphorylation is considerably low. In order to analyze the phosphorylated protein, it is crucial to increase the abundance of the phosphorylated species. This can be done with phosphopeptide enrichment.

Most enrichment techniques take advantage of two main properties that distinguish phosphorylated peptides from their unphosphorylated counterparts: First the negative charge of phosphorylated peptides and second their steric structure (Eyrich et al., 2011). There are many different methods to augment the concentration of phosphorylated peptides. Common techniques are either chromatography-based, such as *strong cation* and *strong anion exchange* (SCX/SAX) or affinity-based such as *immobilized metal ion affinity chromatography* (IMAC) and *metal oxide affinity chromatography* (MOAC). For this work IMAC, MOAC and SCX were used to increase the abundance of the phosphorylated ADRB1 peptides.

Immobilized metal ion affinity chromatography. Immobilized metal ion affinity chromatography exploits the negative charge of the phosphogroup. Different resins

serve as a matrix to which positively charged metal ions can be bound (Porath et al., 1975). This technique is hence based on chelate bonds between the phosphate group of a phosphorylated peptide and metal ions. Common metal chelators like iminodiacetic acid or nitriloacetic acid (Eyrich et al., 2011) are used to immobilize Fe^{3+} (Andersson and Porath, 1986), Al^{3+} (Andersson, 1991) and Ga^{3+} (Posewitz and Tempst, 1999), respectively. The phosphopeptides bound to the metal ions can later be eluted using basic or acidic buffers.

Metal oxide affinity chromatography. Metal oxide affinity chromatography is very similar to IMAC, except that for MOAC the matrix itself is made from metal ions and thus no resins are needed. Several different metals can be used for this, but the by far most common technique is titanium dioxide-based MOAC. Metal oxide affinity chromatography is more robust, selective and sensitive as compared to IMAC. Depending on which metal ions are used, it is possible to preferentially capture mono- or multiphosphorylated peptides. Another advantage of TiO_2-MOAC is that it can be used in a high-throughput online TiO_2 enrichment format. This means that the phosphopeptide enrichment is directly coupled to the mass spectrometer (Fílla et al., 2012).

Sequential elution from IMAC. Sequental elution from IMAC (SIMAC) is a combination of IMAC and MOAC (Thingholm et al., 2007). It combines the advantages of both techniques and results in a greater retrieval of phosphopeptides as compared to each method alone.

Mass spectrometry

For phosphoproteomics usually tandem mass spectrometry is employed. Once the peptides are identified in the first MS scan, the mass spectrometer picks the most abundant peaks (often ten) and these peaks undergo a fragmentation and a second MS scan, the MS/MS scan. During this fragmentation a phosphorylated peptide often loses its phosphogroup through a β-elimination reaction. This results in a neutral loss of either 80 Da (HPO_3) or 98 Da (H_3PO_4) (Mann et al., 2002). This can be taken advantage of by scanning for these neutral losses.

Stable isotope labeling by amino acids in cell culture (SILAC)

SILAC is a method to quantify protein abundance in mass spectrometry using stable heavy isotopes (Ong et al., 2002). One population of cells is cultured in

normal medium, while a second population is cultured in *heavy* medium, where one or two amino acids are labeled with stable heavy isotopes (Figure 1.16).

Different elements can be used for labeling. For example ^{2}H instead of ^{1}H or ^{13}C instead of ^{12}C. After cultivation the cells are mixed and treated together. In a subsequent mass spectrometric analysis the peak from a labeled peptide is several dalton heavier, than the peak originating from the unlabeled peptide. If a peptide contains labeled arginine, usually six ^{12}C are replaced by ^{13}C. This makes a labeled peptide six dalton heavier as compared to the unlabeled peptide. Labeling arginine and lysine is very common, because usually proteins are digested with trypsin before mass spectrometric analysis. Since trypsin digests after arginine and lysine, every tryptic peptide should contain exactly one amino acid which is labeled.

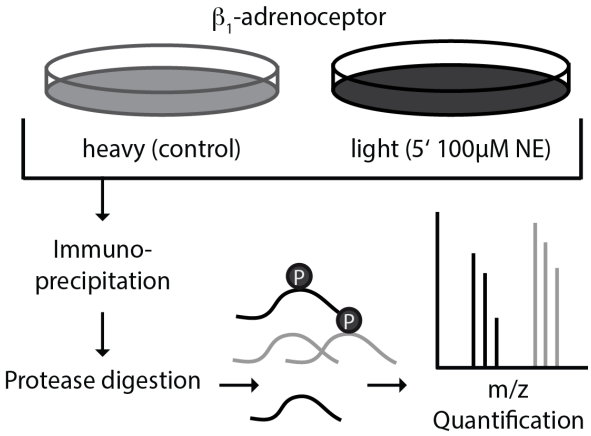

Figure 1.16: **Schematic overview of stable isotope labeling by amino acids in cell culture.** Stably transfected HEK293 cells are either unlabeled (dark grey) or labeled with stable heavy isotopes (light grey). The heavy cells are used as control, while the unlabeled cells are being stimulated. The cells are then lysed and mixed in equal amounts. The lysate mixture is then immunoprecipitated and the immunoprecipitation product is protease-digested, phosphopeptide-enriched and then measured and quantified via mass spectrometry.

The big strength of this method is that the two lysates are mixed early on and the sample losses during sample preparation are equal. On the other hand the drawback is that labeling is needed, which means, that this method cannot be used for human samples.

1.5.3 Radioactive phosphorylation assays

Another method to investigate phosphoproteins is to use radioactive phosphorous. Phosphorous has multiple isotopes, ranging from ^{24}P to ^{46}P (Audi et al., 2003). Only ^{31}P is stable, which is why almost all natural occuring phosphorous is ^{31}P. However there are two radioactive isotopes that can be used for biological research: ^{32}P and ^{33}P. Both of these isotopes are β-emitters.

When cells are cultured in phosphorous-free medium and then exposed to radioactive phosphorous as the only source of phosphorous, they incorporate the radioactive isotopes into their DNA and into phosphoproteins. This incorporation can be visualized using a phosphoimaging system.

1.6 Goal of this thesis

The goal of this work was to decipher the phosphorylation pattern of the β_1-adrenoceptor on a molecular level. By using mass spectrometry, mutagenesis studies and radioactive phosphorylation assays the exact phosphorylation sites of the ADRB1 were identified *in vitro*. Furthermore we aimed to elucidate the function of these newly identified phosphorylation sites.

2 Materials and Methods

2.1 Materials

2.1.1 Chemicals

Unless stated otherwise all chemicals and reagents were purchased in pro analysi quality from the following companies: AppliChem (Darmstadt), Carl Roth (Karlsruhe), Life Technologies (Karlsruhe), Merck (Darmstadt), New England Biolabs (Frankfurt am Main), Qiagen (Hilden), Roche (Mannheim), Sigma-Aldrich (Taufkirchen) and Thermo Fisher Scientific (Waltham).

2.1.2 Plasmids

The following plasmids were used for this work:

Vector	Insert	Source
pDONR221		Life Technologies (Karlsruhe)
pENTR1A		Life Technologies (Karlsruhe)
pT-Rex-DEST30		Life Technologies (Karlsruhe)
$pcDNA_3$	ADRB1	IPT (Munich)
pT-Rex-DEST30	YFP-ARRB2	IPT (Munich)

The sequences depicted in the following table were inserted into the expression vector pT-Rex-DEST30 using the Gateway system (Life Technologies, Karlsruhe). Therefore they exist both in the pDONR221, as well as in the pT-Rex-DEST30 vector. Furthermore all vectors exist both in the Gly389 variant, as well as in the Arg389 variant of the p.Arg389Gly polymorphism (Chapter 1.2.4). For simplicity reasons, the ADRB1 plasmids are listed without the variants.

Insert	Variation description
ADRB1	β_1-adrenoceptor
ADRB1Δphos	completely phosphodeficient ADRB1
ADRB1Δ3rdloop^{a}	S260A
ADRB1Δ3rdloop^{b}	S274A, S276A, 278A, T298A, S312A
ADRB1Δproximal	T404A, S412A, S423A
ADRB1Δmiddle	S428A, T439A
ADRB1Δdistal	S459A, S461A, S462A, S473A, S475A
ADRB1(Ala459/461/462)	S459A, S461A, S462A
ADRB1(Ala461/462)	S461A, S462A
ADRB1(Ala473/475)	S473A, S475A
ADRB1-Cer	Cerulean fused to C-terminus
ADRB1Δphos-Cer	ADRB1Δphos with Cerulean
ADRB1Δ3rdloop^{a}-Cer	ADRB1Δ3rdloop^{a} with Cerulean
ADRB1Δ3rdloop^{b}-Cer	ADRB1Δ3rdloop^{b} with Cerulean
ADRB1Δproximal-Cer	ADRB1Δproximal with Cerulean
ADRB1Δmiddle-Cer	ADRB1Δmiddle with Cerulean
ADRB1Δdistal-Cer	ADRB1Δdistal with Cerulean
ADRB1(Ala459/461/462)-Cer	ADRB1(Ala459/461/462) with Cerulean
ADRB1(Ala461/462)-Cer	ADRB1(Ala461/462) with Cerulean
ADRB1(Ala473/475)-Cer	ADRB1(Ala473/475) with Cerulean
HA-ADRB1	ADRB1 with N-terminal HA tag
ADRB1-HA	ADRB1 with C-terminal HA tag

2.1.3 Gene synthesis

The nucleotide sequence of the completely phosphodeficient ADRB1 (Δphos) mutant was synthesized by GeneArt (Regensburg). This plasmid served as the foundation for the generation of all partially phosphodeficient ADRB1 mutants.

Plasmid	Insert
12ABVKNP_ADRB1_pMK-RQ	ADRB1 (699-1435 Ser/Thr mutated to Ala)

ADRB1 sequence synthesized by GeneArt
5'- C **TAC GTG** CCC CTG TGC ATC ATG GCC TTC GTG TAC CTG CGG GTG TTC CGC GAG GCC CAG AAG CAG GTG AAG AAG ATC GAC GCA TGC GAG CGC CGT TTC CTC GGC GGC CCA GCG CGG CCG CCC GCA CCC GCA CCC GCA CCC GTC CCC GCG CCC GCG CCG CCG CCC GGA CCC CCG CGC CCC GCC GCC GCC GCC GCC GCA GCC CCG CTG GCC AAC GGG CGT GCG GGT AAG CGG CGG CCC GCA CGC CTC GTG GCC CTA CGC GAG CAG AAG GCG CTC AAG ACG CTG GGC ATC ATC ATG GGC GTC TTC ACG CTC TGC TGG CTG CCC TTC TTC CTG GCC AAC GTG GTG AAG GCC TTC CAC CGC GAG CTG GTG CCC GAC CGC CTC TTC GTC TTC TTC AAC TGG CTG GGC TAC GCC AAC TCG GCC TTC AAC CCC ATC ATC TAC TGC CGC AGC CCC GAC TTC CGC AAG GCC TTC CAG GGA CTG CTC TGC TGC GCG CGC AGG GCT GCC CGC CGG CGC CAC GCG GCA CAC GGA GAC CGG CCG CGC GCC GCA GGC TGT CTG GCC CGG CCC GGA CCC CCG CCA GCA CCC GGG GCC GCC GCA GAC GAC GAC GAC GAC GAT GTC GTC GGG GCC GCA CCG CCC GCG CGC CTG CTG GAG CCC TGG GCC GGC TGC AAC GGC GGG GCG GCG GCG GAC GCA GAC GCA GCA CTG GAC GAG CCG TGC CGC CCC GGC TTC GCC GCA GAA GCA AAG GTG TAG ACC CAG CTT TCT TGT ACA AAG TGG TTG ATG GGC GGC CGC **TCT AGA** G - 3'

Marked in bold are the restriction enzyme sites, that were used to cut the part of the β_1-adrenoceptor out of the GeneArt vector and insert it into the pDONR.

2.1.4 Enzymes

Enzyme	**Company**
AccuPrime *Pfx* DNA Polymerase	Life Technologies (Karlsruhe)
Antarctic Phosphatase	Life Technologies (Karlsruhe)
Benzonase	Merck (Darmstadt) Sigma-Aldrich (Taufkirchen)
Gateway BP Clonase II enzyme mix	Life Technologies (Karlsruhe)
Gateway LR Clonase II enzyme mix	Life Technologies (Karlsruhe)
Restriction endonucleases	New England Biolabs (Frankfurt am Main)
T4 DNA Ligase	New England Biolabs (Frankfurt am Main)

2.1.5 Bacteria

Strain	Genotype	Source
E. coli DH10B	F– mcrA Δ(mrr-hsdRMS-mcrBC) Φ80lacZΔM15 ΔlacX74 recA1 endA1 araD139 δ(ara leu) 7697 galU galK rpsL nupG λ–	Life Technologies (Karlsruhe)

2.1.6 Eurkaryotic cell lines

Name	Description	Source
HEK293 cells	Human embryonic kidney cells	Life Technologies (Karlsruhe)

Stable cell lines were created based on the HEK293 cells. All mutants were created in both variants of the p.Arg389Gly polymorphism.

Name	Description
HEK293-ADRB1	ADRB1
HEK293-ADRB1Δphos	completely phosphodeficient ADRB1
HEK293-ADRB1Δ3rdloop^{a}	ADRB1 with Ser260 mutated to Ala
HEK293-ADRB1Δ3rdloop^{b}	ADRB1 with Ser274, Ser276, Ser278, Thr298 and Ser312 mutated to Ala
HEK293-ADRB1Δproximal	ADRB1 with Thr404, Ser412 and Ser423 mutated to Ala
HEK293-ADRB1Δmiddle	ADRB1 with Ser428 and Thr439 mutated to Ala
HEK293-ADRB1Δdistal	ADRB1 with Ser459, Ser461, Ser462, Ser473 and Ser475 mutated to Ala
HEK293-ADRB1(Ala459/461/462)	ADRB1 with Ser459, Ser461 and Ser462 mutated to Ala
HEK293-ADRB1(Ala461/462)	ADRB1 with Ser461 and Ser462 mutated to Ala
HEK293-ADRB1(Ala473/475)	ADRB1 with Ser473 and Ser475 mutated to Ala

Name	Description
HEK293-ADRB1-Cer	ADRB1 with a Cerulean fused to its C-terminus
HEK293-ADRB1Δphos-Cer	completely phosphodeficient ADRB1 with a Cerulean fused to its C-terminus
HEK293-ADRB1Δdistal-Cer	ADRB1 with Ser459, Ser461, Ser462, Ser473 and Ser475 mutated to Ala with a Cerulean fused to its C-terminus
HEK293-HA-ADRB1	ADRB1 with N-terminal HA tag
HEK293-ADRB1-HA	ADRB1 with C-terminal HA tag

2.1.7 Oligonucleotide primers

Primers were either designed manually or with the help of Primer3 (Koressaar and Remm, 2007; Untergasser et al., 2012). All primers were purchased in high purity salt free quality from Eurofins MWG (Ebersberg), Life Technologies (Karlsruhe) or Sigma-Aldrich (Taufkirchen). The lyophilized oligonucleotides were solved in ddH_2O and stored in a stock concentration of 1 mM. They were used in a concentration of 20 pM.

Primer	Sequence (5' → 3')
Conventional cloning	
hADRB1-for	AAAAATGGGCGCGGGGGTGCTCG
hAdrb1-rev	AAAACTACACCTTGGATTCCGAGG
Cer-BseRI-r	TCCTTGAAGTCGATGCCCTT
AscI-for	CGAGACCCTGTGTGTCATTG
ADRB1-NotI-for	AGAAGCAGGTGAAGAAGATCG
ADRB1-7TM-rev	TAGCCCAGCCAGTTGAAGAA
ADRB1-XmaI-rev	CTCGTCCAGGCTCGAGTC
ADRB1-XmaI-rev2	CTCGTCCAGTGCTGCGTC
Gateway cloning	
attBb1A473/475r	GGGGACCACTTTGTACAAGAAAGCTG GGTCCTACACCTTTGCTTCTGCGGCG
attBb1A473/475r2	GGGGACCACTTTGTACAAGAAAGCTG GGTCCTACACCTTTGCTTCTGCGG

Primer	Sequence (5' → 3')
Mutagenesis	
b1-S461/462A-f	GCGACGCAGCACTGGAC
b1-S461/462A-r	GTCCAGTGCTGCGTCGC
Sequencing	
pENTR-ADRB1 for	AGTGACCTGTTCGTTGCAAC
pENTR-ADRB1 for2	GGCCTTTTTGCGTTTCTACA
pENTR-ADRB1 Mitte	CCTGTGCATCATGGCCTTC
pENTR-ADRB1 Mitte	CTCCTTCTTCTGCGAGCTGT
ADRB1- Mitte3	CTCCTTCTTCTGCGAGCTGT
pENTR-ADRB1 rev	CAACGCTACCTTTGCCATGT

2.1.8 Antibodies

Primary antibodies

Epitope	Species	Clonality	Source
ADRB1	mouse	monoclonal	Corimmun (Martinsried)
HSP90	mouse	monoclonal	Santa Cruz (Heidelberg)
MAPK1/3	rabbit	monoclonal	New England Biolabs (Frankfurt a. M.)
pMAPK1/3	rabbit	monoclonal	New England Biolabs (Frankfurt a. M.)

Secondary antibodies

Epitope	Species	Description	Source
mouse-IgG	rabbit	coupled to HRP	Dianova (Hamburg)
rabbit-IgG	goat	coupled to HRP	Dianova (Hamburg)

HRP = horseradish peroxidase

2.2 Methods

2.2.1 Molecular biology methods

Polymerase chain reaction

The polymerase chain reaction (PCR) is a method to amplify nucleic acid sequences. Two oligonucleotide primers are used, which flank the desired region. The primers anneal to the DNA and form the starting points at which the DNA polymerase enzyme transcribes the DNA. After this extension phase the sample is heated to > 90 °C, which leads to the dissolving of the hydrogen bonds between the base pairs. The double stranded DNA is thus transformed to a single strand and new primer pairs can anneal and the cycle starts anew (Bartlett and Stirling, 2003).

	concentration	**volume**
DNA	100 ng/µl	1 µl
ddH_2O		38.5 µl
10 x Accu buffer		5 µl
Primer forward	20 pmol/µl	1 µl
Primer reverse	20 pmol/µl	1 µl
DMSO		2.5 µl
Accu Pfx		1 µl

This is repeated > 30 times, which leads to a rapid amplification of the desired DNA sequence. If the primers are designed to contain single or double nucleotide mismatches, this technique can also be used to introduce desired mutations into the DNA.

Initial denaturation	95 °C	2 min
Denaturation	95 °C	15 s
Annealing	56 °C	30 s
Extension	1 min 45 s	
Cooling	68 °C	1 min
	16 °C	∞

The steps between the double lines are repeated 35 times.

Heat pulse extension polymerase chain reaction

The heat pulse extension (HPE) PCR is a method to amplify GC (guanine and cytosine) -rich constructs (modified after Orpana et al., 2012). Often genes with a GC content over 80 % are hard to amplify. Since the two bases guanine and cytosine are so abundant, it is possible that these genes have several regions with similar base sequences. This can promote hairpin structure formation, which is thought to inhibit the DNA polymerase during the elongation phase. The β_1-adrenoceptor has a GC content of over 70 % on average and in parts of over 95 %. For this reason a normal PCR regularly resulted in a shortened 1000 bp long PCR product instead of 1500 bp. This could be explained by a hairpin structure which leads to a skip of 500 bp by the DNA polymerase.

The basis of the *heat pulse extension PCR* are multiple heat pulses during the elongation phase, which are thought to destroy the hairpin-like structures.

Initial denaturation	94 °C	7 min
Denaturation	95 °C	45 s
	98 °C	10 s
Annealing	64 °C	30 s
Extension	ramp to 78 °C (0.6 °C/s equals 15 % ramp on Eppendorf cycler)	
	86 °C	4 s
	78 °C	4 s
	90 °C	4 s
	78 °C	4 s
Cooling	78 °C	1 min
	4 °C	∞

The steps between the double lines are repeated 35 times.

Another way to amplify GC-rich DNA is to add dimethyl sufoxide (DMSO). DMSO was added in concentrations ranging from 2.5 % to 10 % (Figure 2.1) to test which amount of DMSO would show the best results. After this test, DMSO was routinely added at 5 %.

Agarose gel electrophoresis

1 % agarose gels were made by adding 1 g of agarose to 100 ml of 1x TAE (Tris acetate ethylenediaminetetraacetic acid) buffer and heating the mixture in the mi-

crowave. The heating periods were kept short (< 30 s) in order to prevent a delay in boiling. After water-cooling of the fluid agarose, 5 µl ethidium bromide per 100 ml was added.

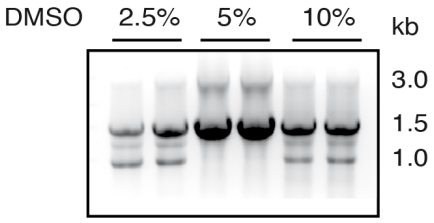

Figure 2.1: **Different DMSO concentrations during heat pulse extension PCR**
DMSO concentrations from 2.5 % to 10 % were added to test which amount of DMSO is optimal for ADRB1 PCR.

50x TAE buffer		**5x DNA loading buffer**	
Tris	0.2 M	Xylencyanol	25 mg
Acetic acid	57.1 ml	EDTA (0,5 M)	1.4 ml
Na_2EDTA x 2 H_2O	37.2 g	Glycerol	3.6 ml
ddH_2O	ad 1 l	ddH_2O	7 ml

Ethidium bromide stock concentration 1 mg/ml

The gels were cast and when completely polymerized transferred into electrophoresis chambers (Peqlab, Erlangen). 1x TAE was used as running buffer.

The samples were mixed with 5x DNA loading buffer and transferred into the wells of the gel. The DNA fragments were separated using a voltage of 140 V and maximal electrical current. Different markers were used to identify the lengths of the different DNA bands. Usually a 1 kb and a 100 bp marker from New England Biolabs (Frankfurt am Main) were used.

The DNA bands were made visible through the intercalation of ethidium bromide into the DNA and subsequent detection under UV light (UV transilluminator, Wealtec, Sparks) with an absorption at 365 nm and an emission of orange light at 605 nm.

DNA extraction from agarose gels

The required DNA band was cut out of the gel under UV light using a scalpel. Whenever possible the low UV setting was used on the gel documentation system

(UV transilluminator, Wealtec, Sparks), in order to avoid UV light-induced thymine dimer formation.

The DNA was then purified using the *QIAQuick Gel Extraction Kit* (Qiagen, Hilden) and following the manufacturer's instructions. The DNA was eluted in 20 µl of ddH_2O and the concentration was determined using a NanoDrop spectrophotometer (Thermo Fisher Scientific, Waltham).

Restriction enzyme digestion

Restriction enzyme digestion was performed either for quality control of Gateway cloning or for conventional cloning. In conventional cloning it was followed by DNA dephosphorylation and ligation.

All restriction enzymes, except when noted otherwise, were purchased from New England Biolabs (Frankfurt am Main). Double digests were planned using the New England Biolabs (Frankfurt am Main) double digest finder tool.

Restriction enzyme digestion

(A) Conventional cloning	
DNA	3 µg
10x BSA	5 µl
Buffer	5 µl
Enzyme 1	2.5 µl
Enzyme 2	2.5 µl
ddH_2O	ad 50 µl

The reaction was incubated at 37 °C for 2 hours.

(B) Gateway cloning /conventional cloning	
Mini-DNA	5 µl
10x BSA	2 µl
Buffer	2 µl
Enzyme 1	0.2 µl
Enzyme 2	0.2 µl
ddH_2O	ad 20 µl

The reaction was incubated at 37 °C for 45 minutes.

DNA dephosphorylation

If the restriction enzyme digestion resulted in blunt 3' and 5' ends, the vector was dephosphorylated to prevent religation.

DNA dephosphorylation	
DNA	2 µg
Buffer	5 µl
ddH_2O	ad 50 µl
Antarctic phosphatase	1 µl

The reaction was incubated for 30 minutes at 37 °C followed by 30 minutes at 50 °C. To inactivate the enzyme after dephosphorylation, the reaction was incubated at 65 °C for 5 minutes.

DNA ligation

DNA ligation was carried out using the T4 DNA Ligase (New England Biolabs (Frankfurt am Main)). The reaction was performed in a 1.5 ml reaction tube on ice.

DNA ligation	
10x T4 DNA Ligase buffer	2 µl
Vector (3 kb)	50 ng
Insert (1 kb)	50 ng
ddH_2O	ad 20 µl
T4 DNA Ligase	1 µl

The ligation was incubated either for 90 minutes at 23 °C or overnight at 16 °C. 2 µl of each reaction were electroporated into electrocompetent DH10B *E. coli*.

Gateway cloning

Whenever possible Gateway cloning (Life Technologies, Karlsruhe) was used. This method is based on homologous recombination. There are three steps in this cloning technique: First the attB PCR, second the BP reaction and third the LR reaction.

attB PCR To add the attB sites to the insert of choice, the attB PCR is performed. The primers were designed according to the manufacturer's instructions. They

contained the attB site and about 15 bases of the beginning and end of the desired insert, respectively.

BP reaction The BP reaction uses the attB sites for homologous recombination into an entry vector. For this project pDONR221 from Life Technologies (Karlsruhe) was used.

BP reaction	
Entry vector	150 ng
attB PCR product	10-150 ng
TE buffer	ad 8 µl
BP clonase II	2 µl

The BP reaction was incubated at 25 °C for one hour and then terminated by adding 1 µl of proteinase K and incubating at 37 °C for 10 minutes. The resulting entry vector was electroporated into DH10B *E. coli* and underwent mini and midi cultures and the respective purifications. The purified entry vector was then used as a template in the LR reaction.

LR reaction The LR reaction uses homologous recombination to transfer the desired insert from the entry vector into an expression vector.

LR reaction	
Entry clone	150 ng
Expression vector	150 ng
TE buffer	ad 8 µl
LR clonase II	2 µl

The LR reaction was incubated at 25 °C for one hour and then terminated by adding 1 µl of proteinase K and incubating at 37 °C for 10 minutes. The resulting expression vector was electroporated into DH10B *E. coli* and underwent mini and midi cultures and the respective purifications. The purified expression vector was then used to transfect HEK293 cells.

Mutagenesis

Site-directed mutagenesis was performed using the QuickChange Mutagenesis kit (Agilent Technologies, Santa Clara) or HPE PCR with primers that contained the desired mismatches.

Bacteria transformation

LB medium	
1 % bacto-trypton	10 g
0.5 % yeast extract	5 g
0.5 % NaCl	5 g
1 M NaOH	1 ml
ddH_2O	ad 1 l
autoclaved	

Bacteria transformation was carried out using electroporation. 50 µl of electrocompetent *E. coli* from the DH10B strain were transformed using the Bio-Rad (Munich) Gene Pulser at the following settings: 200 Ω, 25 µF and 1.8 V. Immediately after transformation 200 µl of LB medium was added and the bacteria were incubated for one hour at 37 °C and 350 rpm in a thermomixer (Eppendorf, Hamburg). After incubation 50 µl of transformed bacteria were plated onto an antibiotic containing agar plate and incubated at 37 °C overnight.

Mini culture and DNA purification from mini cultures

Mini cultures On the following day 5-6 colonies were picked with a pipette tip and put into 5 ml of antibiotic containing LB media. Those mini cultures were incubated at 37 °C and 180 rpm overnight.

DNA purification from mini cultures 1.5 ml of overnight LB culture was spun down at 10,000 x g and the resulting pellet was resuspended in 250 µl of resuspension buffer P1. After 5 minute incubation at room temperature 250 µl of P2 lysis buffer was added. The samples were mixed by inversion and again incubated for 5 minutes at room temperature. To stop the lysis reaction, 300 µl of neutralization buffer P3 was added and the sample was incubated for 5 minutes at 4 °C.

The samples were then centrifuged at 20,000 x g for 10 minutes at 4 °C. The resulting supernatant was transferred into a new 1.5 ml reaction tube and precipitated

with 750 µl of 100 % EtOH for five minutes at room temperature. The sample was again centrifuged at 20,000 x g for five minutes at 4 °C. The resulting pellet was air dried and resuspended in 20 µl ddH_2O. A restriction enzyme digestion and gel electrophoresis were performed to determine whether the mini culture contained the correct plasmid.

Midi culture and DNA purification from midi cultures

1 ml of mini culture was transferred into a new Erlenmeyer flask containing 100 ml of antibiotic-containing LB media. This midi culture was incubated at 37 °C and 180 rpm overnight. The midiprep was carried out using the PureLink midiprep kit from Life Technologies (Karlsruhe) following the manufacturer's instructions.

Measurement of DNA concentration

DNA concentration was determined using the NanoDrop spectrophotometer (Thermo Fisher Scientific, Waltham), which measures the absorbance of UV light at 260 nm. 1 µl of DNA was used per measurement.

Sequencing of plasmid DNA

All DNA sequencing was carried out by Eurofins MWG (Ebersberg), using the a la carte sequencing service.

2.2.2 Cellular biology methods

Cultivation of eukaryotic cell lines

For all experiments HEK293 cells were used. They were cultured in DMEM (Dulbecco's modified Eagle's minimal essential medium) (Thermo Fisher Scientific, Waltham) containing 1 % penicillin/streptomycin and 10 % fetal calf serum (FCS). The media for stably transfected cell lines also contained 0.4-0.8 g/l G-418 as a selecting agent.

Freezing and thawing of cells

Cells can be frozen and stored in liquid nitrogen and thawed again, when needed. Whenever possible cells from early passages were used. Usually cells were not used passed passage 20.

Freezing of cells In order to prevent crystal formation and cell death during the freezing process, DMSO was added as a cryoprotective agent. The cells were washed once with PBS (phosphate buffered saline) and then removed with trypsin. The cells were resuspended in 1 ml per cryotube normal cell medium. One 10 cm plate with confluent cells was sufficient for four cryotubes. The cells were transferred into prechilled cryotubes. To one ml of cells one ml of cold freeze medium was added. The cells were stored for 24 hours at -20 °C and for another 24 hours at -80 °C. On the third day the cells were transferred into liquid nitrogen storage.

Freeze medium (2x)	
FCS	20 %
DMSO	40 %
normal culture medium	40 %
cool freeze medium before use	

Thawing of cells The cells were taken out of liquid nitrogen and directly defrosted at 37 °C. Once the medium was thawed, they were put in a cell culture dish with fresh prewarmed (37°C) medium and incubated until the cells had attached. Then the medium was changed in order to remove the cryoprotective DMSO, which is toxic for cells, when they are not frozen.

Transient transfection of HEK293 cells

HEK293 cells were transfected using Effectene (Qiagen, Hilden). Depending on the following experiment either a regular transfection or a fast-forward transfection was performed. The difference between the two approaches is that for a regular transfection the cells are passaged the day prior to the transfection and cultivated to a confluency of 80 %. They undergo a media exchange and the transfection reagent is pipetted onto the adherent cells. In a fast-forward transfection the cells were passaged on the same day as the transfection and the transfection reagent was pipetted onto the cells, while they were attaching. The transfection efficiency was similar between those two approaches.

To condense the expression vector plasmid, the DNA, EC buffer and Enhancer were mixed and incubated for five minutes. In a following step the transfection reagent Effectene was added. It was mixed and incubated for ten minutes, where it formed a complex with the DNA. This transfection-complex was slowly given onto the cells, where it was able to pass the cell and the nuclear membrane, which led to the production of the desired protein.

Diameter	**3.5 cm**	**10 cm**	**15 cm**
DNA	0.4 µg	2 µg	4 µg
EC buffer	100 µl	250 µl	500 µl
Enhancer	3.2 µl	16 µl	32 µl
	vortex 5 s, incubate at room temperature 5 minutes		
Effectene	10 µl	60 µl	120 µl
	vortex 10 s, incubate at room temperature 10 minutes		
DMEM	600 µl	3 ml	7 ml

The transfection efficiency of the transient transfection was approximately 70 %.

Stable transfection of HEK293 cells

One 10 cm dish of HEK293 cells was transfected as described above. 0.8 g/l of Geneticin (G-418) was added to the normal cell culture medium. Starting on the second day after transfection, the medium was exchanged daily. Only transfected cells, which integrate the G-418 resistance gene into their genome can produce the protein, that is responsible for the antibiotic resistance. These cells survived the selection process, while all untransfected cells and cells that were successfully transfected, but did not integrate the resistance gene into their genome died.

The daily medium exchange was stopped when the cells started to proliferate again. Usually this took 14 days.

Flow cytometry

FACS buffer	
BSA	1 %
EDTA	1 mM
in PBS	
sterile filtered (0.2 µm)	

Cells were measured and sorted in a Bio-Rad S3 sorter. Depending on the experiment 1.5 x 10^6 to 4 x 10^6 cells were used.

The cells were detached by pipetting up and down in PBS and then centrifuged at 300 x g for 5 minutes. The cells were then immediately put on ice and washed once in FACS buffer. The primary antibody was diluted in FACS buffer to a concentration of 5 µg/ml in 200 - 400 µl and the samples were incubated for one hour at 4 °C in an end-over-end shaker. The cells were then washed three times in FACS buffer and incubated in the secondary antibody (5 µg/ml in 200 - 400 µl) for one hour at 4 °C in an end-over-end shaker. After incubation in the secondary antibody the cells were again washed three times and then measured in the Bio-Rad S3 sorter.

When the cells were sorted, all washing steps were carried out in a sterile cell culture hood. The cells were sorted into 500 µl of FACS buffer at 4 °C and immediately after the sorting procedure put on ice. Then they were centrifuged at 300 x g for 5 minutes and the resulting pellet was resuspended in warm DMEM medium containing 2 % penicillin/streptomycin and 0.8 g/l G-418 as antibiotics.

SILAC

For SILAC labeling HEK293 cells were cultivated in heavy and light medium, respectively. For labeling the SILAC-Lys6-Arg10-Kit from Silantes (Munich) was used. The cells were grown in SILAC medium for one week and then a part of the cells was lysed in 3 % NP-40 lysis buffer. Full labeling was verified using mass spectrometry. The labeled cells were then frozen and stored in liquid nitrogen.

2.2.3 Biochemical methods

Protein lysates

SDS lysis buffer

Tris/HCl pH 6.7	50 mM
SDS	2 %
Na_3VO_4	1 mM

1 pill cOmplete Mini protease inhibitor (Roche, Mannheim)
1 pill PhosSTOP phosphatase inhibitor (Roche, Mannheim)

RIPA lysis buffer

NP-40	1 %
Sodiumdeoxycholate	0.1 %
SDS	0.5 %
Tris/HCl pH 7.4	50 mM
NaCl	100 mM
EDTA	2 mM

1 pill cOmplete Mini protease inhibitor (Roche, Mannheim)
1 pill PhosSTOP phosphatase inhibitor (Roche, Mannheim)

NP-40 lysis buffer

HEPES	50 mM
NaCl	250 mM
EDTA	5 mM
NP-40	3 %

1 pill cOmplete Mini protease inhibitor (Roche, Mannheim)
1 pill PhosSTOP phosphatase inhibitor (Roche, Mannheim)

SDS lysates 80 % confluent HEK293 cells were taken out of the 37 °C incubator and put on ice. They were washed three times with ice cold PBS and then incubated on ice in SDS lysis buffer for 30 minutes.

After incubation the cells were scraped off using a cell scraper from Sarstedt (Newton, USA) and transferred into 1.5 ml reaction tubes. 1/10 Vol of Benzonase (Merck, Darmstadt) was added. The lysates were incubated at room temperature for ten minutes. Benzonase was then inactivated by incubation in an ultrasound bath for five minutes at 4 °C. Following this were two sonification steps. The lysates were stored at -20 °C.

RIPA and NP-40 lysates 80 % confluent cells were taken out of the 37 °C incubator and put on ice. They were washed three times with ice cold PBS and then incubated on ice in RIPA lysis buffer or NP-40 lysis buffer, respectively, for 30 minutes.

After incubation the cells were scraped off using a cell scraper from Sarstedt (Newton, USA) and transferred into 1.5 ml reaction tubes. To deplete the lysates of

cell debris, the samples were centrifuged at 13,000 x g at 4 °C for 10 minutes. The supernatant was transferred into new 1.5 ml reaction tubes. 1/10 Vol of Benzonase (Merck, Darmstadt) was added. The lysates were incubated at room temperature for ten minutes. Benzonase was then inactivated by incubation in an ultrasound bath for five minutes at 4 °C. The lysates were stored at -20 °C. Before loading the samples onto an SDS gel, 4x laemmli buffer was added as loading buffer.

BCA assay

For quantification of total protein concentration a BCA assay (Thermo Fisher Scientific, Waltham) was used. Samples were diluted 1:10 and performed in triplicates in a 96 well plate. The BCA reagent was added according to the manufacturer's instructions and the plate was incubated for 30 minutes at 37 °C.

This method is based on the biuret reaction, a protein mediated reduction of Cu^{2+} to Cu^{1+}. BCA forms a chelate complex in the stochiometry of 2:1 with Cu^{1+}. This forms a purple complex with an absorbance at 562 nm that is linear to protein concentration in a range from 20 - 2,000 µg/ml.

The amino acids responsible for the color change are thought to be cysteine, cystine, tryptophan and tyrosine. This means that the target protein should be similar in amino acid content and composition to the protein used for the standard curve. For this work diluted bovine serum albumin was used for the standard curve. A microplate reader (Tecan, Männedorf) was used for colorimetric detection and the results were related to a standard curve.

SDS-PAGE

Upper buffer	
Tris/HCl	61 g
10 % SDS	40 ml
pH 6.7	approx. 60 ml HCl
ddH_2O	ad 1 l

Lower buffer	
Tris/HCl	182 g
10 % SDS	40 ml
pH 8.8	approx. 28 ml HCl
ddH_2O	ad 1 l

10x running buffer	
Tris/HCl	30 g
Glycine	144 g
SDS	15 g
ddH_2O	ad 1 l

10 % SDS polyacrylamide gels were cast:

	Stacking gel	**Separation gel**
Acrylamide/bisacrylamide	0.5 ml	5 ml
ddH_2O	3.2 ml	3.7 ml
Upper buffer	1.25 ml	—
Lower buffer	—	3.8 ml
Glycerol	—	2.5 ml
Tetramethylethyldiamin (TEMED)	6 µl	12 µl
Ammoniumperoxodisulfate (10% solution)	48 µl	72 µl

The Protean 4 Mini (Bio-Rad, Munich) gel electrophoresis system was used. To induce protein denaturation, the samples were heated for 10 minutes at 95 °C. The PageRuler Prestained Protein Ladder (Fermentas, St. Leon-Rot) was used as a protein size marker. The gel running chambers were filled with 1x running buffer and the gels were run at 20 mA per gel for 15 minutes, with maximal voltage and for the rest of the run at 30 mA per gel.

Western blot

Stripping buffer	
Glycine	20 g
SDS	1 g
Tween-20	10 ml
ddH_2O	ad 1 l
titrate to pH 2.0	

10x transfer buffer	
Tris pH 8.3, 1M	25 ml
Glycine	11.26 g
Methanol	100 ml
ddH_2O	ad 1 l

BSA blocking buffer	
Tris pH 7.5	50 mM
NaCl	150 mM
NP-40	0.2 % (v/v)
BSA	2 % (m/v)
NaN_3	0.03 % (m/v)

BSA washing buffer	
Tris pH 7.5	50 mM
NaCl	150 mM
NP-40	0.2 % (v/v)
BSA	0.5 % (m/v)

Blotting procedure PDVF membranes were activated in methanol for 3 minutes. They were rinsed in ultrapure water and then incubated in 1x transfer buffer for > 3 minutes. The gels were incubated in 1x transfer buffer for 3 minutes to avoid methanol-induced shrinking of the gel during the blotting process. Proteins from the gel were transferred onto the membrane by using the Mini-PROTEAN blotting system from Bio-Rad (Munich). The current was set to 300 mA and maximal voltage. The gels were blotted for 90 to 120 minutes. Successful blotting was verified by Coomassie brilliant blue staining of the gel.

After the blotting procedure, the membranes were blocked using BSA blocking buffer. The primary antibody was then diluted according to the manufacturer's instructions (1:500 - 1:10,000) in BSA blocking buffer and the membranes were incubated in the primary antibody.

The membranes were then washed four times for seven minutes using the BSA washing buffer. The secondary antibody was diluted (usually 1:10,000) in BSA washing buffer and the membranes were incubated in the secondary antibody. After the secondary antibody incubation the western blot membranes were washed with BSA washing buffer four times for seven minutes each.

The blocking step and the two antibody incubation steps were performed either for two hours at room temperature or overnight at 4 °C.

Stripping of western blots Western blot membranes were stripped off the antibodies for MAPK1/3 and pMAPK1/3 stainings. The membranes were incubated twice in stripping buffer for 10 minutes each at room temperature, following two washing steps with PBS and two washing steps with BSA washing buffer. Each step was carried out for 10 minutes. Successful stripping was confirmed for each antibody using ECL Plus and the Fujifilm LASmini4000 detection system (Bio-Rad, Munich) as described below. The stripping procedure was followed by another blocking step with BSA blocking buffer for two hours at room temperature or overnight at 4 °C.

Detection The membranes were incubated for one to three minutes in ECL or ECL Plus (Thermo Fisher Scientific, Waltham). The blots were then visualized using the Fujifilm LASmini4000 detection system (Bio-Rad, Munich). Quantification was carried out using the software Multi Gauge (FujiFilm) or ImageJ.

Immunoprecipitation

Immunoprecipitation is a simple affinity-based way to purify proteins out of a cell lysate.

Metal bead immunoprecipitation Metal bead immunoprecipitation was used for the radioactive phosphorylation assays. Either 10 µg of total protein lysate was used to perform the IPs or the lysate resulting from one well of a confluent 12-well plate. The lysate was first incubated with 3 µg of antibody overnight on a shaker at 4 °C. On the next day 40 µl of Dynabeads Protein G (Life Technologies, Karlsruhe) were washed in PBS three times using the DynaMag-2 Magnetic Particle Concentrator (Life Technologies, Karlsruhe). The beads were then mixed with the protein and the antibody for two hours at 4 °C on a shaker. After the incubation the samples were again washed three times with PBS and then 25 µl of Laemmli buffer was added to the antigen-containing beads. The samples were then denaturated for 10 minutes at 95 °C and analyzed on an SDS gel followed by western blot as described above.

Crosslink immunoprecipitation Crosslink immunoprecipitation as shown in figure 1.15) was used to purify the β_1-adrenoceptor prior to mass spectrometric analysis. Crosslink immunoprecipitation was perfomed with agarose beads using the Pierce Crosslink IP Kit (ThermoFisher Scientific, Waltham). Cells were lysed in NP-40 lysis buffer and total protein concentration was determined. 500 µg up to 100 mg of total protein was used for the immunoprecipitations. Apart from the lysis buffer the IP was carried out according to the manufacturer's instructions.

Radioactive phosphorylation

For radioactive phosphorylation assays, HEK293 cells stably expressing the ADRB1 were grown in phosphate-free DMEM containing 1 % FCS and 1 % penicillin/ streptomycin to a confluency of about 80 %. On the day of the experiment ^{32}P-orthophosphoric acid was given to the cells. The cells were either stimulated with 100 µM norepinephrine for five minutes at 37 °C or left untreated. This was followed by a cell lysis using RIPA lysis buffer. Total protein concentration was

determined by BCA assay. 10 µg of total protein lysate was used to perform a metal bead immunoprecipitation and subsequent SDS-PAGE followed by western blotting. The radioactive signal was detected using the Cyclone Plus phospho imager (PerkinElmer, Waltham) and quantified with ImageJ. As a loading control the same membranes were used to perform a western blot analysis detecting ADRB1 as described above.

Membrane preparation

Hypotonic buffer

Tris pH 7.5	5 mM
EDTA	2 mM

HEK293 cells were plated on three 15 cm cell culture dishes and grown until they reached 80 % confluency. The cells were washed three times with ice cold PBS and placed on ice. 5 ml of hypotonic buffer was added to each cell culture dish. The cells were scraped off the plates and transferred into 50 ml reaction tubes. Next they were centrifuged for 30 minutes at 1,400 x g and 4 °C and the supernatant was transferred into ultracentrifuge tubes. The lysates were centrifuged in the Optima L-80 XP ultracentrifuge (Beckman Coulter, Munich) for 45 minutes at 80,000 x g. The membranes were then located in the resulting pellet, which was resuspended in 0.5 ml hypotonic buffer. After homogenization, the resulting membrane preparation was aliquoted and stored at -80 °C.

Radioligand binding on isolated membranes

Binding buffer		**Alprenolol**
Tris pH 7.5	50 mM	400 µM in binding buffer

Guanosine triphosphate (GTP)
100 µM in binding buffer

In order to assess the exact amount of β_1-adrenoceptor that is expressed by the stably transfected HEK293 cells, radioligand binding experiments were performed. 10 µg of total protein from a membrane preparation were diluted in 50 µl binding buffer in a 96 well plate. 50 µl GTP was added to ensure saturation of the

β_1-adrenoceptor with GTP. Half of the samples were incubated with the β-blocker alprenolol to block radioligand binding and thus measure background signal.

To all samples ^{3}H-labeled CGP was added and the samples were incubated for two hours at room temperature. The proteins were then transferred onto a filter using the FilterMate Harvester (PerkinElmer, Waltham). A wax sheet was then melted onto the filter in a 1495-021 microsealer (PerkinElmer, Waltham) and the amount of bound ^{3}H-CGP was measured with the 1450 Microbeta Trilux scintillation counter (PerkinElmer, Waltham). The following formula was used to calculate the amount of β_1-adrenoceptor per µg of total protein: 1 count per minute (cpm) = 5 fmol ADRB1/µg of total membrane protein.

Radioactive internalization assays

FG buffer	
NaCl	130 mM
KCl	5 mM
$CaCl_2$	2 mM
$MgCl_2$	1 mM
HEPES	10 mM
Glucose	10 mM

Internalization was determined as loss of cell surface receptor upon 100 µM norepinephrine stimulation for 0, 2.5, 5 and 30 minutes as described previously (Zindel et al., 2015). HEK293 cells were transiently transfected with the different β_1-adrenoceptor variants. The next day 6-well plates were coated for > 1 hour with poly-D-lysine (Sigma-Aldrich, Taufkirchen). After coating 600,000 cells per well were seeded into the coated plates. On the next day the cells were washed once with 37 °C FG buffer and then stimulated with 100 µM norepinephrine for 0, 2.5, 5 and 30 minutes at 37 °C. After stimuluation the cells were placed on ice and washed twice with ice cold FG buffer. 0.2 µCi ^{3}H-CGP was added per well and incubated at 4 °C overnight. Two wells per condition were also incubated with 10 µM alprenolol, to measure unspecific binding.

On the next day, the cells were washed twice with ice cold PBS. Then 1 ml of 0.5 M NaOH was added and the cells were incubated at room temperature for > 5 min. The lysed cells were then transferred into scintillation tubes and 2 ml of Rotizsint eco plus (Carl Roth, Karlsruhe) scintillation reagent was added. The samples were then measured in the TRI-CARB 2100TR liquid scintillation analyzer (GMI, Ramsey). Analysis was carried out in Microsoft Excel and Graphpad Prism.

2.2.4 Microscopy methods

Confocal microscopy

Confocal microscopy was performed with a TCS SP5II system from Leica (Wetzlar) equipped with a 63x glycerol objective and an Argon laser for excitation of Cer (458 nm) and YFP (514 nm). For internalization assays HEK 293 cells were stimulated with 100 µM norepinephrine at room temperature.

FRET-based β-arrestin recruitment assay

FRET buffer	
NaCl	137 mM
KCl	4.5 mM
$CaCl_2$	2 mM
$MgCl_2$	2 mM
HEPES	10 mM

On day one HEK293 cells were transiently transfected with the different Cerulean-tagged β_1-adrenoceptor constructs and YFP-β-arrestin2 as described in chapter 2.2.2. On day two 15 mm glass coverslips were coated with poly-D-lysine (Sigma-Aldrich, Taufkirchen) and the transfected cells were split onto the coverslips and cultured until day three. During the measurements, the cells were continously superfused with FRET buffer, using the ALA VC3-8 (ALA Scientific Instruments, New York, NY) perfusion system. Adrenergic stimulation was achieved with 10 µM norepinephrine in FRET buffer. The cells were imaged with an Axio Observer Z1 inverted microscope (Zeiss, Oberkochen) equipped with DualView2 and 40x and 100x oil immersion objectives. An Evolve camera (Photometrics, Tucson) was used to detect the emission intensities of the two fluorophores. FRET was calculated as the ratio of YFP emission at 535 nm divided by Cer emission at 480 nm with a correction for spillover of the Cer emission into the YFP channel. Data were analyzed with Microsoft Excel and GraphPad Prism 6.

2.2.5 Mass spectrometry

For the mass spectrometric analyses IP products in 0.25 M glycine were used. The samples were prepared in four steps.

Step 1: Reduction Urea was added to the samples until they contained 8 M urea. 20 mM DTT was added to reduce disulfide bridges. The samples were then incubated on a rotator for one hour at 50 °C. After cooling of the samples at room temperature, 1/10 volume of 550 mM 2-iodoacetamide (IAA) was added so that the end concentration was 55 mM. This led to an irreversible alkylation of the reduced thiol groups. The samples were then incubated for 30 minutes at room temperature in the dark, due to the photosensitivity of IAA. This disrupted the de novo formation of disulfide bridges and thus retained the protein in a linear state.

Step 2: Digestion The second step was the digestion of the proteins with either LysC and trypsin or chymotrypsin alone. The enzymes were lyophilized and solved in 50 mM triethylammonium bicarbonate (TEAB) at a concentration of 0.5 µg/µl. 0.5 µg of enzyme was used per sample.

Digestion with LysC and trypsin. Since LysC works in up to 6 M urea, all samples which were designated for LysC digestion, were diluted in TEAB to a final concentration of 6 M urea. After this dilution 0.5 µg of LysC was added and the samples were incubated at 37 °C and 700 rpm. The rationale for the predigestion using LysC was to cut the β_1-adrenoceptor into several bigger peptides, which were then more accessible to trypsin, as compared to the undigested receptor.

Digestion with chymotrypsin. Before chymotrypsin digestion, samples were diluted in 4 volumes of 50 mM TEAB. 0.5 µg of chymotrypsin was added and the samples were incubated for 5 hours at room temperature on a rotator. After 5 hours another 0.5 µg of enzyme was added and the samples were incubated at 25 °C overnight on a rotator.

Step 3: Desalting To desalt the samples C-18 columns were used. Prior to desalting the samples were acidified with 100 % formic acid (FA) to a pH of 2-3.

Buffer A		**Buffer B**	
FA	0.1 %	Acetonitrile (ACN)	40 %
		FA	0.1 %

The columns were equilibrated with 2 ml of Buffer B for 2 minutes followed by 2 ml of buffer A for 2 minutes. After the preparation of the columns great care was taken to avoid drying of the columns. The samples were then loaded onto the columns and passed through the columns as slowly as possible using a vacuum pump. Next the columns were washed with 4 ml of buffer A and the desalted samples were then eluted with 2 column volumes (2 x 150 µl) of buffer B.

Step 4: Combined IMAC enrichment and desalting The last step in preparing the samples for analysis via mass spectrometry was a combined IMAC enrichment and desalting as described in Villén and Gygi, 2008.

IMAC binding buffer		**IMAC elution buffer**	
ACN	40 %	K_2HPO_4	500 mM
FA	0.1 %	pH 7.0	with 50 % H_3PO_4
StageTip binding buffer		**StageTip elution buffer**	
FA	1 %	ACN	50 %
		FA	0.1 %

IMAC beads (PHOS-Select Iron Affinity Gel, Sigma, Taufkirchen) were stored at -20 °C and first allowed to thaw at room temperature. The beads were then centrifuged for 10 s at 6,000 rpm. The supernatant was discarded. The beads were washed three times with 1 ml of IMAC binding buffer. Per sample 6 µl of IMAC beads were used. Samples and beads were incubated for 60 minutes at 23 °C in a thermomixer mixing at 1200 rpm. During the binding time the StageTips (stop-and-go-extraction tips (Rappsilber et al., 2007)) were prepared.

StageTip preparation Two disks Empore 3M C-18 were punched out using a metal puncher with a diameter of 3 mm. These disks were stacked on top of each other in a 200 µl pipette tip. The StageTips were then allowed to expand in 20 µl of MeOH for 2 minutes. Following this they were centrifuged for 30 s at 2,000 rpm. Next the StageTips were equilibrated with 20 µl of StageTip elution buffer and washed twice with 20 µl of StageTip binding buffer.

IMAC enrichment After samples and beads were incubated for 60 minutes, the samples were centrifuged at 6,000 rpm for 10 s. 250 µl of supernatant was transferred into new 1.5 ml reaction tubes and saved as IMAC flowthrough for later analysis. The rest of the supernatant was resuspended with the beads and put onto the StageTips. The StageTips were washed three times with IMAC binding buffer. The C-18 material of the StageTips was equilibrated using 40 µl of StageTip binding buffer. The StageTips were then washed three times with 70 µl of IMAC elution buffer. This led to the competitive elution of the phosphopeptides from the IMAC beads, which then immediately bound to the C-18 material.

Desalting The StageTips were washed once with 40 µl of StageTip binding buffer, which eliminated phosphate salts. The elution of the StageTips was carried out directly into the SpeedVac plate using 70 µl of StageTip elution buffer, as slowly as possible.

Acquisition Acquisition and analysis was carried out by Benjamin Ruprecht in the laboratory of Prof. Küster (Chair of Proteomics and Bioanalytics, Technische

Universität München). Liquid chromatography and subsequent MS/MS analysis was performed on an Eksigent nanoLC-Ultra 1D+ (Eksigent, Dublin) and an Orbitrap Velos (Thermo Fisher Scientific, Waltham). The peptides were ionized using electrospray ionization at 2.2 kV and 275 °C. The mass spectrometer was operated in data-dependent acquisition mode and switched automatically between full MS and MS/MS scans. Full scan MS spectra (m/z 360 – 1300) were acquired in the Orbitrap mass analyzer at a resolution of 30,000. For MS/MS scans higher-energy collisional dissociation was used to fragment the peptides and the fragment ions were scanned in the Orbitrap with a resolution of 7,500. For analysis Mascot Distiller v2.2.1 (Matrix Science, Boston) was used to extract peak lists from raw files. Mascot v2.3.0 was used to search the human IPI database in order to identify the peptides. Further analysis was carried out using Scaffold v3.

3 Results

3.1 Determination of the β_1-adrenoceptor's phosphorylation pattern

3.1.1 Qualitative assessment of β_1-adrenoceptor phosphorylation

Phosphorylation can be assessed both qualitatively as well as quantitatively. Qualitative methods include radioactive phosphorylation assays, phosphosite-specific monoclonal antibodies in western blotting and qualitative mass spectrometry.

Radioactive phosphorylation

Radioactive phosphorylation assays visualize the amount of protein phosphorylation using radioactive ^{32}phosphorous. To first set the experimental conditions, the concentration of fetal calf serum the stably transfected HEK293 cells were cultured in was tested. Figure 3.1 depicts this test. Four different FCS concentrations were used ranging from 0.25 % up to 10 % of FCS as medium supplement. The cells were stimulated with 100 µM norepinephrine for five minutes. This induced receptor phosphorylation. Since the largest differences between the unstimulated and the stimulated conditions were observed in 1 % FCS, all subsequent experiments were performed using 1 % of FCS in the cell culture medium (Figures 3.2 and 3.12).

The radioactive phosphorylation assay further shows that the β_1-adrenoceptor is phosphorylated in its basal state and that its phosphorylation increases upon adrenergic stimulation (Figure 3.2).

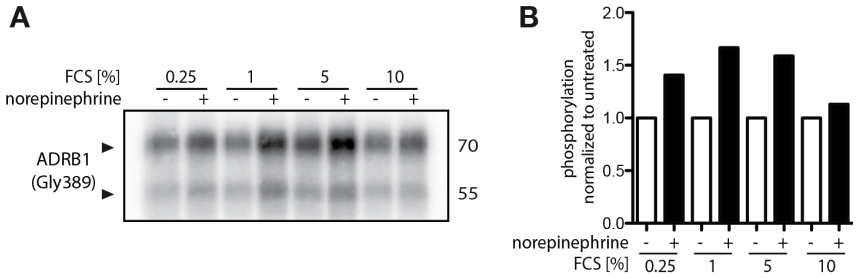

Figure 3.1: **Supplementing FCS in cell culture medium impacts ADRB1 phosphorylation.** (**A**) Radioactive phosphorylation assay with HEK293 cells stably overexpressing the β_1-adrenoceptor. The cells were cultivated in FCS concentrations ranging from 0.25 % to 10 %. After incubation with ^{32}P an immunoprecipitation against the β_1-adrenoceptor was performed and the radioactive western blot was exposed on a film for three weeks. Radioactivity was then measured using a phosphoimaging system. (**B**) Quantification of (A). n = 1

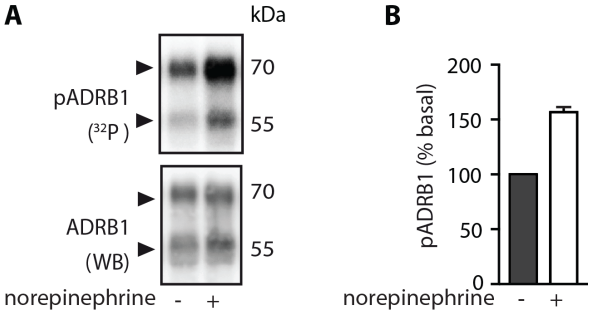

Figure 3.2: **The β_1-adrenoceptor is basally phosphorylated and its phosphorylation increases upon norepinephrine stimulation.** (**A**) Upper panel: Radioactive phosphorylation assay using unstimulated and stimulated HEK293 cells stably overexpressing the β_1-adrenoceptor. Lower panel: Western blot of the radioactive blot, to control for equal protein loading. (**B**) Quantification of (A). n=3

3.1.2 Purification of the β_1-adrenoceptor

In order to determine the phosphorylation pattern of the β_1-adrenoceptor via mass spectrometry, the receptor first needed to be purified. The purified receptor could then be separated by sodium dodecyl sulfate polyacrylamide gel electrophoresis (SDS-PAGE) and the two receptor bands were cut out of the gel and underwent mass spectrometric analysis. The ADRB1 usually displays a two-band pattern on an SDS-PAGE and western blot (Figure 3.3 (A) - (C)), with one band at 55 kDa and the other at 68 kDa. It is proposed that this double band pattern is due to glycosylation and N-terminal cleavage (Hakalahti et al., 2013).

During a conventional immunoprecipitation the precipitating antibody is degraded together with its precipitated target. This leads to the degradation of the antibody into its light and heavy chain. The molecular weights of both moieties are 25 and 50 kDa, respectively. With the β_1-adrenoceptor as antigen, this leads to a very prominent antibody band at nearly the same height as the lower band of the ADRB1 (Figure 3.3 (A)). While this is not problematic in a western blot, as anti-light chain antibodies can be used for detection, this is not feasible in a gel that is designated to be further analyzed by mass spectrometry. To circumvent this problem and to ensure a higher purity of the immunoprecipitated ADRB1 a crosslink immunoprecipitation was performed. 1-15 mg of total protein was used in the crosslink immunoprecipitations in order to maximize the amount of ADRB1 protein available for MS analysis. The crosslink immunoprecipitation products were then separated on an SDS-PAGE gel and underwent western blotting (Figure 3.3 (B)) and silver staining (Figure 3.3 (C)), respectively.

Silver staining was performed to visualize the β_1-adrenoceptor after purification. After the staining the two ADRB1 bands were cut out off the gel, digested and analyzed via mass spectrometry. On a western blot the untransfected negative control was very clean as seen in Figure 3.3 (B). This shows the robustness of the assay, i.e. the antibody crosslinking seemed to be very effective, with no co-elution of the antibody with the desired antigen. In the silver staining, however, a very prominent band appeared at approximately 55 kDa. This band looked very similar to the lower band in the stably transfected HEK293 cells expressing the ADRB1. This led to the conclusion that the upper band corresponded to the upper band of the ADRB1, but the lower band seemed to be a mixture of unknown proteins and the lower band of the ADRB1. Subsequent MS analysis suggested that this band consisted mostly of tubulin.

As the silver staining turned out to be relatively clean, apart from the band at 55 kDa there were no other unexplained bands, the in-gel digestion was dis-

continued in favor of an in-solution digestion of the immunoprecipitation eluate. This means that the whole immunoprecipitation product was used for the mass spectrometry scans and not just the bands, that were cut out of the silver gels.

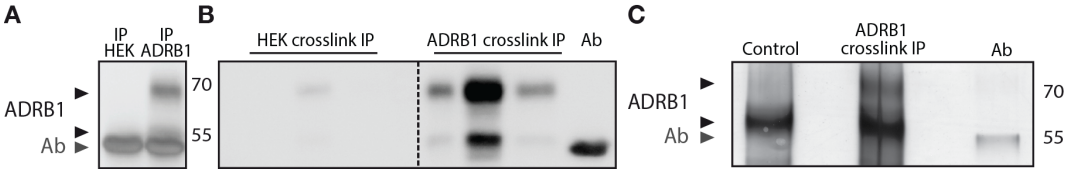

Figure 3.3: **Immunoprecipitation and silver staining of the β_1-adrenoceptor.**
(**A**) Purification of the ADRB1 using conventional immunoprecipitation. Untransfected HEK293 cells were immunoprecipitated as a negative control. Due to the antibody degradation into the heavy and light chain in SDS, the antibody band at 50 kDa is very prominent. (**B**) Crosslink immunoprecipitation. Untransfected HEK293 cells were immunoprecipitated as a negative control. The three lanes containing immunoprecipitated ADRB1 represent different elution steps after the crosslink IP. (**C**) Purified β_1-adrenoceptor from a crosslink immunoprecipitation was separated on an SDS gel and then silver-stained to assess the amount of purified receptor. An immunoprecipitation from untransfected HEK293 cells was used as negative control. To ensure that no antibody was co-eluting together with the ADRB1, additionally denatured IgG was used as a control. Ab = antibody

Qualitative mass spectrometry

In order to determine the β_1-adrenoceptor's phosphorylation pattern, a qualitative mass spectrometry approach was implemented. To elucidate which amino acid residues on the ADRB1 can actually become phosphorylated, HEK293 cells stably expressing the β_1-adrenoceptor were stimulated with 100 µM norepinephrine for five minutes to induce maximal activation of the receptors and thus maximal phosphorylation of the receptor itself. Figure 3.4 depicts the workflow of sample preparation for MS analysis.

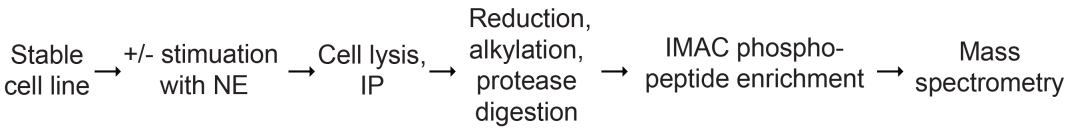

Figure 3.4: **Workflow of sample preparation for mass spectrometry.**
IMAC = immobilized metal ion affinity chromatography, IP = immunoprecipitation, NE = norepinephrine

The cells were lysed in a 3 % NP-40 lysis buffer and the lysates were crosslink-immunoprecipitated. The IP products were then reduced, alkylated and protease digested. Since the ADRB1 proved to be difficult to digest with trypsin alone, three different proteases were used: LysC combined with trypsin and chymotrypsin. The resulting mixture of peptides underwent an IMAC phosphopeptide enrichment to increase the abundance of the phosphorylated species over its unphosphorylated counterpart and was subsequently analyzed in the mass spectrometer.

The resulting phosphorylation pattern of the β_1-adrenoceptor after mass spectrometric analysis is shown in Figure 3.5.

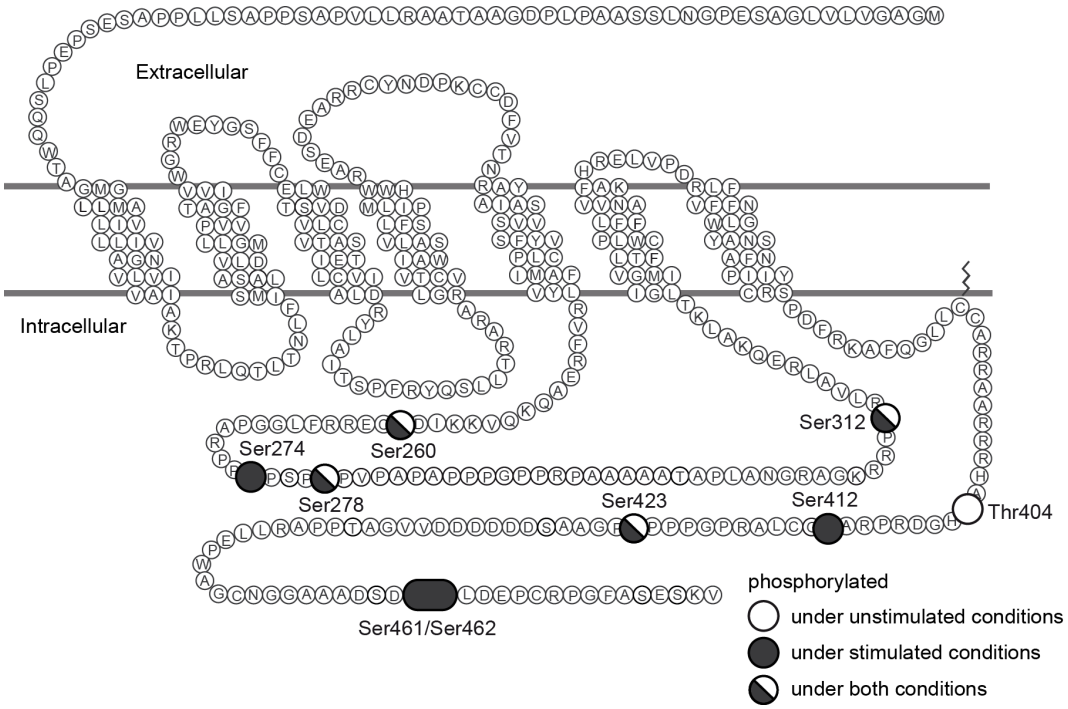

Figure 3.5: **Qualitative assessment of β_1-adrenoceptor phosphorylation by mass spectrometry.**
Phosphorylation pattern of the β_1-adrenoceptor. Amino acids marked in white and black indicate phosphorylation under basal conditions and after stimulation with 100 µM norepinephrine for 5 min, respectively.

Marked are all serines and threonines, which could be confidently identified as phosphorylation sites, namely

3rd ICL	C-terminus
Ser260	Thr404
Ser274	Ser412
Ser278	Ser423
Ser312	Ser461/Ser462

Serine 312 and serine 412 have been previously described to be phosphorylated by protein kinase A and B, respectively. All other sites were newly identified. Data from five measurements were pooled to get an overview of the maximal phosphorylation pattern of the β_1-adrenoceptor.

3.1.3 Quantitative assessment of β_1-adrenoceptor phosphorylation

To assess the regulation of the found β_1-adrenoceptor phosphosites, a quantitative SILAC experiment was performed. For this experiment HEK293 cells stably expressing the ADRB1 were labeled with medium containing ^{13}C in every lysine instead of ^{12}C and ^{13}C plus ^{15}N in every arginine instead of ^{12}C and ^{14}N. The cells incorporated the heavy amino acids into their proteome. This population of cells was then used as control. A second population of cells, which was cultivated in normal, "light" medium, but was otherwise identical, was stimulated with 100 µM norepinephrine for five minutes.

After stimulation the cells were lysed in 3 % NP-40 lysis buffer and then the heavy and the light lysates were mixed in equal ratios as determined by BCA assay. All subsequent MS preparation steps were performed with this mixture, so the protein losses during sample preparation were equal for both groups. After cell lysis, the proteins were crosslink immunoprecipitated. The immunoprecipitation products were protease-digested and analyzed via mass spectrometry.

After the samples were measured in the mass spectrometer, the phosphorylation was quantified using the Mascot database. Four phosphorylation sites were identified in the SILAC experiment: Ser260, Ser274, Ser312 and Ser412 as depicted in figure 3.6. Three amino acids exhibited an upregulation of phosphorylation after adrenergic stimulation: Ser260 (upregulation by a factor of 7.35 $\pm$ 0.01), Ser312 (upregulation by a factor of 1.85 $\pm$ 0.06) and Ser412 (upregulation by a factor of 3.10). The fourth amino acid identified in the SILAC experiment (Ser274)

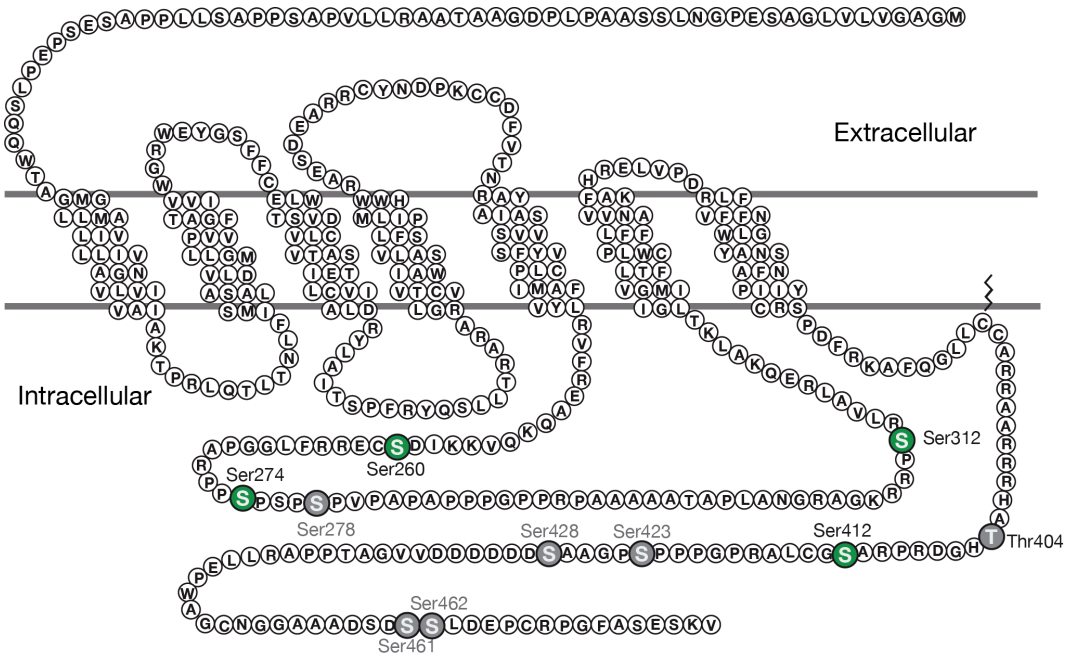

Figure 3.6: **Quantitative assessment of β_1-adrenoceptor phosphorylation: Overview of the identified phosphorylation sites in the SILAC experiment.**
Regulated phosphorylation sites of the β_1-adrenoceptor as determined by SILAC labeling and subsequent mass spectrometric analysis. Amino acids marked in green were found to be phosphorylated in the SILAC experiments. Ser260, Ser312 and Ser412 exhibited an upregulation of phosphorylation after adrenergic stimulation, while Ser274 showed a very slight downregulation. Amino acids marked in grey were found to be phosphorylated in previous mass spectrometry experiments, but were not detected in the SILAC experiments.

showed a slight downregulation of phosphorylation upon stimulation by a factor of 0.938 ± 0.002.

Figure 3.7 (A) depicts the MS/MS spectrum of the peptide REAQKQVKKID-SCERRF containing phosphorylated serine 260, which exhibited the strongest regulation of phosphorylation in the SILAC experiment, as determined in the extracted ion chromatogram (Figure 3.8).

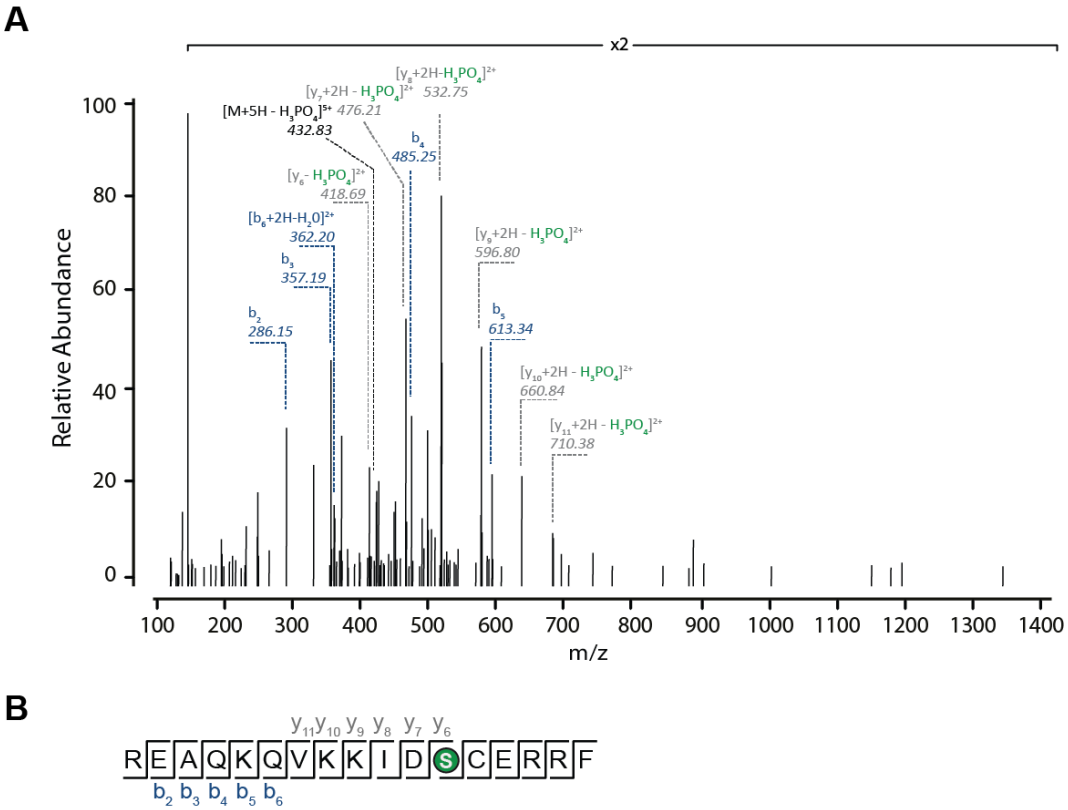

Figure 3.7: **Quantitative assessment of β_1-adrenoceptor phosphorylation: MS/MS spectrum of phosphorylated serine 260.**
(**A**) MS/MS spectrum of ADRB1 peptide REAQKQVKKIDSCERRF containing phosphorylated serine 260. b-ions are depicted in blue, y-ions in grey and neutral losses in green. (**B**) Fragmentation of REAQKQVKKIDSCERRF peptide.

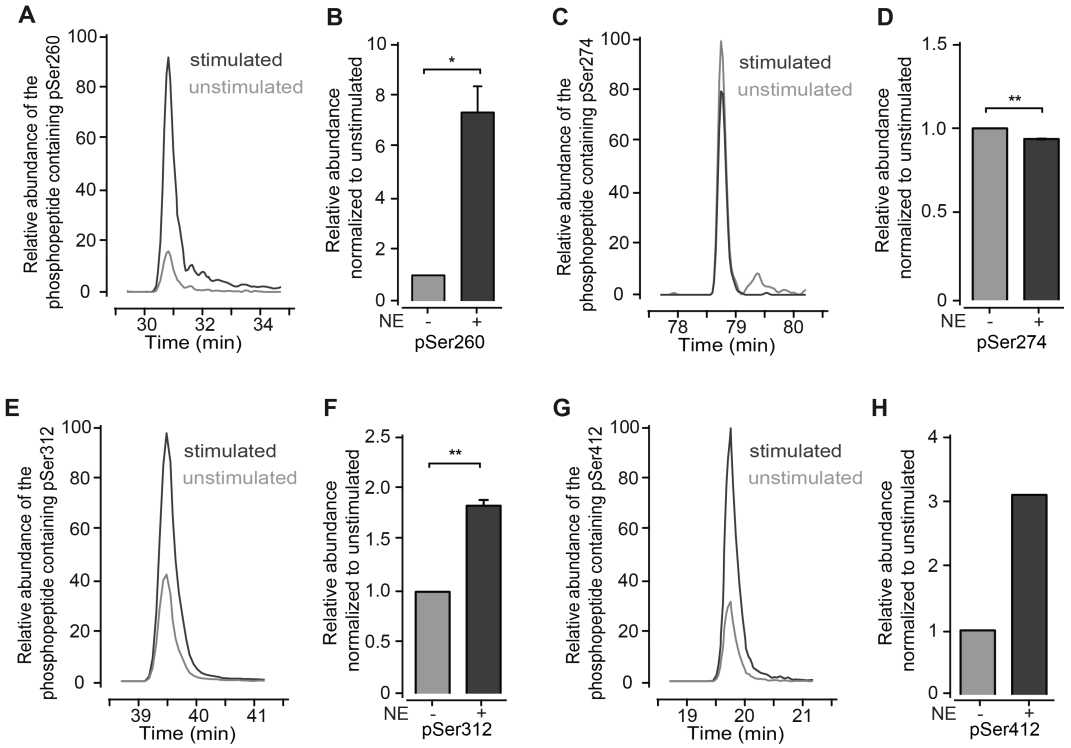

Figure 3.8: **Quantitative assessment of β_1-adrenoceptor phosphorylation: Extracted ion chromatogram of phosphorylated Ser260, Ser274, Ser312 and Ser412.**
(A) Extracted ion chromatogram (XIC) of raw intensities of the heavy and light phosphopeptide (REAQKQVKKIDSCERRF) containing Ser260. **(B)** Quantification of (A) by integration of the area under the curve using the software ImageJ. **(C)** XIC of the heavy and light phosphopeptide (FLGGPARPPSPSPSPVPAPAPPPGPPRPAAAAATAPLANGR) containing Ser274. **(D)** Quantification of (C). **(E)** XIC of the heavy and light phosphopeptide (RRPSRLVALR) containing Ser312. **(F)** Quantification of (E). **(G)** XIC of the heavy and light phosphopeptide (HATHGDRPRASGCLAR) containing Ser412. **(H)** Quantification of (G). n=1-3. **P*<0.05, ***P*<0.01 determined by unpaired t test.

3.2 Assessment of downstream signal transduction

There are two different pathways concerning downstream signal transduction of the β_1-adrenoceptor. First the G protein-dependent signaling and second the G protein-independent signal transduction (Figure 1.10). Since the latter is thought to be phosphorylation and arrestin binding dependent, this work focuses on the alternative signal transduction.

In order to elucidate the impact of different phosphorylation sites throughout the β_1-adrenoceptor, eight different ADRB1 mutants lacking various phosphosites were created. One stable HEK293 cell line was created with each of these different β_1-adrenoceptor variants.

3.2.1 Generation of phosphodeficient β_1-adrenoceptor mutants

To generate the eight different phosphodeficient ADRB1 variants, first the completely phosphodeficient ADRB1Δphos was created. The protein coding DNA sequence, which codes for the third intracellular loop and the receptor's C-terminus was synthesized by GeneArt (Chapter 2.1.3). Every codon, which codes for a threonine or a serine, was substited by the alanine codon GCA (Figures 3.9 and 3.10). The nucleotide sequence was flanked by two restriction enzyme sites: BsaAI was used to cut the 5' end of the nucleotide sequence and XbaI for the 3' end. An entry vector (pDONR) was digested with the same two enzymes and both vector and insert were separated using agarose gel electrophoresis. The DNA was then extracted from the gel and the two parts were ligated. This pDONR vector and the resulting pTRex expression vector were both used as a starting point for the other ADRB1 variants, which were

ADRB1 variant	**E1**	**E2**	**Mutated serine/threonine residues**
Δphos3rdloop^{a}	BsaAI	NotI	Ser360
Δphos3rdloop^{b}	NotI	SgrAI	Ser274, Ser276, Ser278, Thr298, Ser312
Δproximal	SgrAI	XmaI	Thr404, Ser412, Ser423
Δmiddle	XmaI	PasI	Ser428, Thr439
Δdistal	PasI	XbaI	Ser459, Ser461, Ser462, Ser473, Ser475

E = enzyme

ADRB1Δ3rdloop^{a}, ADRB1Δ3rdloop^{b}, Δproximal, Δmiddle and Δdistal were cloned using restriction enzyme digestion and ligation. All mutants were cloned in the

same way: pDONR-ADRB1Δphos was used to generate the inserts and pDONR-ADRB1 wild-type was used as destination vector in which the insert was ligated. The different C-terminal phosphodeficient variants were generated using heat pulse extension PCR (Chapter 2.2.1) with primers, that had specific mismatches to introduce the desired mutations. Figures 3.9 and 3.10 provide an overview of the different phosphodeficient ADRB1 mutants.

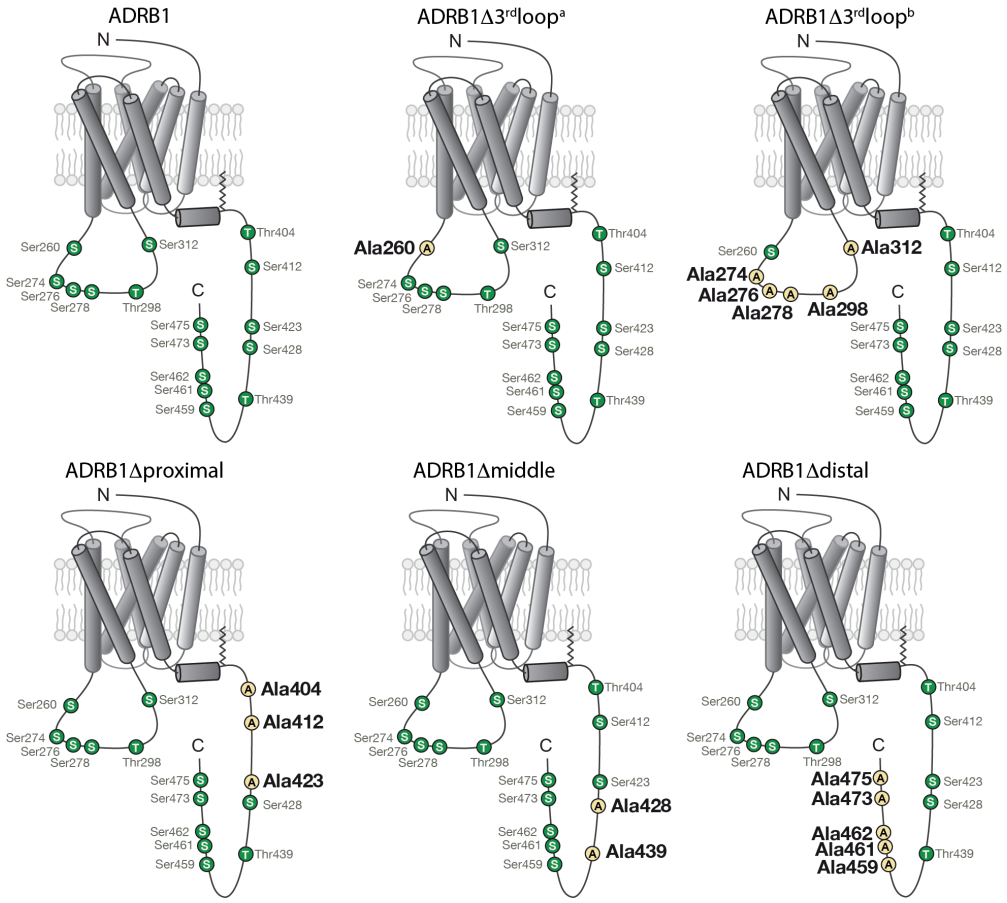

Figure 3.9: **Generation of different β_1-adrenoceptor mutants I.**
Different phosphodeficient ADRB1 mutants. From left to right and top to bottom: ADRB1 wild-type, Δphos3rdloopa, Δphos3rdloopb, Δproximal, Δmiddle, Δdistal. Green amino acids indicate native serine or threonine residues. Yellow amino acids indicate mutated alanine residues.

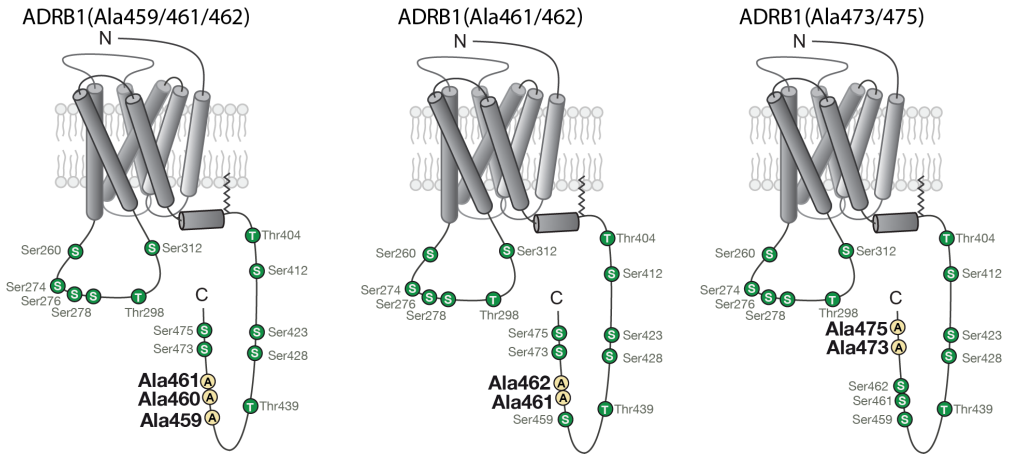

Figure 3.10: **Generation of different β_1-adrenoceptor mutants II.**
Different phosphodeficient ADRB1 mutants were created. From left to right: Ala459/462/462, Ala462/462 and Ala473/475. Green amino acids indicate native serine or threonine residues. Yellow amino acids indicate mutated alanine residues.

Similar protein expression was verified with radioligand binding as seen in figure 3.11 and described in chapter 2.2.3.

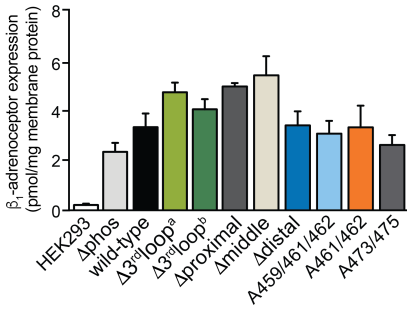

Figure 3.11: **Expression levels of the different ADRB1 variants.**
Expression of the different ADRB1 variants stably transfected in HEK293 cells determined by radioligand binding on membrane fractions. n = 3-7.

Verification of phosphodeficiency of the ADRB1 mutants To test whether the ADRB1Δphos was truly phosphodeficient, a radioactive phosphorylation assay was conducted (Figure 3.12). The ADRB1Δphos was compared to the Δphos3rdloop^{a}, Δphos3rdloop^{b} and the Δdistal variants.

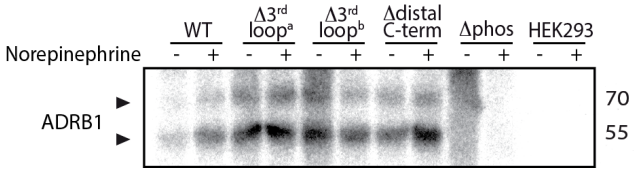

Figure 3.12: **Radioactive phosphorylation of different β_1-adrenoceptor variants.** Radioactive phosphorylation assay. HEK293 cells stably transfected with different ADRB1 variants were stimulated for five minutes with 100 µM norepinephrine and then immunoprecipitated. Radioactive ^{32}phosphorous was detected using a phosphoimaging system.

The radioactive phosphorylation assay confirmed the assumption, that the completely phosphodeficient ADRB1 could no longer become phosphorylated. However, when looking at ADRB1 mutants where more than one phosphorylation site had been mutated, it becomes clear, that the radioactive phosphorylation assay is not very sensitive. For this experiment several phosphosites have been mutated to alanine residues, however this still does not result in a noticeable change in phosphorylation as detected by the radioactive phosphorylation assay.

3.2.2 Arrestin recruitment to the β_1-adrenoceptor

It is believed that intracellular phosphorylation is a prerequisite for arrestin binding to G protein-coupled receptors. Therefore we investigated arrestin binding to the β_1-adrenoceptor using a FRET-based arrestin recruitment assay as described in chapter 1.4.3.

To verify accurate membrane and intracellular localization of the Cer-tagged β_1-adrenoceptor and the YFP-tagged β-arrestin2, respectively, a transient transfection following confocal microscopy was performed. Figure 3.13 depicts the membrane localization of serveral ADRB1-Cer variants and the cytosolic localization of YFP-β-arrestin2.

Impact of the third intracellular loop on arrestin recruitment

The strongest phosphorylation regulation, that was observed in the SILAC experiment (Chapter 3.1.3), was in the third intracellular loop, namely at serine 260. We therefore investigated the impact of phosphorylation in the third intracellular loop on arrestin recruitment to the ADRB1 using two ADRB1 mutants to cover the potential phosphorylation sites. The first mutant, ADRB1$\Delta 3^{rd}loop^{a}$, was a single site mutant: only Ser260 was mutated to Ala260. The second receptor variant, ADRB1$\Delta 3^{rd}loop^{b}$, contained five potential phosphorylation sites: Ser274, Ser276, Ser278, Thr298 and Ser312. These five residues had all been mutated to alanine (Figure 3.14 (A)).

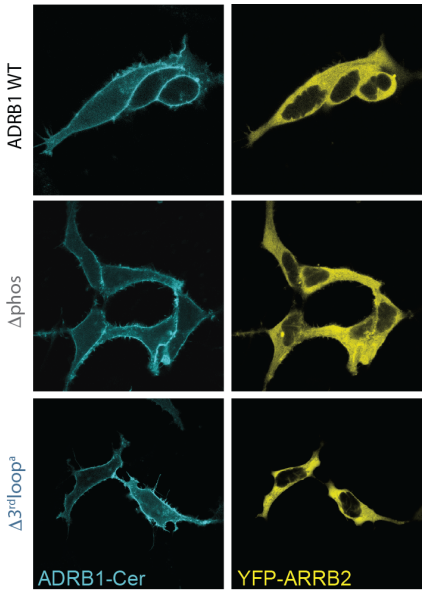

Figure 3.13: **Membrane localization of different β_1-adrenoceptor mutants.**
Confocal microscopy of different cerulean-tagged β_1-adrenoceptor mutants and YFP-tagged β-arrestin2. The receptors are correctly located in the membrane, while β-arrestin2 exhibits a cytosolic expression pattern.

The different receptor variants were all Cer-tagged and β-arrestin2 was N-terminally fused to YFP. When the two fluorophores were in close proximity, this led to an increase in FRET ratio. The completely phoshodeficient β_1-adrenoceptor exhibited a significantly lower FRET ratio compared to wild-type (Figure 3.14 (B) and

(C)). However, neither ADRB1Δ3rdloopa nor ADRB1Δ3rdloopb showed any change in β-arrestin recruitment as compared to wild-type ADRB1 (Figure 3.14 (C)).

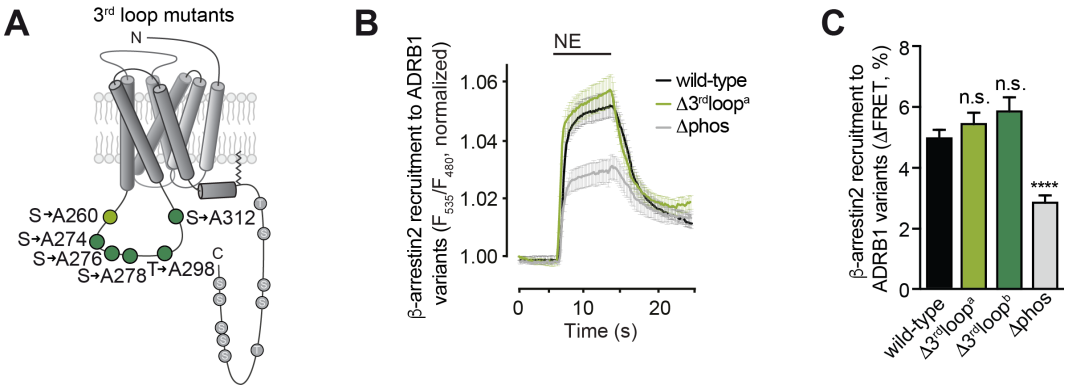

Figure 3.14: **Phosphorylation sites in the third intracellular loop do not influence arrestin recruitment to the ADRB1.**
(**A**) β_1-adrenoceptor schematic highlighting the phosphosite mutants of the third intracellular loop. Light green: ADRB1Δ3rdloopa, dark green: ADRB1Δ3rdloopb (**B**) Mean ± SEM of 10-12 representative FRET tracings comparing wild-type ADRB1, ADRB1Δ3rdloopa and ADRB1Δphos. In ADRB1Δphos all serine and threonine residues in the third intracellular loop and in the C-terminus were mutated to alanine residues. (**C**) Quantification of β-arrestin2 recruitment to different ADRB1 variants. Mean + SEM of 44-74 FRET amplitudes. In ADRB1Δ3rdloopb all serines and threonines in the third intracellular loop except for Ser260 have been mutated to alanine residues. Kruskal-Wallis-Test with Dunn's post test. **** $p \leq 0.0001$ vs. wild-type and n.s. = not significant.

Impact of the C-terminus on arrestin recruitment

To elucidate, where the significant decrease in β-arrestin2 recruitment seen with the ADRB1Δphos variant (Figure 3.14 (B) and (C)) originated, the C-terminal phosphorylation sites of the β_1-adrenoceptor were investigated. The large size of the C-terminus made it favorable to cover it by three different phosphodeficient β_1-adrenoceptor mutants, as opposed to two in case of the third intracellular loop. ADRB1Δproximal covered two serines and one threonine residue. Thr404, Ser412 and Ser423 had been exchanged for alanine in this receptor mutant. For the ADRB1 mutant ADRB1Δmiddle, two amino acids were mutated to alanine: Ser428 and Thr439. The last ADRB1 variant, ADRB1Δdistal, spanned five serine residues: Ser459, Ser461, Ser462, Ser473 and Ser475 (Figure 3.15 (A)).

Both ADRB1Δproximal as well as ADRB1Δdistal showed an impairment in β-arrestin2 recruitment to the β_1-adrenoceptor (Figure 3.15 (B)). For the Δdistal mutant the effect was comparable to the reduction in β-arrestin2 recruitment seen with the completely phosphodeficient ADRB1 mutant Δphos. ADRB1Δmiddle showed no change in arrestin recruitment as compared to wild-type ADRB1 (Figure 3.15 (C)).

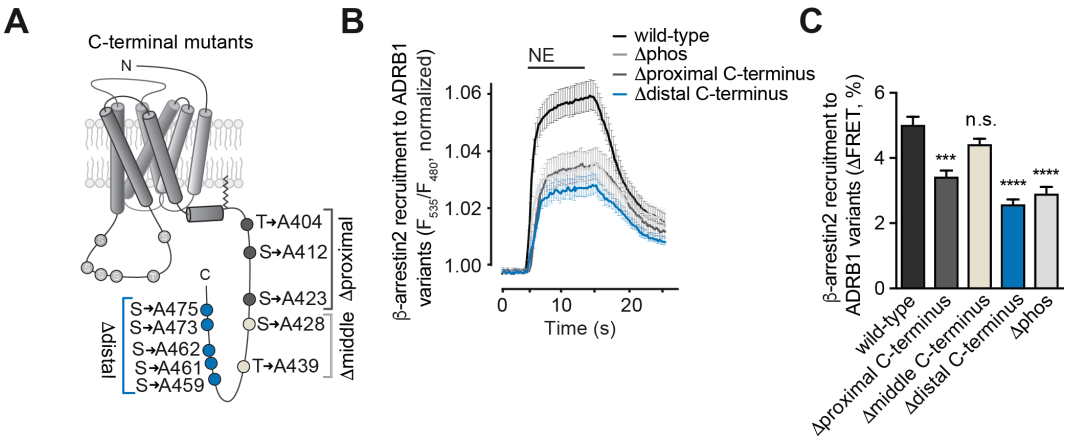

Figure 3.15: **Phosphorylation sites in the C-terminus are crucial for β-arrestin2 recruitment.** (**A**) Schematic of the C-terminally phosphodeficient ADRB1 variants: ADRB1Δproximal (dark grey), Δmiddle (ivory) and Δdistal (blue) C-terminus. (**B**) Mean ± SEM of 10-15 FRET tracings comparing wild-type ADRB1, ADRB1Δphos, ADRB1Δproximal and Δdistal C-terminus. (**C**) Quantification of β-arrestin2 recruitment of different ADRB1 variants. Mean + SEM of 30-78 FRET tracing amplitudes. Kruskal-Wallis-Test with Dunn's post test. **** $p \leq 0.0001$, *** $p \leq 0.001$ vs. wild-type and n.s. = not significant.

These results led to a thorough investigation of the distal C-terminus of the β_1-adrenoceptor.

Another three mutants were created to take a closer look at the very end of the receptor: Ala459/461/462, Ala461/462 and Ala473/475 (Figure 3.16 (A)). The two mutants Ala459/461/462 and Ala461/462 both exhibited a significant decrease in β-arrestin2 recruitment to the receptor variants, while the Ala473/475 mutant showed no change as compared to wild-type ADRB1 (Figure 3.16 (B) and (C)).

Ser461/462, which are important for β-arrestin2 recruitment to the ADRB1 show a strong conservation among different vertebrate species. This conservation seems similar to the conservation of the PDZ type I domain, which is located at the very end of the receptor and includes the two serine residues 473 and 475 (Figure 3.17).

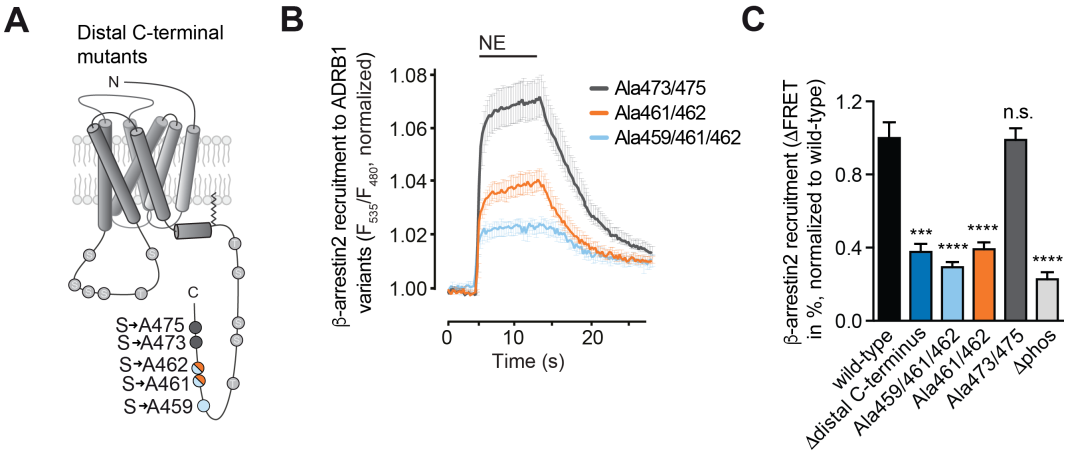

Figure 3.16: **Phosphorylation at serine 461 / serine 462 in the C-terminus determines arrestin binding.**
(**A**) Schematic of the ADRB1 variants representing the distal C-terminus: ADRB1(Ala459/461/462) (light blue), ADRB1(Ala461/462) (orange) and ADRB1 (Ala473/475) (dark grey). (**B**) Mean ± SEM of 6-13 FRET tracings comparing ADRB1(Ala459/461/462), ADRB1(Ala461/462) and ADRB1(Ala473/475). (**C**) Quantification of β-arrestin2 recruitment to ADRB1 variants. Mean + SEM of 9-36 FRET tracing amplitudes. Kruskal-Wallis test with Dunn's post test. *** $p \leq 0.001$ vs. wild-type, **** $p \leq 0.0001$ and n.s. = not significant.

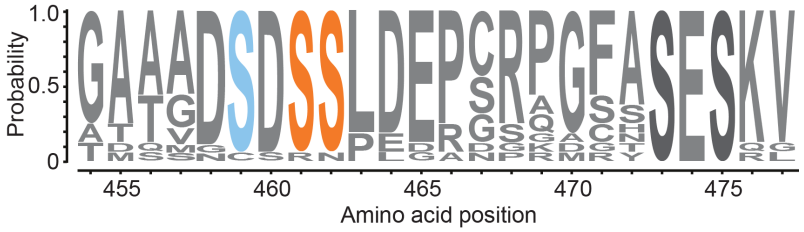

Figure 3.17: **The ADRB1 arrestin binding site is highly conserved among vertebrates.**
Positions 459 (light blue), 461 and 462 (orange) are compared among 12 different vertebrate species (human, mouse, zebrafish, duck, cow, guinea pig, dog, squirrel, elephant, turkey, gorilla and chicken). This image was created with Weblogo (Crooks et al., 2004).

3.2.3 Arrestin-mediated downstream signal transduction

Recruitment of arrestins to adrenoceptors is suggested to trigger receptor internalization and to initiate alternative signal transduction, e.g. activation of the MAP kinase pathway.

Internalization

To address the question whether phosphorylation of the β_1-adrenoceptor's distal C-terminus has an impact on receptor internalization, Cer-tagged β_1-adrenoceptor variants overexpressed in living HEK293 cells were analyzed via confocal microscopy (Figure 3.18 (A)). HEK293 cells were transiently co-transfected with either cerulean-tagged ADRB1 wild-type and YFP-β-arrestin2 or ADRB1Δdistal-Cer (ADRB1 lacking the five most distal C-terminal phosphosites) and YFP-β-arrestin2. Stimulation with 100 µM norepinephrine for 5 and 30 minutes, respectively, led to a stronger internalization of the wild-type receptor as compared to the ADRB1Δphosdistal-Cer variant, suggesting a link between receptor phosphorylation and its internalization.

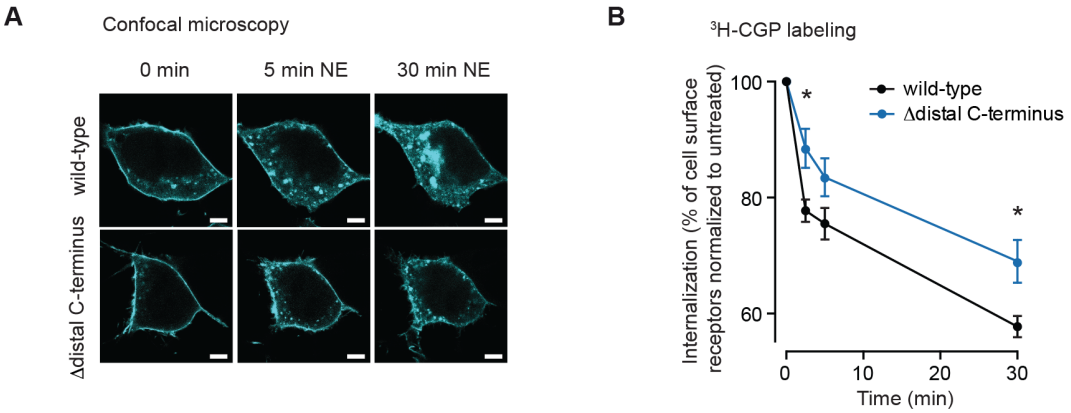

Figure 3.18: **Phosphorylation at the distal C-terminus of the ADRB1 determines receptor internalization.**
(**A**) Internalization of different ADRB1 variants determined by confocal microscopy after stimulation with 100 µM norepinephrine for 0, 5 and 30 minutes. Scale bar represents 5 µm. NE = norepinephrine. Representative of 6 independent experiments. (**B**) Internalization of ADRB1 wild-type and ADRB1Δdistal-C-terminus determined by loss of cell surface receptors labeled with ^{3}H-CGP. Stimulation with 100 µM norepinephrine for 0, 2.5, 5 and 30 minutes, respectively. Two-way ANOVA with Sidak's multiple comparisons test. * $P < 0.05$. n=4

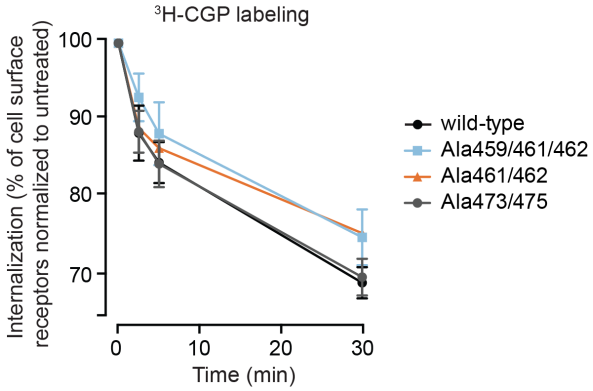

Figure 3.19: **Phosphorylation of serine 461 / 462 determines β_1-adrenoceptor internalization upon adrenergic stimulation.**
Internalization of ADRB1 wild-type, ADRB1(Ala459/461/462), ADRB1(Ala461/462), ADRB1(Ala473/475) determined by loss of cell surface receptors labeled with ^{3}H-CGP. Stimulation with 100 µM norepinephrine for 0, 2.5, 5 and 30 minutes, respectively. n=4

This qualitative observation was quantified by radioactive analysis of loss of ADRB1 surface expression upon stimulation with norepinephrine for 0, 2.5, 5 and 30 minutes (Figure 3.19 (B)). Wild-type ADRB1 and ADRB1Δdistal, which exhibited a similar reduction in receptor-arrestin interaction as mutation of Ser461/Ser462 alone (Chapter 3.2.2), were expressed in HEK293 cells along with Cerulean-tagged β-arrestin2. Norepinephrine stimulation led to both a significantly slower internalization of the ADRB1 lacking the five most distal serines as well as an overall reduced internalization resulting in a higher percentage of residual receptor at the cell surface after 2.5 and 30 minutes of stimulation compared to the wild-type ADRB1 (Figure 3.18 (B)).

To elucidate, whether this internalization impairment originated from phosphorylation of Ser461/462 or from the PDZ type I domain in the far-distal C-terminus, another radioactive internalization experiment was performed (Figure 3.19). ADRB1 (Ala459/461/462) and ADRB1(Ala461/462) both exhibited a decrease in internalization upon norepinephrine stimulation as compared to wild-type ADRB1. However, ADRB1(Ala473/475), which contains the PDZ type I domain, does not show any difference in stimulation-dependent internalization behavior, as compared to wild-type ADRB1.

These data point towards Ser461/462 being crucial for ADRB1 internalization.

MAPK1/3 activation

GPCR agonist-induced MAP kinase activation has been reported to result from G_s-dependent (Tilley, 2011), $G_{\beta\gamma}$-dependent (Hawes et al., 1995) and arrestin-dependent (Kim et al., 2005) signal transduction. Since arrestin binding is phosphorylation-dependent, the next question was whether the differences in β-arrestin recruitment to the various phosphosite-mutated receptor variants would be reflected in their ability to activate MAP kinase signaling.

To investigate this, we assessed MAP kinase activation (i.e. phosphorylation) in stably transfected HEK293 cells by quantitative western blot analyses. These assays were performed with and without agonist stimulation (5 minutes 100 µM norepinephrine). Interestingly, and in contrast to many other GPCRs, there was no change in MAPK1/3 phosphorylation in any of the phosphodeficient ADRB1 mutants, including ADRB1Δphos, ADRB1Δdistal, ADRB1(Ala459/461/462) and ADRB1(Ala461/462). These four ADRB1 mutants had all exhibited a significant reduction in β-arrestin recruitment, however, no decrease in MAP kinase activation was found (Figure 3.20).

To further investigate this unexpected finding, a western blot-based assay was performed, where the canonical signal transduction of the ADRB1 was blocked using the PKA inhibitor PKI (Figure 3.21). Untransfected HEK293 cells and cells expressing ADRB1 wild-type and ADRB1Δphos were compared at three different stimulation time points: unstimulated, stimulation for 5 and 15 minutes with 100 nM isoprenaline (ISO). It is proposed that stimulation for a short time period (i.e. 5 minutes) results in G protein-dependent MAPK activation and longer stimulation (i.e. 15 minutes) leads to arrestin-dependent MAPK phosphorylation (Ahn et al., 2004; Shenoy et al., 2006). Therefore we expected a significant decrease in MAPK activation after PKI treatment in wild-type ADRB1 stimulated with ISO for 5 minutes. We furthermore anticipated a reduction of MAPK phosphorylation after 15 minute stimulation and PKI treatment in the ADRB1Δphos as compared to wild-type ADRB1. Surprisingly, we could not verify either assumption.

Interestingly we found the ADRB1Δphos to be expressed significantly lower as compared to the other ADRB1 mutants, which was verified by radioligand binding (Figure 3.11). Furthermore this mutant seemed to run a few kDa lower on an SDS-PAGE than the other ADRB1 variants, which can be explained by the lack of phosphorylation and therefore smaller size.

These data suggest that agonist-induced MAPK1/3 activation through the ADRB1 does not depend on phosphorylation of the receptor.

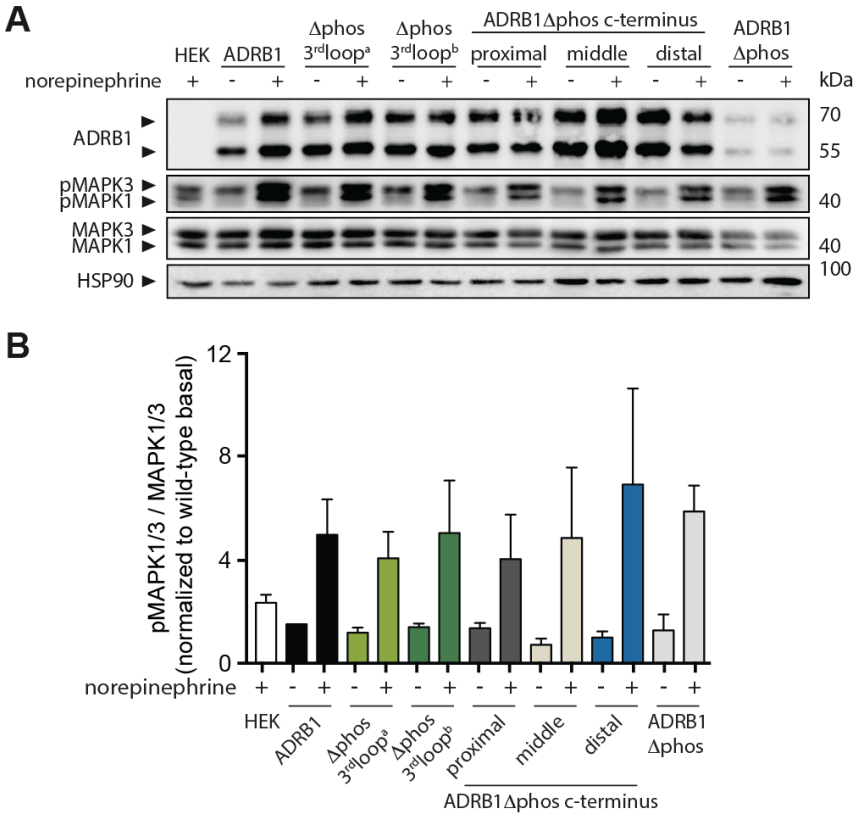

Figure 3.20: **MAP kinase 1/3 activation is preserved in the different phosphodeficient ADRB1 mutants.**
(**A**) Representative western blot of the different ADRB1 mutants with and without 100 µM norepinephrine stimulation for five minutes. Untransfected HEK293 cells are used as a negative control. (**B**) Quantification of (A). n = 3.

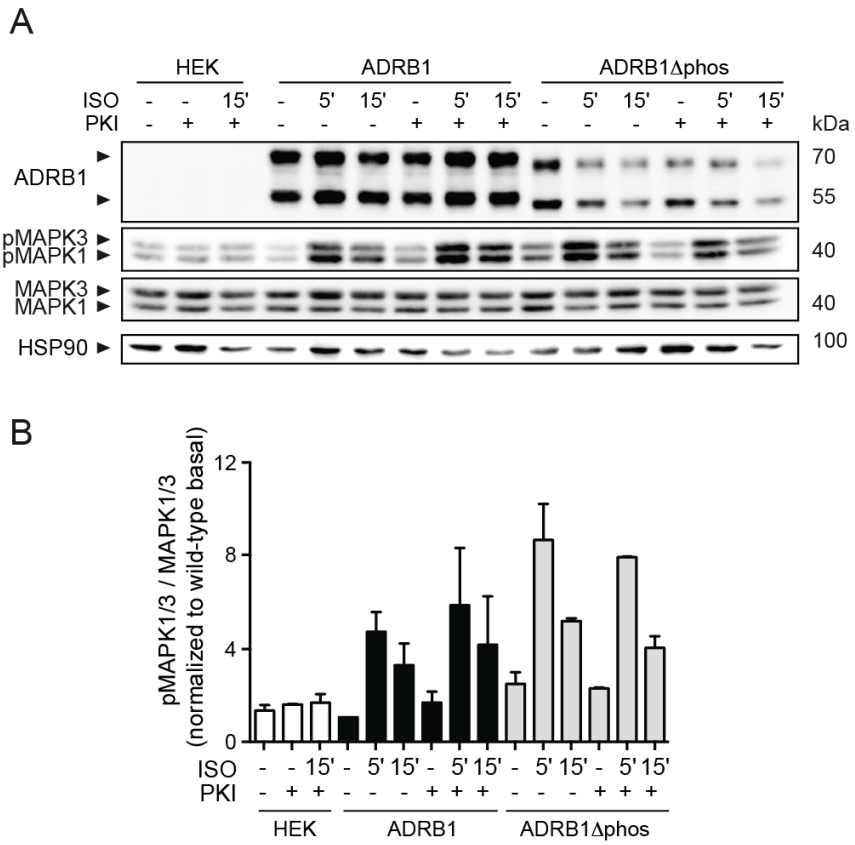

Figure 3.21: **Inhibition of canonical ADRB1 signaling does not impact MAP kinase activation.** Representative western blot analysis of ADRB1 wild-type and ADRB1Δphos with and without isoprenaline stimulation (100 nM) and with and without inhibition of canonical signal transduction using the PKA inhibitor PKI. (**A**) HEK293 cells either untransfected or stably expressing ADRB1 wild type and ADRB1Δphos were either left untreated or stimulated for 5 and 15 minutes, respectively. (**B**) Quantification of (A). ISO = isoprenaline. n = 4.

4 Discussion

Phosphorylation of G protein-coupled receptors is a key mechanism for their regulation. It facilitates the binding of arrestin proteins, which leads to uncoupling of the receptor from its cognate G protein. This stops the canonical signal transduction, i.e. leads to receptor desensitization. Apart from their function in terminating G protein-dependent signaling, arrestins can further act as docking proteins for other signaling proteins and thus initiate alternative signal transduction (Tilley et al., 2009; Ostermaier et al., 2014).

Even though phosphorylation is a very important regulatory mechanism, phosphorylation of the human ADRB1 is still poorly understood. The goal of this thesis was to investigate which sites in the ADRB1 are phosphorylated and how this phosphorylation impacts downstream signal transduction.

Using mass spectrometry and mutagenesis studies, we were able to elucidate the phosphorylation pattern of the β_1-adrenoceptor. Furthermore the receptor's arrestin recognition site could be identified: pSer461/462 determines arrestin recruitment to the ADRB1. Through binding of arrestins this site is also essential for agonist-dependent internalization of the receptor.

4.1 Phosphorylation of the β_1-adrenoceptor

Deciphering the receptor's phosphorylation via mass spectrometry

Mass spectrometry is a very common technique to discover and identify phosphorylation sites in proteins (Mann et al., 2002; Steen et al., 2006; Olsen and Mann, 2013). Our approach led to the identification of two phosphosites in the human β_1-adrenoceptor, which were previously known (Gardner et al., 2004; Gavi et al., 2007) and six novel ones. However, despite the successful identification of two (Ser312 and Ser412) of the three (Ser475, Nooh et al., 2014) known phosphosites, which proved that our approach was effective in identifying phosphorylation sites, we cannot exclude that there might be other phosphorylation sites, which were missed using our methodology. When looking at the number of phosphorylation sites and

comparing it to other GPCRs, the number and distribution of phosphorylation sites we found seem reasonable. The closely related ADRB2 contains 13 phosphorylation sites, three in the third intracellular loop and ten in the C-terminus (Nobles et al., 2011), the endothelin A receptor contains 14 serine/threonine phosphorylation sites, which are mostly located in the C-terminus (Gärtner et al., 2013).

The standard course of action in mass spectrometry is to first digest the protein using trypsin. Trypsin is a very powerful intestinal serine protease, which cleaves at the C-terminal sites of arginine and lysine. Given the unfavorable distribution of arginine and lysine residues within the ADRB1 and several missed cleavage sites, a tryptic digestion of the ADRB1 leads to a peptide mixture with some peptides being so big that they are hard to ionize in the mass spectrometer. The optimal peptide size for a mass spectrometry analysis is 9-10 amino acids (Swaney et al., 2010). In case of the ADRB1 peptides as big as 41 amino acids were found after the tryptic digest. This might be one of the reasons why there have not been any systematic studies of phosphorylation sites in the β_1-adrenoceptor so far.

We were able to overcome this problem by using three different proteases: trypsin, chymotrypsin and LysC. Before protein digestion, the samples were divided in half. One part was digested with chymotrypsin and the other with LysC. Both chymotrypsin and LysC are endoproteinases, used in sample preparation for mass spectrometry analysis (Giansanti et al., 2016). Chymotrypsin is similar to trypsin a protease from the digestive system. It cleaves at the C-terminal side of big hydrophobic amino acids such as tyrosine, tryptophan and phenylalanine. Due to its preference for hydrophobic residues, chymotrypsin is ideal for digestion of transmembrane proteins (Giansanti et al., 2016), such as the β_1-adrenoceptor. LysC cleaves at the C-terminal sites of lysine residues (Jekel et al., 1983; Giansanti et al., 2016) and leads to the formation of somewhat big protein pieces. Due to its cleaving site LysC digested peptides and tryptic peptides show a big overlap. The rationale for using LysC is therefore not to have another peptidase, which cleaves at additional sites, but rather to increase the efficiency of trypsin, which is generally used after a digestion with LysC and was also used in this study.

Norepinephrine stimulation

In order to induce maximal phosphorylation of the β_1-adrenoceptor, we used 100 µM of norepinephrine to stimulate the β_1-adrenoceptors prior to cell lysis and immunoprecipitation. Norepinephrine has a K_i of 3.57 µM regarding the ADRB1 (Hoffmann et al., 2004). This means that the norepinephrine concentration used for stimulation of the cells prior to mass spectrometry was approximately 28 times the K_i. This

is a supraphysiological concentration which was used to ensure full activation of the receptors when determining the phosphorylation pattern by mass spectrometry. For the FRET-based arrestin recruitment assays, a dose-response curve (data not shown) was recorded, which showed the maximal arrestin recruitment at 10 µM. Therefore this concentration was used for the arrestin recruitment assays.

4.2 Arrestin recruitment and arrestin-dependent signal transduction

4.2.1 Arrestin recruitment

We were able to newly identify the ADRB1 recognition site for β-arrestin2. Our data show that the amino acid sequence 459-SDSS-462 is crucial for binding of β-arrestin2 to the ADRB1. This β-arrestin2 recognition site does not seem to be conserved throughout different G protein-coupled receptors (Tobin et al., 2008).

While our FRET-based approach was very successful regarding the interaction of the β_1-adrenoceptor and β-arrestin2, we were not able to detect any interaction between the receptor and the other non-visual arrestin, β-arrestin1.

This could be explained by two scenarios. One would be that the ADRB1 belongs to the class A receptors regarding arrestin recruitment. These receptors, such as the β_2-adrenoceptor preferably interact with β-arrestin2 over β-arrestin1 and not with the visual arrestins. Class B receptors do not discriminate between the two non-visual arrestins and also interact with the visual arrestins. The fact that the ADRB2 is a class A receptor might be a hint that the ADRB1 could also be class A. However the GPCR classes regarding arrestin interaction are not only defined by the types of arrestins a given GPCR interacts with, but also by the recycling properties of that GPCR. After internalization class A receptors undergo a rapid recycling back to the plasma membrane, due to the more transient nature of their interaction with β-arrestin2. In contrast to that, class B receptors bind arrestins stronger and thus show a slower recycling. To ultimately assign the ADRB1 to class A or class B receptors, one would need to know its recycling timeline. It is known that the ADRB1 undergoes a recycling back to the membrane (Nakagawa and Asahi, 2013; Nooh et al., 2014) but so far the time line of that recycling remains elusive, which is why no clear categorization of the ADRB1 into class A or B can be undertaken at the moment.

The other explanation for our lack of success in observing β_1-adrenoceptor-β-arrestin1-interaction could be that the two fluorophores fused to the receptor and β-arrestin1, respectively, are not optimally orientated on the proteins and no energy transfer occurs even though the two proteins might interact. This could be tested by optimizing the fluorophores or changing the linker between fluorophore and protein. Another possibility would be to switch to another assay to observe the putative interaction, for example doing a BRET assay (Nobles et al., 2011) or a co-immunoprecipitation (McCrink et al., 2016).

Another very interesting technique to further investigate arrestin recruitment to the ADRB1 would be the newly developed β-arrestin FlAsH (fluorescein arsenical hairpin) sensors. Nuber et al., 2016 have been able to investigate not only the FRET change derived from arrestin recruitment to the GPCR, they also visualized the ligand-induced conformational change within the arrestin molecule itself. They found the arrestin protein to remain active for a short time even after dissociation from their GPCR. This work studied several GPCRs including the ADRB2, the M2 muscarinic acetylcholine receptor and the parathyroid hormone type 1 receptor, however not the ADRB1. It would be fascinating to use this tool to drill deeper into ADRB1-β-arrestin2 interaction.

4.2.2 Arrestin-mediated downstream signal transduction

Internalization of the ADRB1

Arrestin binding to G protein-coupled receptors leads to receptor internalization through the interaction of arrestins with clathrin and/or the clathrin adaptor protein AP2 (Goodman et al., 1996; Goodman et al., 1997; Oakley et al., 1999; Laporte et al., 2002).

Internalization of the β_1-adrenoceptor has been studied by several groups with very different outcomes, which range from no internalization at all (Eichel et al., 2016) to a strong endophilin-dependent ADRB1 internalization (Boucrot et al., 2015). Our own results showed differences regarding the wild-type ADRB1 internalization. The first set of experiments showed a maximal receptor internalization of the wild type ADRB1 after 30 minutes of norepinephrine stimulation of 42 % (Figure 3.18). In the second experiment we observed a lower maximal internalization of 30 % (Figure 3.19). All experimental conditions had remained exactly the same. The only difference between the two sets of experiments was that the first set was conducted in summer, while the second set was carried out in winter. This could be a possible explanation for the smaller degree of internalization in the second set of

experiments, as internalization is strongly temperature dependent (Penheiter et al., 2002).

There are many reasons for the discrepancies in the field regarding internalization findings. Some groups study the murine Adrb1 (Rapacciuolo et al., 2003), while we and others study the human receptor. Most of these studies are performed in HEK293 cells, which should make them very comparable. However, even slight differences in the expression levels of the receptors or the GRKs can result in big differences for the recruitment of arrestins and therefore internalization. This becomes clear when looking closely at the methodology used by different researchers. Some groups need to co-transfect the ADRB1 together with β-arrestins and GRKs to see an effect (Zindel et al., 2015), while others only transfect the receptor (Eichel et al., 2016) or the receptor together with β-arrestin, as we did. This infers that the same cell line in different laboratories can show differences in protein expression, which could explain the different findings.

It is generally believed that the β_1-adrenoceptor internalizes to a much smaller extent as compared to the β_2-adrenoceptor (Shiina et al., 2000; Liang et al., 2003; Eichel et al., 2016). This is thought to be due to a relatively weak interaction of the ADRB1 with β-arrestin (Shiina et al., 2000). Our own data confirm that the ADRB1 both interacts weaker with β-arrestin2 and also internalizes less than the ADRB2. Nonetheless, we were able to observe a consistent internalization of the ADRB1 with and without co-transfection of β-arrestin2, with the extent of internalization being stronger with co-transfection (data not shown). While our data hint at Ser461/462 being the β_1-adrenoceptor's arrestin recognition site and therefore also the driver of internalization (Chapter 3.2.3), others have found Ser312 to be the main phosphosite responsible for internalization (Gardner et al., 2004; Nooh et al., 2014). This internalization is thought to be dependent on the β_1-adrenoceptor's PDZ type I domain and on the subsequent interaction with SAP97. As far as the involvement of kinases goes, Ser312 is known to be phosphorylated by PKA (Gardner et al., 2004). Due to this the authors conclude that ADRB1 internalization is strictly protein kinase A dependent. This is in contrast to the internalization of most other GPCRs.

It is moreover generally accepted that phosphorylation by G protein-coupled receptor kinases is the prerequisite for arrestin binding and therefore internalization (Vaughan et al., 2006). Our data did not show differences in internalization for the Ala312 mutant as compared to wild-type ADRB1 as determined by confocal internalization assay (data not shown). These different findings could be due to slight differences in protein expression in the HEK293 cells or the different methodology used.

Another very interesting finding is that the internalization pathway may differ depending on which kinases phosphorylate the receptor. Rapacciuolo et al., 2003 have found that PKA phosphorylation leads to a β_1-adrenoceptor internalization via caveolae, while GRK-mediated phosphorylation leads to clathrin-mediated endocytosis. However, this study was performed on the mouse Adrb1 and since there is no complete conservation of phosphorylation sites between the murine and human ADRB1, this finding cannot be directly translated to the model we used in our study.

Apart from the mode of internalization, several recent studies demonstrated the ability of different GPCRs to continue signaling after they have been internalized (Ferrandon et al., 2009; Kuna et al., 2013; Merriam et al., 2013; Irannejad et al., 2013). This is a very interesting finding, as the predominant opinion used to be that G protein-coupled receptors completely stop signaling after internalization. For the ADRB1 this phenomenon has not been shown yet. There has been one study (Eichel et al., 2016), where the authors have attributed continuous ADRB1 signaling to clathrin-coated structures rather than endosomes. They propose arrestin activation 'at a distance', meaning β-arrestin is not bound to the GPCR which activated it, during the internalization process (before endocytotic scission). During this state it can stay active and cause MAP kinase signaling from clathrin-coated structures. This is different from the previous model, which the authors call 'activation from the complex', meaning that β-arrestin has to be bound to its GPCR in order to induce alternative signal transduction.

Therefore internalization of the ADRB1 remains a very controversial topic. Additional studies are needed to elucidate which mechanism or which combination of mechanisms is used by the ADRB1 for internalization and which (phospho-) sites and kinases are of main importance.

Activation of MAPK1/3

Apart from arrestin binding leading to receptor internalization it is shown for many GPCRs that arrestin recruitment to the receptor can lead to an alternative signal transduction (Luttrell and Gesty-Palmer, 2010). This G protein-independent, arrestin-dependent signaling targets effector proteins of several prominent signal transduction cascades such as MAPK1/3, c-Src, JNK and Akt (Noor et al., 2011).

It is generally thought that, when stimulating a GPCR it first initiates a G protein-dependent response i.e. an increase/decrease in cAMP or IP3 concentration, respectively. Following this response is a G protein-independent response, that is triggered by binding of arrestins and subsequent binding of other signal transduction

proteins to the arrestin proteins. The time frame for the two responses is about five minutes for the G protein-dependent response and about 20 to 30 minutes for the arrestin-dependent response (Ahn et al., 2004). This is termed the *two waves of signaling*. The best studied adrenoceptor in this regard is the ADRB2 (Luttrell et al., 1999).

Since arrestin recruitment is phosphorylation-dependent, alternative signal transduction must hence be also phosphorylation-dependent. Therefore we wanted to test this phenomenon for the β_1-adrenoceptor with our phosphorylation-deficient ADRB1 mutants. For these receptor variants either all potential phosphorylation sites had been removed (ADRB1Δphos) by mutating the serine and threonine residues to alanines or the phosphorylation sites where only partially mutated. All receptors, which contained alanine residues at position 461/462 instead of serines had already exhibited a severe reduction in arrestin recruitment (Chapter 3.14) and should therefore be ideal tools to investigate arrestin-dependent biased alternative signal transduction of the β_1-adrenoceptor. However, our data could not reproduce the two waves of signaling for the ADRB1 as they did not show an arrestin-based MAPK1/3 activation (Chapter 3.2.3). If there was a G protein-independent, arrestin-based activation of these kinases, their activation should have been diminished in the phosphorylation-deficient ADRB1 mutants. These mutants showed a significant impairment in β-arrestin2 recruitment, but no change in MAPK1/3 activation as assessed by western blotting.

Possible explanations for this could be that 1) our methodology did not pick up the changes in the activated states of the proteins, 2) our phosphorylation-deficient mutants, where up to 16 serine and threonine residues are exchanged for alanine residues, do not fold correctly, or 3) this effect is not present in case of β_1-adrenoceptor signal transduction. The first possible explanation is hard to exclude. It could only be ruled out if this data was reproduced in other laboratories. Against the second possibility argues that the phosphorylation-deficient mutants exhibited a correct running pattern on an SDS-PAGE gel, they showed normal cAMP production and normal activation upon agonist stimulation in FRET-based experiments. This leaves us with the third explanation, which cannot be conclusively proven until this data has been reproduced and a systematic error is ruled out.

4.3 Outlook

This work determined the phosphorylation pattern of the β_1-adrenoceptor as well as the receptor's arrestin recognition site, which controls arrestin recruitment and receptor internalization. This thesis can therefore be seen as the basis for a number of very interesting questions, which could be pursued in the future. Knowing these sites enables the community to develop phosphosite-specific antibodies to further study β_1-adrenoceptor phosphorylation. The availability of such antibodies would facilitate the identification of the responsible kinases by employing an siRNA-mediated knockdown of likely candidates such as GRK2, 3 and 5, and protein kinase A, B and C. This will give more insight into the receptor's function and regulation.

These antibodies could also be used as tools to examine diagnostic samples obtained from patients. It is unlikely that they could be used for primary diagnostics, as each test would require a heart biopsy, so that the antibodies could be used on tissue. However, phosphosite-specific monoclonal antibodies could nonetheless be a great asset which would help us to deeper understand the underlying principles of different cardiac diseases, such as heart failure. To date we know that heart failure is accompanied by a supraphysiological norepinephrine concentration in the blood (Cohn et al., 1984). It is very conceivable, that this high norepinephrine concentration results in a very strong receptor phosphorylation. So far we can only hypothesize about these circumstances. Using the Ser461/462 phosphorylation site, that was identified in this thesis, to generate these tools, could enable researchers to close this gap and investigate the molecular basis of heart failure.

We determined the receptor's phosphorylation pattern upon supraphysiological norepinephrine stimulation. It is shown for other GPCRs, that there can be both a dose-dependent as well as a ligand-dependent change in receptor phosphorylation (Lehmann et al., 2016). Since the β_1-adrenoceptor is the target of one of the most prescribed medications worldwide, the β-blockers, it would be of great interest to determine whether the phosphorylation pattern and potentially also the arrestin recruitment change upon antagonist treatment. As it is described for many other GPCRs, there might be an antagonist-dependent arrestin-mediated MAP kinase activation (Erickson et al., 2013). This has been reported especially for carvedilol (Wisler et al., 2007), but also for metoprolol (Nakaya et al., 2012), which is the most used β-blocker in Germany. On these grounds it is of high interest to elucidate the potential β-blocker-initiated arrestin-dependent signaling.

Another aspect, which is still not fully understood is the role of the p.Arg389Gly polymorphism regarding the receptor's phosphorylation. It is known, that the Arg389

variant of the β_1-adrenoceptor is both hyperfunctional and stronger phosphorylated. While the association between the p.Arg389Gly polymorphism and susceptibility for heart failure and hypertension remains controversial (Ahles and Engelhardt, 2014), there seems to be a strong link between the more common Arg389 variant and a stronger response to β-agonists and -antagonists. Whether there is a causal link between ADRB1(Arg389) hyperphosphorylation and the increased responsiveness to ligands, remains to be studied.

Dealing with such a prominent and important protein, there are obviously many more interesting aspects to investigate. Developing phosphosite-specific antibodies, identifying the kinases, characterizing the impact of β-blocker treatment on receptor phosphorylation and studying the potential link between the p.Arg389Gly polymorphism, phosphorylation and responsiveness to β-blockers would get us a lot closer to understanding the β_1-adrenoceptor.

List of Figures

Bibliography

Ahles, Andrea and Stefan Engelhardt (2014). “Polymorphic variants of adrenoceptors: pharmacology, physiology, and role in disease.” In: *Pharmacological reviews* 66.3, pp. 598–637 (cit. on pp. 8–10, 89).

Ahles, Andrea et al. (2015). “Interhelical interaction and receptor phosphorylation regulate activation kinetics of different human β1-adrenoceptor variants.” In: *The Journal of biological chemistry* (cit. on pp. 9, 16).

Ahn, Seungkirl et al. (2004). “Differential kinetic and spatial patterns of β-arrestin and G protein-mediated ERK activation by the angiotensin II receptor.” In: *The Journal of biological chemistry* 279.34, pp. 35518–35525 (cit. on pp. 78, 87).

Alexander, Stephen P H et al. (2013). “The concise guide to pharmacology 2013/14: G protein-coupled receptors.” In: *British Journal of Pharmacology* 170.8, pp. 1459–1581 (cit. on p. 3).

Andersson, Lennart (1991). “Recognition of phosphate groups by immobilized aluminium(III) ions.” In: *Journal of Chromatography A* 539.2, pp. 327–334 (cit. on p. 28).

Andersson, Lennart and Jerker Porath (1986). “Isolation of phosphoproteins by immobilized metal (Fe3+) affinity chromatography.” In: *Analytical Biochemistry* 154.1, pp. 250–254 (cit. on p. 28).

Arshavsky, Vadim Y. (2002). “Rhodopsin phosphorylation: From terminating single photon responses to photoreceptor dark adaptation.” In: *Trends in Neurosciences* 25.3, pp. 124–126 (cit. on p. 16).

Attwood, T. K. and J. B. C. Findlay (1994). “Fingerprinting G-protein-coupled receptors.” In: *Protein Engineering, Design and Selection* 7.2, pp. 195–203 (cit. on p. 3).

Audi, G. et al. (2003). “The NUBASE evaluation of nuclear and decay properties.” In: *Nuclear Physics A* 729.1, pp. 3–128 (cit. on p. 30).

Barak, L S et al. (1995). “The conserved seven-transmembrane sequence NP(X)2, 3Y of the G-protein-coupled receptor superfamily regulates multiple properties of the β2-adrenergic receptor.” In: *Biochemistry* 34.47, pp. 15407–14 (cit. on p. 5).

Bartlett, John M S and David Stirling (2003). “A short history of the polymerase chain reaction.” In: *Methods in molecular biology* 226, pp. 3–6 (cit. on p. 37).

Belmonte, Stephen L and Burns C Blaxall (2011). “G protein-coupled receptor kinases as therapeutic targets in cardiovascular disease.” In: *Circulation research* 109.3, pp. 309–19 (cit. on p. 12).

Bemben, Michael A et al. (2014). “CaMKII phosphorylation of neuroligin-1 regulates excitatory synapses.” In: *Nature neuroscience* 17.1, pp. 56–64 (cit. on p. 22).

Benovic, J L et al. (1986). “β-adrenergic receptor kinase: identification of a novel protein kinase that phosphorylates the agonist-occupied form of the receptor.” In: *Proceedings of the National Academy of Sciences of the United States of America* 83.9, pp. 2797–801 (cit. on p. 12).

Birnbaumer, Lutz (2007). “Expansion of signal transduction by G proteins. The second 15 years or so: from 3 to 16 alpha subunits plus betagamma dimers.” In: *Biochimica et biophysica acta* 1768.4, pp. 772–93 (cit. on p. 7).

Blundell, Michael P et al. (2009). “Phosphorylation of WASp is a key regulator of activity and stability in vivo.” In: *Proceedings of the National Academy of Sciences of the United States of America* 106.37, pp. 15738–15743 (cit. on p. 22).

Börjesson, M et al. (2000). “A novel polymorphism in the gene coding for the β1-adrenergic receptor associated with survival in patients with heart failure.” In: *European heart journal* 21.22, pp. 1853–8 (cit. on p. 9).

Boucrot, Emmanuel et al. (2015). “Endophilin marks and controls a clathrin-independent endocytic pathway.” In: *Nature* 517.7535, pp. 460–5 (cit. on pp. 18, 84).

Bouvier, M et al. (1988). “Removal of phosphorylation sites from the β2-adrenergic receptor delays onset of agonist-promoted desensitization.” In: *Nature* 333.6171, pp. 370–3 (cit. on p. 16).

Bruck, Heike et al. (2005). “The Arg389Gly beta1-adrenoceptor polymorphism and catecholamine effects on plasma-renin activity.” In: *Journal of the American College of Cardiology* 46.11, pp. 2111–5 (cit. on p. 10).

Cantin, Greg T. et al. (2007). “Optimizing TiO2-based phosphopeptide enrichment for automated multidimensional liquid chromatography coupled to tandem mass spectrometry.” In: *Analytical chemistry* 79.12, pp. 4666–73 (cit. on p. 21).

Cao, T T et al. (1999). “A kinase-regulated PDZ-domain interaction controls endocytic sorting of the β2-adrenergic receptor.” In: *Nature* 401.6750, pp. 286–90 (cit. on pp. 5, 18).

Catterall, W A (2000). “Structure and regulation of voltage-gated Ca2+ channels.” In: *Annual review of cell and developmental biology* 16, pp. 521–55 (cit. on p. 9).

Celver, J P et al. (2001). “Threonine 180 is required for G-protein-coupled receptor kinase 3- and β-arrestin2-mediated desensitization of the mu-opioid receptor in Xenopus oocytes.” In: *Journal of Biological Chemistry* 276.7, pp. 4894–4900 (cit. on p. 15).

Clapham, D E and E J Neer (1997). “G protein betagamma subunits.” In: *Annual review of pharmacology and toxicology* 37, pp. 167–203 (cit. on p. 6).

Cohn, J N et al. (1984). “Plasma norepinephrine as a guide to prognosis in patients with chronic congestive heart failure.” In: *The New England journal of medicine* 311.13, pp. 819–23 (cit. on p. 88).

Cotecchia, Susanna, Laura Stanasila, and Dario Diviani (2012). “Protein-Protein Interactions at the Adrenergic Receptors.” In: *Current Drug Targets* 13.1, pp. 15–27 (cit. on p. 13).

Crooks, Gavin E et al. (2004). “WebLogo: a sequence logo generator.” In: *Genome research* 14.6, pp. 1188–90 (cit. on p. 75).

Daaka, Y, L M Luttrell, and R J Lefkowitz (1997). “Switching of the coupling of the β2-adrenergic receptor to different G proteins by protein kinase A.” In: *Nature* 390.6655, pp. 88–91 (cit. on p. 19).

De Lean, A, J M Stadel, and R J Lefkowitz (1980). “A ternary complex model explains the agonist-specific binding properties of the adenylate cyclase-coupled β-adrenergic receptor.” In: *The Journal of biological chemistry* 255.15, pp. 7108–17 (cit. on p. 15).

Deupi, Xavier and Brian Kobilka (2007). “Activation of G protein-coupled receptors.” In: *Advances in protein chemistry* 74.07, pp. 137–66 (cit. on p. 3).

Drake, Matthew T., Sudha K. Shenoy, and Robert J. Lefkowitz (2006). *Trafficking of G protein-coupled receptors* (cit. on p. 12).

Eichel, K., D. Jullié, and M. von Zastrow (2016). “β-Arrestin drives MAP kinase signalling from clathrin-coated structures after GPCR dissociation.” In: *Nature cell biology* 18.3, pp. 303–10 (cit. on pp. 18, 84–86).

Erickson, Catherine E. et al. (2013). “The β-blocker Nebivolol Is a GRK/β-arrestin Biased Agonist.” In: *PLoS ONE* 8 (cit. on p. 88).

Eyrich, Beate, Albert Sickmann, and René Peiman Zahedi (2011). “Catch me if you can: mass spectrometry-based phosphoproteomics and quantification strategies.” In: *Proteomics* 11.4, pp. 554–70 (cit. on pp. 27, 28).

Ferguson, S S (2001). “Evolving concepts in G protein-coupled receptor endocytosis: the role in receptor desensitization and signaling.” In: *Pharmacological reviews* 53.1, pp. 1–24 (cit. on p. 16).

Ferrandon, Sébastien et al. (2009). “Sustained cyclic AMP production by parathyroid hormone receptor endocytosis.” In: *Nature chemical biology* 5.10, pp. 734–42 (cit. on p. 86).

Fílla, Jan et al. (2012). “Enrichment techniques employed in phosphoproteomics.” In: *Amino Acids* 43.3, pp. 1025–1047 (cit. on p. 28).

Fredriksson, Robert et al. (2003). “The G-protein-coupled receptors in the human genome form five main families. Phylogenetic analysis, paralogon groups, and fingerprints.” In: *Molecular pharmacology* 63.6, pp. 1256–72 (cit. on p. 3).

Frielle, Thomas et al. (1987). “Cloning of the cDNA for the human β1-adrenergic receptor.” In: *Proceedings of the National Academy of Sciences of the United States of America* 84.22, pp. 7920–4 (cit. on p. 3).

Fritze, Olaf et al. (2003). “Role of the conserved NPxxY(x)5,6F motif in the rhodopsin ground state and during activation.” In: *Proceedings of the National Academy of Sciences of the United States of America* 100.5, pp. 2290–5 (cit. on p. 5).

Gardner, Lidia a et al. (2004). “Role of the cyclic AMP-dependent protein kinase in homologous resensitization of the β1-adrenergic receptor.” In: *The Journal of biological chemistry* 279.20, pp. 21135–43 (cit. on pp. 13, 18, 81, 85).

Gardner, Lidia a, Anjaparavanda P Naren, and Suleiman W Bahouth (2007). “Assembly of an SAP97-AKAP79-cAMP-dependent protein kinase scaffold at the type 1 PSD-95/DLG/ZO1 motif of the human β1-adrenergic receptor generates a receptosome involved in receptor recycling and networking.” In: *The Journal of biological chemistry* 282.7, pp. 5085–99 (cit. on p. 18).

Gärtner, Florian et al. (2013). “Desensitization and internalization of endothelin receptor A: impact of G protein-coupled receptor kinase 2 (GRK2)-mediated phosphorylation.” In: *The Journal of biological chemistry* 288.45, pp. 32138–48 (cit. on p. 82).

Gavi, Shai et al. (2007). “Insulin-Like Growth Factor-I Provokes Functional Antagonism and Internalization of β1 -Adrenergic Receptors.” In: *Endocrinology* 148.6, pp. 2653–2662 (cit. on pp. 13, 81).

Gerber, Kyle J, Katherine E Squires, and John R Hepler (2016). “Roles for Regulator of G Protein Signaling Proteins in Synaptic Signaling and Plasticity.” In: *Molecular pharmacology* 89.2, pp. 273–86 (cit. on p. 7).

Giansanti, Piero et al. (2016). “Six alternative proteases for mass spectrometry-based proteomics beyond trypsin.” In: *Nature protocols* 11.5, pp. 993–1006 (cit. on p. 82).

Gilman, Alfred G (1987). “G proteins: transducers of receptor-generated signals.” In: *Annual review of biochemistry* 56, pp. 615–649 (cit. on p. 6).

Gjesing, A P et al. (2007). “Studies of associations between the Arg389Gly polymorphism of the beta1-adrenergic receptor gene (ADRB1) and hypertension and obesity in 7677 Danish white subjects.” In: *Diabetic medicine : a journal of the British Diabetic Association* 24.4, pp. 392–7 (cit. on p. 9).

Goodman, O B et al. (1996). “β-arrestin acts as a clathrin adaptor in endocytosis of the β2-adrenergic receptor.” In: *Nature* 383.6599, pp. 447–50 (cit. on pp. 17, 84).

Goodman, O B et al. (1997). “Arrestin/clathrin interaction. Localization of the arrestin binding locus to the clathrin terminal domain.” In: *The Journal of biological chemistry* 272.23, pp. 15017–22 (cit. on pp. 17, 84).

Gurevich, Vsevolod V and Eugenia V Gurevich (2004). “The molecular acrobatics of arrestin activation.” In: *Trends in pharmacological sciences* 25.2, pp. 105–11 (cit. on pp. 13, 14).

Gurevich, Vsevolod V. and Eugenia V. Gurevich (2006). “The structural basis of arrestin-mediated regulation of G-protein-coupled receptors.” In: *Pharmacology & therapeutics* 110.3, pp. 465–502 (cit. on p. 18).

Hakalahti, Anna E et al. (2013). “β-adrenergic agonists mediate enhancement of β1-adrenergic receptor N-terminal cleavage and stabilization in vivo and in vitro.” In: *Molecular pharmacology* 83.1, pp. 129–41 (cit. on p. 61).

Hanks, S K and Tony Hunter (1995). “Protein kinases 6. The eukaryotic protein kinase superfamily: kinase (catalytic) domain structure and classification.” In: *FASEB journal* 9.8, pp. 576–96 (cit. on p. 11).

Hawes, B. E. et al. (1995). *Distinct pathways of Gi- and Gq-mediated mitogen-activated protein kinase activation.* (Cit. on pp. 19, 78).

Hoffmann, C et al. (2004). “Comparative pharmacology of human β-adrenergic receptor subtypes–characterization of stably transfected receptors in CHO cells.” In: *Naunyn-Schmiedeberg’s archives of pharmacology* 369.2, pp. 151–9 (cit. on p. 82).

Hou, Bi-Huei et al. (2011). “Optical sensors for monitoring dynamic changes of intracellular metabolite levels in mammalian cells.” In: *Nature protocols* 6.11, pp. 1818–33 (cit. on p. 20).

Huang, Jianyun et al. (2013). “Crystal structure of oligomeric β1-adrenergic G protein-coupled receptors in ligand-free basal state.” In: *Nature structural & molecular biology* 20.4, pp. 419–25 (cit. on p. 6).

Hustoft, Hanne Kolsrud et al. (2010). “A Critical Review of Trypsin Digestion for LC-MS Based Proteomics.” In: *Integrative Proteomics*, pp. 73–92 (cit. on p. 27).

Insel, Paul A et al. (2007). “Impact of GPCRs in clinical medicine: monogenic diseases, genetic variants and drug targets.” In: *Biochimica et biophysica acta* 1768.4, pp. 994–1005 (cit. on p. 8).

Irannejad, Roshanak et al. (2013). “Conformational biosensors reveal GPCR signalling from endosomes.” In: *Nature* 495.7442, pp. 534–8 (cit. on pp. 19, 86).

Jekel, P A, W J Weijer, and J J Beintema (1983). “Use of endoproteinase Lys-C from Lysobacter enzymogenes in protein sequence analysis.” In: *Analytical biochemistry* 134.2, pp. 347–54 (cit. on p. 82).

Johnson, Andrew D et al. (2011). “Association of hypertension drug target genes with blood pressure and hypertension in 86,588 individuals.” In: *Hypertension (Dallas, Tex. : 1979)* 57.5, pp. 903–10 (cit. on p. 9).

Joost, Patrick and Axel Methner (2002). “Phylogenetic analysis of 277 human G-protein-coupled receptors as a tool for the prediction of orphan receptor ligands.” In: *Genome biology* 3.11, RESEARCH0063 (cit. on p. 3).

Kaboord, Barbara and Maria Perr (2008). “Isolation of proteins and protein complexes by immunoprecipitation.” In: *Methods in molecular biology* 424, pp. 349–64 (cit. on pp. 23, 25).

Kenakin, Terry (2007). “Functional selectivity through protean and biased agonism: who steers the ship?” In: *Molecular pharmacology* 72.6, pp. 1393–1401 (cit. on p. 19).

Kennedy, M B (1995). “Origin of PDZ (DHR, GLGF) domains.” In: *Trends in biochemical sciences* 20.9, p. 350 (cit. on p. 18).

Kim, Jihee et al. (2005). “Functional antagonism of different G protein-coupled receptor kinases for β-arrestin-mediated angiotensin II receptor signaling.” In: *Proceedings of the National Academy of Sciences of the United States of America* 102.5, pp. 1442–7 (cit. on pp. 12, 78).

Kirchberg, Kristina et al. (2011). “Conformational dynamics of helix 8 in the GPCR rhodopsin controls arrestin activation in the desensitization process.” In: *Proceedings of the National Academy of Sciences of the United States of America* 108.46, pp. 18690–5 (cit. on p. 4).

Koressaar, Triinu and Maido Remm (2007). “Enhancements and modifications of primer design program Primer3.” In: *Bioinformatics* 23.10, pp. 1289–1291 (cit. on p. 35).

Krasel, Cornelius et al. (2005). “β-arrestin binding to the β2-adrenergic receptor requires both receptor phosphorylation and receptor activation.” In: *The Journal of biological chemistry* 280.10, pp. 9528–35 (cit. on p. 20).

Krasel, Cornelius et al. (2008). “Dual role of the β2-adrenergic receptor C-terminus for the binding of β-arrestin and receptor internalization.” In: *The Journal of biological chemistry* 283.46, pp. 31840–8 (cit. on pp. 15, 20).

Kuna, Ramya S et al. (2013). “Glucagon-like peptide-1 receptor-mediated endosomal cAMP generation promotes glucose-stimulated insulin secretion in pancreatic β-cells.” In: *American journal of physiology. Endocrinology and metabolism* 305.2, E161–70 (cit. on p. 86).

Kunapuli, P., V. V. Gurevich, and J. L. Benovic (1994). “Phospholipid-stimulated autophosphorylation activates the G protein-coupled receptor kinase GRK5.” In: *The Journal of biological chemistry* 269.14, pp. 10209–12 (cit. on p. 12).

Lambert, N. A. (2008). “Dissociation of Heterotrimeric G Proteins in Cells.” In: *Science Signaling* 1.25, re5–re5 (cit. on p. 6).

Laporte, Stephane A et al. (2002). “β-Arrestin/AP-2 interaction in G protein-coupled receptor internalization: identification of a beta-arrestin binging site in beta 2-adaptin.” In: *The Journal of biological chemistry* 277.11, pp. 9247–54 (cit. on pp. 17, 84).

Lefkowitz, R. J. (2007). “Seven transmembrane receptors: something old, something new.” In: *Acta physiologica* 190.1, pp. 9–19 (cit. on p. 3).

Lefkowitz, Robert J and Sudha K Shenoy (2005). “Transduction of receptor signals by β-arrestins.” In: *Science* 308.5721, pp. 512–7 (cit. on pp. 8, 20).

Lehmann, Andreas et al. (2016). “Identification of Phosphorylation Sites Regulating sst3 Somatostatin Receptor Trafficking.” In: *Molecular endocrinology* 30.6, pp. 645–59 (cit. on p. 88).

Liang, Wei et al. (2003). “Resistance of the human β1-adrenergic receptor to agonist-mediated down-regulation. Role of the C terminus in determining beta-subtype degradation.” In: *The Journal of biological chemistry* 278.41, pp. 39773–81 (cit. on p. 85).

Lohse, M J, V Lenschow, and U Schwabe (1984). “Two affinity states of Ri adenosine receptors in brain membranes. Analysis of guanine nucleotide and temperature effects on radioligand binding.” In: *Molecular pharmacology* 26.1, pp. 1–9 (cit. on p. 15).

Lohse, Martin J and Carsten Hoffmann (2014). “Arrestin interactions with G protein-coupled receptors.” In: *Handbook of experimental pharmacology*. Handbook of Experimental Pharmacology 219. Ed. by Vsevolod V. Gurevich, pp. 15–56 (cit. on p. 15).

Lohse, Martin J et al. (1990). “β-Arrestin: a protein that regulates β-adrenergic receptor function.” In: *Science* 248.4962, pp. 1547–50 (cit. on p. 16).

Lohse, Martin J, Stefan Engelhardt, and Thomas Eschenhagen (2003). “What is the role of β-adrenergic signaling in heart failure?” In: *Circulation research* 93.10, pp. 896–906 (cit. on p. 9).

Lohse, Martin J et al. (2008). “Optical techniques to analyze real-time activation and signaling of G-protein-coupled receptors.” In: *Trends in pharmacological sciences* 29.3, pp. 159–65 (cit. on p. 20).

Luttrell, L M et al. (1999). “β-arrestin-dependent formation of β2 adrenergic receptor-Src protein kinase complexes.” In: *Science* 283.5402, pp. 655–61 (cit. on p. 87).

Luttrell, Louis M and Diane Gesty-Palmer (2010). “Beyond desensitization: physiological relevance of arrestin-dependent signaling.” In: *Pharmacological reviews* 62.2, pp. 305–330 (cit. on pp. 18, 86).

Lymperopoulos, Anastasios, Giuseppe Rengo, and Walter J. Koch (2013). “Adrenergic nervous system in heart failure: pathophysiology and therapy.” In: *Circulation research* 113.6, pp. 739–53 (cit. on p. 8).

Mann, Matthias et al. (2002). “Analysis of protein phosphorylation using mass spectrometry: deciphering the phosphoproteome.” In: *Trends in biotechnology* 20.6, pp. 261–8 (cit. on pp. 10, 28, 81).

Manning, G et al. (2002). “The protein kinase complement of the human genome.” In: *Science* 298.5600, pp. 1912–34 (cit. on p. 10).

Maqbool, A et al. (1999). “Common polymorphisms of β1-adrenoceptor: identification and rapid screening assay.” In: *Lancet* 353.9156, p. 897 (cit. on p. 9).

Marion, Sébastien et al. (2006). “A β-arrestin binding determinant common to the second intracellular loops of rhodopsin family G protein-coupled receptors.” In: *The Journal of biological chemistry* 281.5, pp. 2932–8 (cit. on p. 5).

Marx, S O et al. (2000). “PKA phosphorylation dissociates FKBP12.6 from the calcium release channel (ryanodine receptor): defective regulation in failing hearts.” In: *Cell* 101.4, pp. 365–376 (cit. on p. 9).

Mason, D. a. et al. (1999). “A gain-of-function polymorphism in a G-protein coupling domain of the human β1-adrenergic receptor.” In: *The Journal of biological chemistry* 274.18, pp. 12670–4 (cit. on p. 9).

McCrink, Katie A et al. (2016). “β1-adrenoceptor Arg389Gly polymorphism confers differential β-arrestin-binding tropism in cardiac myocytes.” In: *Pharmacogenomics* 17.15, pp. 1611–1620 (cit. on pp. 16, 84).

McDonald, P. H. (2000). “β-arrestin 2: A Receptor-Regulated MAPK Scaffold for the Activation of JNK3.” In: *Science* 290.5496, pp. 1574–1577 (cit. on p. 15).

Merriam, Laura A et al. (2013). “Pituitary adenylate cyclase 1 receptor internalization and endosomal signaling mediate the pituitary adenylate cyclase activating polypeptide-induced increase in guinea pig cardiac neuron excitability.” In: *The Journal of neuroscience* 33.10, pp. 4614–22 (cit. on p. 86).

Miller, W. E. and R. J. Lefkowitz (2001). “Expanding roles for β-arrestins as scaffolds and adapters in GPCR signaling and trafficking.” In: *Current Opinion in Cell Biology* 13.2, pp. 139–145 (cit. on p. 15).

Morgan, Alexander A. and Edward Rubenstein (2013). “Proline: The Distribution, Frequency, Positioning, and Common Functional Roles of Proline and Polyproline Sequences in the Human Proteome.” In: *PLoS ONE* 8.1, pp. 1–9 (cit. on p. 11).

Nakagawa, Takatoshi and Michio Asahi (2013). “β1-adrenergic receptor recycles via a membranous organelle, recycling endosome, by binding with sorting nexin27.” In: *The Journal of membrane biology* 246.7, pp. 571–9 (cit. on p. 83).

Nakamura, K, R W Hipkin, and M Ascoli (1998). “The agonist-induced phosphorylation of the rat follitropin receptor maps to the first and third intracellular loops.” In: *Molecular endocrinology* 12.4, pp. 580–91 (cit. on p. 15).

Nakaya, Michio et al. (2012). “Induction of cardiac fibrosis by β-blocker in G protein-independent and GRK5/β-arrestin2-dependent signaling pathways.” In: *The Journal of biological chemistry* (cit. on p. 88).

Neubig, R R, R D Gantzos, and W J Thomsen (1988). “Mechanism of agonist and antagonist binding to alpha 2 adrenergic receptors: evidence for a precoupled receptor-guanine nucleotide protein complex.” In: *Biochemistry* 27.7, pp. 2374–2384 (cit. on p. 6).

Nobles, Kelly N et al. (2011). “Distinct phosphorylation sites on the β(2)-adrenergic receptor establish a barcode that encodes differential functions of β-arrestin.” In: *Science signaling* 4.185, ra51 (cit. on pp. 12, 13, 82, 84).

Nobles, Muriel, Amy Benians, and Andrew Tinker (2005). “Heterotrimeric G proteins precouple with G protein-coupled receptors in living cells.” In: *Proceedings of the National Academy of Sciences of the United States of America* 102.51, pp. 18706–11 (cit. on p. 6).

Noma, Takahisa et al. (2007). “β-arrestin-mediated β1-adrenergic receptor transactivation of the EGFR confers cardioprotection.” In: *The Journal of clinical investigation* 117.9, pp. 2445–58 (cit. on p. 19).

Nooh, Mohammed M. et al. (2014). “Sorting of β1-adrenergic receptors is mediated by pathways that are either dependent on or independent of type I PDZ, protein kinase A (PKA), and SAP97.” In: *The Journal of biological chemistry* 289.4, pp. 2277–94 (cit. on pp. 13, 81, 83, 85).

Noor, Nabila, Chetan B. Patel, and Howard A. Rockman (2011). “Beta-arrestin: a signaling molecule and potential therapeutic target for heart failure.” In: *Journal of molecular and cellular cardiology* 51.4, pp. 534–41 (cit. on p. 86).

Nuber, Susanne et al. (2016). “β-Arrestin biosensors reveal a rapid, receptor-dependent activation/deactivation cycle.” In: *Nature* 531.7596, pp. 661–664 (cit. on p. 84).

Oakley, Robert H. et al. (1999). “Association of β-arrestin with G protein-coupled receptors during clathrin-mediated endocytosis dictates the profile of receptor resensitization.” In: *The Journal of biological chemistry* 274.45, pp. 32248–57 (cit. on pp. 17, 84).

Oakley, Robert H. et al. (2000). “Differential affinities of visual arrestin, β-arrestin1, and β-arrestin2 for G protein-coupled receptors delineate two major classes of receptors.” In: *The Journal of biological chemistry* 275.22, pp. 17201–10 (cit. on p. 16).

Oka, Yuichiro et al. (2009). “The fifth class of Galpha proteins.” In: *Proceedings of the National Academy of Sciences of the United States of America* 106.5, pp. 1484–9 (cit. on p. 6).

Olivares-Reyes, J A et al. (2001). “Agonist-induced signaling, desensitization, and internalization of a phosphorylation-deficient AT1A angiotensin receptor.” In: *The Journal of biological chemistry* 276.41, pp. 37761–8 (cit. on p. 12).

Olsen, Jesper V and Matthias Mann (2013). “Status of large-scale analysis of post-translational modifications by mass spectrometry.” In: *Molecular & cellular proteomics : MCP* 12.12, pp. 3444–52 (cit. on p. 81).

Olsen, Jesper V. et al. (2006). “Global, In Vivo, and Site-Specific Phosphorylation Dynamics in Signaling Networks.” In: *Cell* 127.3, pp. 635–648 (cit. on p. 10).

Ong, Shao-En et al. (2002). “Stable Isotope Labeling by Amino Acids in Cell Culture, SILAC, as a Simple and Accurate Approach to Expression Proteomics.” In: *Molecular & Cellular Proteomics* 1.5, pp. 376–386 (cit. on p. 28).

Orpana, Arto K, Tho H Ho, and Jakob Stenman (2012). “Multiple heat pulses during PCR extension enabling amplification of GC-rich sequences and reducing amplification bias.” In: *Analytical chemistry* 84.4, pp. 2081–7 (cit. on p. 38).

Ostermaier, Martin K., Gebhard F X Schertler, and Joerg Standfuss (2014). “Molecular mechanism of phosphorylation-dependent arrestin activation.” In: *Current Opinion in Structural Biology* 29, pp. 143–151 (cit. on p. 81).

Overington, John P, Bissan Al-Lazikani, and Andrew L Hopkins (2006). “How many drug targets are there?” In: *Nature reviews. Drug discovery* 5.12, pp. 993–6 (cit. on p. 2).

Palczewski, K, J H McDowell, and P A Hargrave (1988). “Purification and characterization of rhodopsin kinase.” In: *The Journal of biological chemistry* 263.28, pp. 14067–73 (cit. on p. 12).

Palczewski, Krzysztof et al. (1991). “Mechanism of rhodopsin kinase activation.” In: *The Journal of biological chemistry* 266.20, pp. 12949–55 (cit. on pp. 12, 13).

Palczewski, Krzysztof et al. (2000). “Crystal structure of rhodopsin: A G protein-coupled receptor.” In: *Science* 289.5480, pp. 739–45 (cit. on p. 4).

Pearson, Gray et al. (2001). “Mitogen-activated protein (MAP) kinase pathways: regulation and physiological functions.” In: *Endocrine reviews* 22.2, pp. 153–83 (cit. on p. 10).

Penheiter, Sumedha G et al. (2002). “Internalization-dependent and -independent requirements for transforming growth factor β receptor signaling via the Smad pathway.” In: *Molecular and cellular biology* 22.13, pp. 4750–9 (cit. on p. 85).

Pierce, Kristen L, Richard T Premont, and Robert J Lefkowitz (2002). “Seven-transmembrane receptors.” In: *Nature reviews. Molecular cell biology* 3.9, pp. 639–50 (cit. on pp. 2, 3, 6).

Pitcher, Julie A et al. (1992). “Role of beta gamma subunits of G proteins in targeting the beta-adrenergic receptor kinase to membrane-bound receptors.” In: *Science* 257.5074, pp. 1264–7 (cit. on pp. 12, 13).

Porath, Jerker et al. (1975). “Metal chelate affinity chromatography, a new approach to protein fractionation.” In: *Nature* 258.5536, pp. 598–599 (cit. on p. 28).

Posewitz, M C and P Tempst (1999). “Immobilized gallium(III) affinity chromatography of phosphopeptides.” In: *Analytical chemistry* 71.14, pp. 2883–92 (cit. on p. 28).

Preininger, Anita M and Heidi E Hamm (2004). “G protein signaling: insights from new structures.” In: *Science’s STKE : signal transduction knowledge environment* 2004.218, re3 (cit. on p. 6).

Premont, R T et al. (1994). “Identification, purification, and characterization of GRK5, a member of the family of G protein-coupled receptor kinases.” In: *The Journal of biological chemistry* 269.9, pp. 6832–41 (cit. on p. 12).

Premont, Richard T and Raul R Gainetdinov (2007). “Physiological roles of G protein-coupled receptor kinases and arrestins.” In: *Annual review of physiology* 69, pp. 511–34 (cit. on pp. 14, 20).

Qi, Ai-Dong et al. (2011). “Ser352 and Ser354 in the carboxyl terminus of the human P2Y(1) receptor are required for agonist-promoted phosphorylation and internalization in MDCK cells.” In: *British journal of pharmacology* 162.6, pp. 1304–13 (cit. on p. 15).

Rapacciuolo, Antonio et al. (2003). “Protein kinase A and G protein-coupled receptor kinase phosphorylation mediates β-1 adrenergic receptor endocytosis through different pathways.” In: *The Journal of biological chemistry* 278.37, pp. 35403–11 (cit. on pp. 18, 85, 86).

Rappsilber, Juri, Matthias Mann, and Yasushi Ishihama (2007). “Protocol for micro-purification, enrichment, pre-fractionation and storage of peptides for proteomics using StageTips.” In: *Nature protocols* 2.8, pp. 1896–1906 (cit. on p. 57).

Rasmussen, Søren G F et al. (2007). “Crystal structure of the human β2 adrenergic G-protein-coupled receptor.” In: *Nature* 450.7168, pp. 383–7 (cit. on p. 6).

Rasmussen, Søren G F et al. (2011a). “Crystal structure of the β2 adrenergic receptor-Gs protein complex.” In: *Nature* 477.7366, pp. 549–55 (cit. on p. 6).

Rasmussen, Søren G F et al. (2011b). “Structure of a nanobody-stabilized active state of the β(2) adrenoceptor.” In: *Nature* 469.7329, pp. 175–80 (cit. on p. 6).

Reiner, Susanne et al. (2009). “β -Arrestin-2 Interaction and Internalization of the Human P2Y 1 Receptor Are Dependent on C-Terminal Phosphorylation Sites.” In: *Molecular pharmacology* 76.6, pp. 1162–1171 (cit. on p. 15).

Reiter, Eric and Robert J Lefkowitz (2006). “GRKs and β-arrestins: roles in receptor silencing, trafficking and signaling.” In: *Trends in endocrinology and metabolism: TEM* 17.4, pp. 159–65 (cit. on p. 12).

Ridge, Kevin D. et al. (2003). “Phototransduction: Crystal clear.” In: *Trends in Biochemical Sciences* 28.9, pp. 479–487 (cit. on p. 16).

Rockman, HA, WJ Koch, and RJ Lefkowitz (2002). “Seven-transmembrane-spanning receptors and heart function.” In: *Nature* 415.6868, pp. 206–12 (cit. on pp. 3, 18).

Salon, John a, David T Lodowski, and Krzysztof Palczewski (2011). “The significance of G protein-coupled receptor crystallography for drug discovery.” In: *Pharmacological reviews* 63.4, pp. 901–37 (cit. on p. 2).

Schiess, Ralph, Bernd Wollscheid, and Ruedi Aebersold (2009). “Targeted proteomic strategy for clinical biomarker discovery.” In: *Molecular oncology* 3.1, pp. 33–44 (cit. on p. 23).

Sheng, M and C Sala (2001). “PDZ domains and the organization of supramolecular complexes.” In: *Annual review of neuroscience* 24, pp. 1–29 (cit. on p. 18).

Shenoy, Sudha K and Robert J Lefkowitz (2003). “Multifaceted roles of β-arrestins in the regulation of seven-membrane-spanning receptor trafficking and signalling.” In: *The Biochemical journal* 375.Pt 3, pp. 503–15 (cit. on p. 18).

Shenoy, Sudha K et al. (2006). “β-arrestin-dependent, G protein-independent ERK1/2 activation by the β2 adrenergic receptor.” In: *The Journal of biological chemistry* 281, pp. 1261–1273 (cit. on pp. 18, 78).

Shi, Yigong (2009). “Serine/threonine phosphatases: mechanism through structure.” In: *Cell* 139.3, pp. 468–84 (cit. on p. 12).

Shiina, T. et al. (2000). “Interaction with β-arrestin determines the difference in internalization behavor between β1- and β2-adrenergic receptors.” In: *The Journal of biological chemistry* 275.37, pp. 29082–90 (cit. on p. 85).

Shukla, Arun K., Garima Singh, and Eshan Ghosh (2014). “Emerging structural insights into biased GPCR signaling.” In: *Trends in Biochemical Sciences* 39, pp. 594–602 (cit. on pp. 13, 18).

Simmerman, H K and L R Jones (1998). “Phospholamban: protein structure, mechanism of action, and role in cardiac function.” In: *Physiological reviews* 78.4, pp. 921–947 (cit. on p. 9).

Smith, Jeffrey S. and Sudarshan Rajagopal (2016). “The β-Arrestins: Multifunctional Regulators of G Protein-coupled Receptors.” In: *The Journal of biological chemistry* 291.17, pp. 8969–77 (cit. on p. 19).

Sofowora, G G et al. (2003). “A common beta1-adrenergic receptor polymorphism (Arg389Gly) affects blood pressure response to beta-blockade.” In: *Clinical pharmacology and therapeutics* 73.4, pp. 366–71 (cit. on p. 10).

Steen, Hanno et al. (2006). “Phosphorylation analysis by mass spectrometry: myths, facts, and the consequences for qualitative and quantitative measurements.” In: *Molecular & cellular proteomics : MCP* 5.1, pp. 172–81 (cit. on pp. 27, 81).

Strada, S. J., P. Uzunov, and B. Weiss (1974). “Ontogenetic Development of a Phosphodiesterase Activator and the Multiple Forms of Cyclic Amp Phosphodiesterase of Rat Brain.” In: *Journal of Neurochemistry* 23.6, pp. 1097–1103 (cit. on p. 7).

Strosberg, A D (1993). “Structure, function, and regulation of adrenergic receptors.” In: *Protein science : a publication of the Protein Society* 2.8, pp. 1198–209 (cit. on p. 8).

Swaney, Danielle L, Craig D Wenger, and Joshua J Coon (2010). “Value of using multiple proteases for large-scale mass spectrometry-based proteomics.” In: *Journal of proteome research* 9.3, pp. 1323–9 (cit. on p. 82).

Tesson, F et al. (1999). “Characterization of a unique genetic variant in the β1-adrenoceptor gene and evaluation of its role in idiopathic dilated cardiomyopathy. CARDIGENE Group.” In: *Journal of molecular and cellular cardiology* 31.5, pp. 1025–32 (cit. on p. 9).

Thingholm, Tine E et al. (2007). “SIMAC (sequential elution from IMAC), a phosphoproteomics strategy for the rapid separation of monophosphorylated from multiply phosphorylated peptides.” In: *Molecular & cellular proteomics : MCP* 7.4, pp. 661–71 (cit. on p. 28).

Tikhonoff, V et al. (2008). “Blood pressure and metabolic phenotypes in relation to the ADRB1 Arg389Gly and ADRA2B I/D polymorphisms in a White population.” In: *Journal of human hypertension* 22.12, pp. 864–7 (cit. on p. 9).

Tilley, Douglas G (2011). “G protein-dependent and G protein-independent signaling pathways and their impact on cardiac function.” In: *Circulation research* 109.2, pp. 217–30 (cit. on p. 78).

Tilley, Douglas G et al. (2009). “β-Arrestin mediates β1-adrenergic receptor - epidermal growth factor receptor interaction and downstream signaling.” In: *The Journal of biological chemistry* 284.30, pp. 20375–86 (cit. on pp. 13, 81).

Tobin, Andrew B., Adrian J. Butcher, and Kok Choi Kong (2008). “Location, location, location. . . site-specific GPCR phosphorylation offers a mechanism for cell-type-specific signalling.” In: *Trends in Pharmacological Sciences* 29.8, pp. 413–420 (cit. on p. 83).

Tolkovsky, A M and A Levitzki (1978). “Mode of coupling between the β-adrenergic receptor and adenylate cyclase in turkey erythrocytes.” In: *Biochemistry* 17.18, p. 3795 (cit. on p. 6).

Ubersax, Jeffrey a and James E Ferrell (2007). “Mechanisms of specificity in protein phosphorylation.” In: *Nature reviews. Molecular cell biology* 8.7, pp. 530–41 (cit. on pp. 10–12).

Uhlén, Mathias et al. (2015). “Tissue-based map of the human proteome.” In: *Science* 347.6220, pp. 1260419–1260419 (cit. on pp. 9, 12, 14).

Untergasser, Andreas et al. (2012). “Primer3-new capabilities and interfaces.” In: *Nucleic Acids Research* 40.15, pp. 1–12 (cit. on p. 35).

Vaughan, David J. et al. (2006). “Role of the G protein-coupled receptor kinase site serine cluster in βadrenergic receptor internalization, desensitization, and beta-arrestin translocation.” In: *The Journal of biological chemistry* 281.11, pp. 7684–92 (cit. on p. 85).

Venter, J C et al. (2001). “The sequence of the human genome.” In: *Science* 291.5507, pp. 1304–51 (cit. on p. 11).

Vilardaga, Jean-Pierre et al. (2003). “Measurement of the millisecond activation switch of G protein-coupled receptors in living cells.” In: *Nature biotechnology* 21.7, pp. 807–12 (cit. on p. 20).

Villén, Judit and Steven P Gygi (2008). “The SCX/IMAC enrichment approach for global phosphorylation analysis by mass spectrometry.” In: *Nature protocols* 3.10, pp. 1630–8 (cit. on p. 57).

Vishnivetskiy, Sergey A et al. (2007). “Regulation of arrestin binding by rhodopsin phosphorylation level.” In: *The Journal of biological chemistry* 282.44, pp. 32075–83 (cit. on p. 14).

Warne, Tony et al. (2008). “Structure of a β1-adrenergic G-protein-coupled receptor.” In: *Nature* 454.7203, pp. 486–91 (cit. on pp. 5, 6).

Warne, Tony et al. (2011). “The structural basis for agonist and partial agonist action on a β(1)-adrenergic receptor.” In: *Nature* 469.7329, pp. 241–4 (cit. on p. 6).

Warne, Tony et al. (2012). “Crystal structures of a stabilized β1-adrenoceptor bound to the biased agonists bucindolol and carvedilol.” In: *Structure* 20.5, pp. 841–9 (cit. on p. 6).

Weiss, Ellen R et al. (2001). “Species-specific differences in expression of G-protein-coupled receptor kinase (GRK) 7 and GRK1 in mammalian cone photoreceptor cells: implications for cone cell phototransduction.” In: *Cloning* 21.23, pp. 9175–9184 (cit. on p. 12).

Wisler, James W et al. (2007). “A unique mechanism of β-blocker action: carvedilol stimulates β-arrestin signaling.” In: *Proceedings of the National Academy of Sciences of the United States of America* 104.42, pp. 16657–16662 (cit. on pp. 19, 88).

Wynne, Brandi M., Chin-Wei Chiao, and R. Clinton Webb (2009). “Vascular Smooth Muscle Cell Signaling Mechanisms for Contraction to Angiotensin II and Endothelin-1.” In: *Journal of the American Society of Hypertension : JASH* 3.2, pp. 84–95 (cit. on p. 7).

Zhang, Peng, Celinda M. Kofron, and Ulrike Mende (2015). “Heterotrimeric G protein-mediated signaling and its non-canonical regulation in the heart.” In: *Life Sciences* 129, pp. 35–41 (cit. on p. 3).

Zhao, X L et al. (1994). “The alpha 1-subunit of skeletal muscle L-type Ca channels is the key target for regulation by A-kinase and protein phosphatase-1C.” In: *Biochemical and biophysical research communications* 198.1, pp. 166–173 (cit. on p. 9).

Zindel, Diana et al. (2015). “Engineered hyperphosphorylation of the β2-adrenoceptor prolongs arrestin-3 binding and induces arrestin internalization.” In: *Molecular pharmacology* 87.2, pp. 349–62 (cit. on pp. 15, 54, 85).

Appendix

1 List of abbreviations

ACN	Acetonitrile
ADP	Adenosine monophosphate
ADRB1	β_1-adrenoceptor
ADRB2	β_2-adrenoceptor
Akt	Protein kinase B (PKB)
Ala	Alanine
AMP	Adeonosine monophosphate
Arg	Arginine
ATM	Ataxia teleangiectasia mutated
ATP	Adenosine triphosphate
ATR	Ataxia telangiectasia and Rad3-related protein
AUC	Area under the curve
BCA	Bicinchoninic acid
BSA	Bovine serum albumin
cAMP	Cyclic adenosine monophosphate
Cer	Cerulean
CFP	Cyan fluorescent protein
c-Src	Proto-oncogene tyrosine-protein kinse src
DMEM	Dulbecco's modified Eagle's minimal essential medium
DMSO	Dimethyl sulfoxide
DSS	Disuccinimidyl suberate
DTT	Dithiothreitol
ECL	Extracellular loop
EDTA	Ethylenediaminetetraacetic acid
EGFR	Epidermal growth factor receptor
EtOH	Ethanol
FA	Formic acid
FACS	Fluorescence activated cell sorting
FCS	Fetal bovine serum
FlAsH	Fluorescein arsenical hairpin
FRET	Fluorescence resonance energy transfer

GDP	Guanosine diphosphate
GFP	Green fluorescent protein
GPCR	G protein-coupled receptor
G protein	Guanine nucleotide binding protein
G_i	Inhibitory G protein
G_s	Stimlatory G protein
GTP	Guanosine triphosphate
GRK	G protein-coupled receptor kinase
HPE PCR	Heat pulse extension PCR
IAA	2-iodoacetamide
ICL	Intracellular loop
IMAC	Immobilized metal ion affinity chromatography
IP	Immunoprecipitation
JNK	c-Jun N-terminal kinase
LC	Liquid chromatography
MAPK	Mitogen-activated protein kinase
MeOH	Methanol
MOAC	Metal oxide affinity chromatography
MS	Mass spectrometry
PBS	Phosphate buffered saline
PCR	Polymerase chain reaction
PDE	Phosphodiesterase
PDVF	Polyvinylidene fluoride
PDZ	post synaptic density protein 95, Drosophila disc large tumor suppressor and zonula occludens-1 protein
PKA	Protein kinase A
PKC	Protein kinase C
pSer	Phosphoserine
pThr	Phosphothreonine
PTM	Post-translational modification
pTyr	Phosphotyrosine
RGS	Regulator of G protein signaling
RIPA buffer	Radioimmunoprecipitation assay buffer

SAP97	Synapse-associated protein 97
SAX	Strong anion exchange
SCX	Strong cation exchange
SDS	Sodium dodecyl sulfate
Ser	Serine
SILAC	Stable isotope labeling by amino acids in cell culture
SIMAC	Sequential elution from IMAC
SNP	Single nucleotide polymorphism
TAE	Tris acetate EDTA
TEAB	Triethylammonium bicarbonate
Thr	Threonine
Tris	Tris-(hydroxymethyl)-aminomethan
Tyr	Tyrosine
YFP	Yellow fluorescent protein

2 Acknowledgements

First I want to thank Prof. Engelhardt for giving me the opportunity to do my PhD in his lab. I have learned so much in the past four years and I am truly grateful for this.

Next, I would like to thank my supervisor Dr. Andrea Ahles, who has taught me countless things. Starting from how to make PowerPoint slides look good and how to convincingly present data to almost every method I used in the research for my dissertation. She took the time to help me prepare for the first lecture I had to give and she even sat in the back row and listened to the lecture because it helped me not to be so nervous. She always had an open ear for me, when I was stuck and didn't know how to continue and she always encouraged me. Andrea, I want to thank you for everything. This thesis wouldn't be if it weren't for you. You have become a good friend over the past years and I truly hope that we stay in touch!

Another thanks goes to Dr. Kathleen Meyer and to Lucia Koblitz. You two have made my life in the lab so much more fun! I will miss having a glass of wine after work with you two! But of course I also want to thank you for helping me professionally. Thank you Lulu for always helping out with small, but very time consuming tasks! You really made my life easier. And Kathleen, thank you for countless discussions of my data. You really helped me to focus on what is important.

The other two people I had countless very helpful discussions with were Dr. Bernhard Laggerbauer and Dr. Anne Dück. Thank you two for all the input!

Additionally I would like to thank the lab of Prof. Küster, who did the mass spectrometry. Especially I want to thank Benjamin Ruprecht, who performed the experiments.

Apart from the researchers I also want to thank Michaela Hennig, the secretary at the IPT. Thank you for always looking out for me. It is really appreciated.

Another thank you goes to Desislava Zlatanova and Dr. Katrin Offe, who manage the Ph.D. Program. You two really helped me out at the end of my thesis. Thank you!

Last, I thank my family and especially my fiancee, Adrian Stoewer, who had to put up with a lot due to my research. I am so thankful that you agreed to me commuting from Berlin to Munich, to finish up my studies. Thank you!